

UNIVERSITY OF OKLAHOMA

GRADUATE COLLEGE

FLUCTUATION-INDUCED FRICTIONAL EFFECTS
ON ATOMS AND NANOPARTICLES

A DISSERTATION

SUBMITTED TO THE GRADUATE FACULTY

in partial fulfillment of the requirements for the

degree of

DOCTOR OF PHILOSOPHY

By

Xin Guo

Norman, Oklahoma

2023

FLUCTUATION-INDUCED FRICTIONAL EFFECTS
ON ATOMS AND NANOPARTICLES

A DISSERTATION APPROVED FOR THE
HOMER L. DODGE DEPARTMENT OF PHYSICS
AND ASTRONOMY

BY THE COMMITTEE CONSISTING OF

Dr. Howard A. Baer, Chair

Dr. Kimball A. Milton

Dr. Max B. Forester

Dr. Phillip Gutierrez

Dr. Bruno Uchoa

Dedicated to the Lord Jesus Christ my savior for what he has done for me.

Acknowledgements

Almost seven years passed. I have been completely transformed in these years, not according to my plan, but my God's plan.

By the Spring of 2018, I was about to abandon my Lord, Jesus Christ, for the sake of a fake freedom — sin. I wanted to be myself and go on my own way, not His way. It, however, pushed me into a deepest pit. When I realized I even got to the point of wanting to end my life, I had to tell my advisor Kim that I was very depressed and felt hopeless. Thankfully, he was very concerned and helped me to return to China before that semester ended. Arriving back to home that summer, I found my mom, a very strong willed woman, became so humbled and tender. She prayed for me with tears every day. I still remember that cold night. She persuaded me to go with her to the church. I argued with her wildly on the street on our way back to home. She suddenly stopped arguing, bowed to pray, and then took her coat and put it on me. That night, her love warmed up not only my body but my heart. Through that move, I had a glimpse of God's love, mighty and considerate. God won me back to Him, and pulled me out of the darkness into his wonderful light.

I was back to school and worked with Kim again in the fall of 2018. Kim is excellent in physics and he cares his students. I, however, was not making much progress because I only wanted to achieve great things but was not willing to make small, concrete efforts to learn. Instead of finding problems of my own, I thought I should change research field and go to another institution to realize my ambition. I talked to Kim about my rebellious plan and he was, of course, not happy about it. Surprisingly, he later changed his mind ¹ and told me that he would still like to support me, even with the knowledge that I was trying to leave. Needless to say, I was very grateful for that grace. But, I was still stubborn enough to want to leave. I did pray very hard at the time and hoped God would lead me to a right place for me. He answered and blocked my way of leaving with His word and circumstances. I eventually obeyed His guidance and gave up leaving. Soon, I found myself starting to learn and enjoy the research we were doing. This was another turning point, where my vain conceits were exposed and replaced with God's wisdom.

¹I knew from Kim later that, Dr. Strauss, had helped in the middle.

In January 2020, I went on a trip for a supposedly short visit to my family in China. I had planned to come back on February 3rd. However, Covid hit China and my flights back to Norman were canceled on February 1st. This, of course, looked terrible at the time, since I had little idea about what would have happened next. Very thankfully, Kim not only allowed me to participate in research remotely from China but also kept paying me through his research grant during this time. These were essential and allowed me to continue my study and research while I was in China. During the lock down days, my relationship with Chuanyu, a Christian girl I met in the local church at my hometown, quickly improves. The two of us would chat and pray together through video calls every day, even though we did not get to see each other face to face due to the lock down. On April 12th, this girl becomes my wife. Later, our daughter, Qianrou, was born in February, 2021. Of course, I wasn't planning for a marriage or to become a father when I went onto that special trip in January, but God did.

Praise God, my rock, who saves me! Without his mercy and love, I would really have died. When I was ever more closer to death, I doubted that He would ever want me back or have anything to do with me. Right at that time, he lifted me out of the slimy pit, out of the mud and mire. He set my feet on a rock and gave me a firm place to stand — Christ. In this way, he loved me back, washed me clean and gave me a new life, the eternal life of Christ. Therefore I learned a most important lesson: He who did not spare His own perfect son for me on the cross will never forsake me. The salvation he grants me is as secure as Christ is precious to Him! What a love is poured on me! In response to this love, I desire to live for the one who died for me. I have decided to follow Jesus, with no turning back.

There are also so many people and things to be grateful for in the seven years. I am grateful for my advisor, Kim, and his wife, Margarita, for teaching me physics, guiding my research, and the love that they have shown towards me and my family. I am grateful for our research group, from whom I have learned a lot. I am grateful for all the professors who had taught me physics over the years at OU. I am grateful for our department, which provided me an environment to learn, to make mistakes and to grow. I am grateful for the university, and its library in particular, for providing excellent resources

and services to facilitate the study of a student. Finally, I am grateful for the US National Science Foundation, grant Nos. 1707511, 2008417, for financial support during my PhD study.

Xin Guo
Norman, Oklahoma

List of Figures

- 2.1 Illustration of the two-layer geometry.
- 2.2 The temperature-dependent damping parameter for metal gold.
- 4.1 Illustration of an atom flying above a perfectly conducting (PC) plate.
- 4.2 The dimensionless functions that determine the contributions to the quantum friction in the presence of a PC plate (QFPC) from each polarization state is plotted as a function of a distance scaled inverse temperature, $z = \beta/2a$.
- 4.3 The temperature dependence of the quantum frictional force on a Cs atom moving above a PC plate.
- 4.4 The distance dependence of the quantum frictional force on a Cs atom moving above a PC plate.
- 4.5 The velocity dependence of the quantum frictional force on a Cs atom moving above a PC plate (a) at nonrelativistic velocities (b) at relativistic velocities.
- 5.1 Illustration of a charged particle flying above a medium with a finite index of refraction.
- 5.2 Plots of the dimensionless functions f^E and f^H , which controls the magnitude of the induced Cherenkov friction (ICF) on a moving charged particle.
- 5.3 Illustration of a neutral but polarizable particle flying above a medium with a finite index of refraction.

- 5.4 The distance dependence of ICF on a gold nanosphere.
- 5.5 The velocity dependence of ICF on a gold nanosphere.
- C.1 The dimensionless function, f^{XZ} , which determines the strength of the contribution to QFPC from the XZ polarization ($\alpha_{xx}\alpha_{zz}$) is plotted as a function of a distance scaled inverse temperature, $z = \beta/2a$.

Table of Contents

| | |
|--|-----|
| Acknowledgements | v |
| Table of Contents | x |
| Abstract | xii |
| 1 Introduction | 1 |
| 2 Theoretical Minimum | 5 |
| 2.1 First Principles | 6 |
| 2.2 Fluctuation-Dissipation Theorem | 11 |
| 2.3 Quantization | 18 |
| 2.4 Electromagnetic Green's tensor | 20 |
| 2.4.1 General symmetry properties | 21 |
| 2.4.2 Equations of motion | 22 |
| 2.4.3 Vacuum Green's tensor | 25 |
| 2.4.4 Green's tensor in planar geometry | 27 |
| 2.5 Polarizability Tensor | 31 |
| 2.5.1 Polarizability of a nanoparticle | 31 |
| 2.5.2 Polarizability of an atom | 34 |
| 3 Quantum Vacuum Frictional Effects (QVF) | 36 |
| 3.1 Quantum Vacuum Frictional Effects on a Dissipative Nanoparticle . | 37 |
| 3.1.1 Radiative heat transfer of a particle at rest | 38 |
| 3.1.2 Radiative heat transfer of a uniformly moving particle and the nonequilibrium steady state (NESS) | 40 |
| 3.1.3 Quantum vacuum friction in the rest frame of the particle . . | 45 |
| 3.1.4 Quantum vacuum frictional force in the rest frame of radiation | 47 |
| 3.1.5 Interrelations between the powers and forces in different frames | 51 |
| 3.2 Quantum Vacuum Frictional Effects on a Nondissipative Particle in Vacuum | 54 |
| 3.2.1 Second order in polarizability | 54 |
| 3.2.2 Effective polarizability | 59 |
| 3.2.3 Numerical estimates of the quantum vacuum friction for a gold atom | 64 |
| 4 Quantum Friction in the Presence of a Perfectly Conducting Plate (QFPC) | 67 |

TABLE OF CONTENTS

| | | |
|-------|--|-----|
| 5 | Induced Cherenkov Friction (ICF) | 81 |
| 5.1 | Induced Cherenkov Friction on a Charged Particle | 82 |
| 5.1.1 | A nondispersive medium | 83 |
| 5.1.2 | A dispersive medium | 87 |
| 5.2 | Quantum Cherenkov Friction on a Neutral Polarizable Particle . . . | 90 |
| 6 | Conclusions and Outlook | 98 |
| A | Lorentz Transformations of Dipole, Field and Green's Tensor | 102 |
| B | The Absence of Zero Temperature Quantum Friction in the Presence of a Diaphanous Medium | 104 |
| C | Analytical Method for Extracting Limits of QFPC | 106 |
| | List of Publications | 110 |
| | References | 111 |

Abstract

Fluctuations can cause extraordinary effects on atoms and nanoparticles. For example, a neutral but polarizable particle sitting close to a planar surface feels an attraction force towards the surface. This is the well-known Casimir-Polder (CP) force. Fluctuations could also induce a quantum frictional force on a moving particle.

This quantum frictional force is different from the classical frictional phenomenon, where a particle slides above a rough surface, because it originates from the quantum and thermal fluctuations of the electromagnetic fields and it is non-contact. In fact, we will see that the frictional force may not even require a surface. It can occur on a particle moving in vacuum, not in contact or close to any other object. But it is also similar to the classical friction, in that both are nonconservative and cause energy transfer between the particle and the background. At finite temperature, the energy transfer accompanying the quantum frictional force is called the radiative heat transfer. This dissertation is devoted to study the quantum frictional force and radiative heat transfer in some simple backgrounds.

Chapter 1 gives a brief introduction of the historical works which had provided us a road map to enter the fascinating research area of quantum friction. We also remark on the difficulties and possibilities of measuring the quantum frictional effects.

In Chapter 2, we lay out the theoretical foundation for studying quantum frictional effects. The idea is to start with the first principles in classical electrodynamics, namely the Lorentz law for force and Joule heating law for power. Then, we quantize them using the fluctuation-dissipation theorem, which will directly give the quantum frictional force and the rate of radiative heat transfer (quantum frictional power) induced by fluctuations in terms of two important susceptibility tensors: the electromagnetic Green's tensor and the polarizability tensor. Each of

these are discussed in some detail later in the chapter as well.

Starting from Chapter 3 to Chapter 5, we apply the principles introduced in Chapter 2, to calculate the frictional force and radiative heat transfer in different backgrounds. Chapter 3 is devoted to the discussion of the frictional effects in vacuum, the simplest background. But, it also provides a paradigm for discussing frictional effects due to fluctuations in other more complicated backgrounds. The concept of nonequilibrium steady state is introduced in this chapter. The different treatments required for dissipative and nondissipative particles are also discussed. In Chapter 4, a detailed analysis of the quantum friction on an atom moving above a perfectly conducting plate is presented. Here, we emphasize that the contributions to the frictional force from different polarization states exhibit different dependences on distance, temperature and velocity. Interestingly, the contribution from one particular polarization state corresponds to a push instead of a drag on the atom. In Chapter 5, we discuss the friction induced on a particle moving above a dielectric plate with a finite and nondissipative index of refraction. This discussion extends the classic Cherenkov effect in two aspects. First, the particle can be moving outside of the medium and still experience the induced Cherenkov friction. Second, due to the fluctuations, a neutral, polarizable particle can still emit Cherenkov radiation, even though it is not charged.

In the concluding Chapter 6, we summarize the discussions presented in this short thesis and possible extensions for future investigations. We then point out that fluctuations can also induce effects other than quantum frictional forces and radiative heat transfer, especially when nonreciprocity or inhomogeneity is involved. Based on the experimental considerations on temperature and velocity, we give some comments on the challenge for a direct measurement of the frictional force. Finally, we propose that, for a moving nanoparticle, the deviation of its nonequilibrium steady state temperature from the radiation temperature could serve as a feasible signature for detecting the quantum frictional effects.

Chapter 1

Introduction

Fluctuations, once treated being a synonym for noise and merely an unwanted experimental reality, have now taken a prominent place in our understanding of physics, ranging from the van der Waals interaction between neutral atoms and molecules to the expanding universe. More pertinently, fluctuations give rise to all the frictional effects we will be discussing in the present thesis.

In the beginning of 20th century, Max Planck [1, 2] correctly derived the spectrum for the blackbody radiation, which marked the start of quantum mechanics. Crucial in Planck's work is the average energy of a harmonic oscillator in thermal equilibrium with radiation at temperature, T ,

$$U = \frac{\hbar\omega}{e^{\hbar\omega/k_B T} - 1} + \frac{1}{2}\hbar\omega. \quad (1.1)$$

The two terms in the above expression reflect precisely the thermal fluctuation and quantum fluctuation that give rise to the frictional effects which will be discussed in this thesis. Most physicists at the time, including Planck himself, did not believe that the second term, which is also referred to as zero-point energy, corresponded to any physical reality.

There was one famous exception, though. Einstein, at least for a short period of time after Planck's discovery, recognized the physical significance of Planck's zero-point energy. This had to do with his earlier work together with Hopf [3] on the drag force for an oscillating dipole in thermal equilibrium with the electromagnetic fields. Only after introducing a zero-point energy in the internal energy of the

oscillating dipole, Einstein and Stern [4] was able to rederive the correct spectral energy density of radiation, which results in their claim that the existence of a zero-point energy of size $\frac{1}{2}\hbar\nu$ is probable [5].

Based on the existence of a zero-point energy for electromagnetic fields,¹ Casimir, in 1948, was able to derive his famous effect of attraction between two perfectly conducting plate in vacuum [6]. Prior to that, Casimir and Polder had used quantum electrodynamics to calculate the retarded interaction between an atom and a perfectly conducting plate, which is now known as Casimir-Polder force [7]. Casimir, later, was also able to reproduce this Casimir-Polder force using the more radical approach of calculating the change in the electromagnetic zero-point energy [6]. Both the Casimir effect and Casimir-Polder force have been experimentally confirmed [8, 9] and therefore serve as direct physical manifestations of the zero-point energy [10].

Casimir forces are conservative forces between neutral bodies. When motion is involved, a nonconservative force should arise due to zero-point energy as well. Such an idea can be traced back to Ref. [11] or even earlier Refs. [12, 13, 14, 15]. In Ref. [11], Pendry calculated the frictional force between two dissipative surfaces when they are sheared parallel to their surfaces and he was the first to name the frictional force quantum friction.

Not only the zero-point energy (quantum fluctuations) but also the thermal fluctuations can induce frictional forces. In Ref. [16], Mkrtchian and collaborators claim that a universal drag exists on a single particle in relative motion with black-body radiation at finite temperature. Even though the authors had not mentioned it, this frictional force is, in fact, a direct generalization of the Einstein-Hopf drag from a single-frequencied oscillating dipole to a polarizable and intrinsically dissipative particle. Such a connection is made very clear by other authors later, for example, in Refs. [17, 18].

This is also our entry point to quantum friction. Prior to our investigation on quantum friction, we had studied the friction felt by a charged particle [19] as well as by a moving neutral particle carrying either an electric or a magnetic

¹In Milonni's book, Ref. [5], he recorded a private communication from Casimir, where Casimir mentioned that a conversation with Niels Bohr, in which Bohr mumbled something about zero point energy, had put him on a new track.

dipole moment [20]. What serves as a frictional force in these situations is just the classical electromagnetic force given by the Lorentz force law. In Ref. [20], we find, by quantizing our expression for friction on moving classical dipoles, we could obtain Mkrtchian's universal drag or Einstein-Hopf drag. We also notice that, to recover the Einstein-Hopf formula correctly, both dipoles and fields must be properly quantized and each will give a contribution to the total quantum frictional force. These observations guide us to investigate the quantum vacuum friction for a nondissipative atom in Ref. [21] and that for a dissipative nanoparticle in Ref. [22]. For the former case, the dipole fluctuation is induced by the field fluctuation, while, for the latter case, the dipole fluctuation is independent from the field fluctuations. Both of these works [21, 22] feature a fully relativistic treatment of the problem as well as some detailed discussions on the energetics. As a next step, we study the quantum frictional force on a nondissipative atom when it moves parallel to a perfectly conducting plate in Ref. [23]. This friction, though being a transverse component of the famous Casimir-Polder force, seems to not have been explored by others. Such an omission of exploration may be due to the intuition that quantum friction arises only because the image particle inside an imperfect surface lags behind the actual particle [11], which therefore would not arise in the presence of a perfectly conducting surface. However, we have learned that frictional force can arise even without a surface, as in the case for quantum vacuum friction, because the free space filled with blackbody radiation is dissipative and modifies the motion of objects in it [24]. We conclude in Ref. [23] that, not only quantum friction exists in the presence of a perfectly conducting plate, but exhibits interesting dependence on the polarization state of the atom, temperature, velocity and distance (to the plate). One step further, we replace the perfectly conducting plate by a nondissipative dielectric plate with a finite index of refraction and ask how friction arises for a particle moving above such a plate. We find, even at zero temperature, a friction can be induced on a particle moving at a velocity greater than the speed of light in the dielectric. Indeed, this very much resembles the classic Cherenkov effect, except that the particle under investigation moves outside the medium instead of in the medium. The work on this induced Cherenkov friction has not been published in a journal but first appears here in this thesis.

Of course, apart from us, many other authors have also surveyed the exciting field of quantum friction. Here, we do not have room to review all of them but just mention a few that we have learned from. Volokitin and Persson’s discussion on blackbody friction in their book [25] inspired us to study the nonequilibrium steady state temperature of a nanoparticle moving in vacuum [22]. Intravaia et al., in Ref. [26], have studied quantum friction on a nondissipative particle moving above a surface. This is similar to our work in Ref. [21], where the quantum friction is second order in the particle’s intrinsic polarizability. There have also been several recent review articles on the subject [27, 28, 29] from the same group. Pieplow and Henkel’s work on Cherenkov friction in Ref. [30] gives us hints on how to calculate the friction on an isotropic particle in the rest frame of radiation.

Despite the enthusiasm in quantum frictional effects among the theoretical community, these effects have so far eluded a definitive experimental confirmation. The frictional forces seem too small to be within the current experimental reach [31]. In very recent years, renewed optimism has been sparked, though, especially through a proposal that the quantum frictional effects could be probed by measuring the geometric phase induced while a neutral particle travels above an imperfect conductor in vacuum [32, 33]. A concrete experiment was designed, which measures the geometric phase associated with a diamond NV center² placed above a rotating Au-coated or n-doped Si coated disk of a radius of 6 cm, which could be rotated up to a frequency of 7000 /s³. In particular, for the n-doped Si coated disk, the correction of the geometric phase due to the friction becomes detectable at a velocity within the experimental reach. We, therefore, could remain hopeful for the detection of the quantum frictional effects, perhaps even in the near future [34].

²The NV center consists of a vacancy, or missing carbon atom in the diamond lattice, lying next to a nitrogen atom which has substituted one of the nearest neighbors of the vacancy [34].

³The maximum linear velocity obtained on the edge of the disk is, therefore, 2640 m/s.

Chapter 2

Theoretical Minimum

In this thesis, we study quantum frictional effects, the frictional (parallel to the direction of motion) force or radiative heat transfer for a moving polarizable particle which possesses neither any charge nor any intrinsic dipole moment. Of course, a polarizable particle can still be polarized under the influence of some external field. More extraordinarily, when fluctuations are taken into account, a polarizable particle can be polarized even in the absence of any external fields. It is precisely these fluctuations that account for the quantum frictional effects we discuss here.

In this chapter, we provide the approach we take for calculating the quantum frictional force and radiative heat transfer. In Sec. 2.1, we start by reviewing first principles, namely the Lorentz force law and the Joule heating law, encountered in classical electrodynamics. Applying these principles to calculate the electromagnetic force and power on a uniformly moving dipole, we find they can both be recast into the form of the principle of virtual work. That is, both the force and the power can be obtained by differentiating a free energy. In Sec. 2.2, we introduce a most powerful tool to quantize the first-principle forces and powers—the fluctuation dissipation theorem (FDT). Some important historical works on FDT are briefly summarized here, though the list is incomplete. We first derive the simplest form of FDT for the case where the response of the system is described simply by a scalar function. Later, we generalize the obtained relation to the case of a vector field. In Sec. 2.3, we quantize the particle-radiation system by applying the proper form of FDT. In particular, FDT relation, which links field fluctuations with the electromagnetic Green’s tensor, and the FDT, which links dipole fluctuations with

the polarizability tensor, are derived. Sec. 2.4 is devoted to a detailed account of the electromagnetic tensor, which includes its symmetry, equation of motion, along with useful forms of the tensor in vacuum and for planar geometry. In Sec. 2.5, we discuss the polarizability tensor both for a nanoparticle and an atom.

In all formulas throughout this chapter, we will set the speed of light, c to be 1, but keep the reduced Planck constant, \hbar , whenever it appears, to emphasize the quantum nature of the relations.

2.1 First Principles

We are already familiar with how to calculate the electromagnetic force and power in the classical realm.

The electromagnetic force on a system could be obtained by integrating the Lorentz force density over space. This is the famous Lorentz force law (LFL):

$$\mathbf{F}(t) = \int d\mathbf{r} [\rho(t, \mathbf{r})\mathbf{E}(t, \mathbf{r}) + \mathbf{j}(t, \mathbf{r}) \times \mathbf{B}(t, \mathbf{r})]. \quad (2.1)$$

On the other hand, the electromagnetic power or the rate of radiative heat transfer into a system could be calculated using the Joule heating law (JHL),

$$P(t) = \int d\mathbf{r} \mathbf{j}(t, \mathbf{r}) \cdot \mathbf{E}(t, \mathbf{r}). \quad (2.2)$$

To apply these first principles, the charge and current densities of the configuration, ρ and \mathbf{j} , need to be specified.

In this thesis, we are interested in frictional effects. So, naturally, we are concerned with a particle moving in some background. We will also assume uniform motion so as to avoid the complicated issue of acceleration radiation [35]. Classically, the simplest source is a uniformly moving charged particle, say, an electron. Intuitively, the source (charge and current) densities can be written down as

$$\rho_e(t, \mathbf{r}) = e\delta(\mathbf{r} - \mathbf{v}t), \quad \mathbf{j}_e(t, \mathbf{r}) = e\mathbf{v}\delta(\mathbf{r} - \mathbf{v}t). \quad (2.3)$$

When these are inserted into Eq. (2.1) and Eq. (2.2), we find, for the moving

electron, the Lorentz force on it,

$$\mathbf{F}_e(t) = e[\mathbf{E}(t, \mathbf{vt}) + \mathbf{v} \times \mathbf{B}(t, \mathbf{vt})], \quad (2.4)$$

and the rate of electromagnetic work done on it,

$$P_e(t) = e\mathbf{v} \cdot \mathbf{E}(t, \mathbf{vt}). \quad (2.5)$$

More relevant to most of the considerations in the thesis, however, is a uniformly moving particle which possesses intrinsic dipole moments. For generality, let us assume the particle to carry an electric dipole moment, \mathbf{d} , and a magnetic dipole moment, $\boldsymbol{\mu}$, both being time-dependent. Now, the source densities, ρ and \mathbf{j} should be inferred from the electric polarization field, \mathbf{P} , and the magnetic polarization field, \mathbf{M} , due to the moving dipoles,

$$\begin{aligned} \mathbf{P}(t, \mathbf{r}) &= [\mathbf{d}(t) - \boldsymbol{\mu}(t) \times \mathbf{v}] \delta(\mathbf{r} - \mathbf{vt}), \\ \mathbf{M}(t, \mathbf{r}) &= [\boldsymbol{\mu}(t) + \mathbf{d}(t) \times \mathbf{v}] \delta(\mathbf{r} - \mathbf{vt}). \end{aligned} \quad (2.6)$$

In general, the source densities are related to the more fundamental field quantities via

$$\rho(t, \mathbf{r}) = -\boldsymbol{\nabla} \cdot \mathbf{P}(t, \mathbf{r}), \quad \mathbf{j}(t, \mathbf{r}) = \boldsymbol{\nabla} \times \mathbf{M}(t, \mathbf{r}) + \frac{\partial}{\partial t} \mathbf{P}(t, \mathbf{r}), \quad (2.7)$$

which can be easily derived by isolating the source terms in the Maxwell equations. It can be easily check that the source densities so constructed will automatically satisfy the continuity equation, $\partial_t \rho + \boldsymbol{\nabla} \cdot \mathbf{j} = 0$.¹

We find, for a moving dipolar particle, the charge density to be

$$\rho_d(t, \mathbf{r}) = [-\mathbf{d}(t) \cdot \boldsymbol{\nabla} + \boldsymbol{\mu}(t) \times \mathbf{v} \cdot \boldsymbol{\nabla}] \delta(\mathbf{r} - \mathbf{vt}), \quad (2.8)$$

¹Note, however, for a given charge density, the current density is only defined through the continuity equation up to a total curl, because it is only its divergence that enters the continuity equation. On the contrary, deriving the source densities from the more fundamental polarization fields leaves no such ambiguity.

and the current density to be

$$\mathbf{j}_d(t, \mathbf{r}) = \left[\dot{\mathbf{d}}(t) - \mathbf{v} \mathbf{d}(t) \cdot \nabla + \nabla \times \boldsymbol{\mu}(t) - \dot{\boldsymbol{\mu}}(t) \times \mathbf{v} + \boldsymbol{\mu}(t) \times \mathbf{v} (\mathbf{v} \cdot \nabla) \right] \delta(\mathbf{r} - \mathbf{vt}). \quad (2.9)$$

In reality, it is usually a good approximation to neglect the magnetic properties.² We will therefore most often use the source densities in Eq. (2.8) and Eq. (2.9) without the terms involving $\boldsymbol{\mu}$ and drop the subscript on them,

$$\rho(t, \mathbf{r}) = -\mathbf{d}(t) \cdot \nabla \delta(\mathbf{r} - \mathbf{vt}), \quad \mathbf{j}(t, \mathbf{r}) = \left[\dot{\mathbf{d}}(t) - \mathbf{v} \mathbf{d}(t) \cdot \nabla \right] \delta(\mathbf{r} - \mathbf{vt}). \quad (2.10)$$

Let us now insert the source densities in Eq. (2.10) into Eq. (2.1) to find out the force on a moving electric dipole,

$$\mathbf{F}(t) = \mathbf{d}(t) \cdot \nabla \mathbf{E}(t, \mathbf{vt}) + \mathbf{d}(t) \cdot \nabla [\mathbf{v} \times \mathbf{B}(t, \mathbf{vt})] + \dot{\mathbf{d}}(t) \times \mathbf{B}(t, \mathbf{vt}). \quad (2.11)$$

The second term in Eq. (2.11) can be written as

$$\begin{aligned} \mathbf{d}(t) \cdot \nabla [\mathbf{v} \times \mathbf{B}(t, \mathbf{vt})] &= -\mathbf{d}(t) \times [\nabla \times (\mathbf{v} \times \mathbf{B}(t, \mathbf{vt}))] + \nabla [\mathbf{d}(t) \cdot (\mathbf{v} \times \mathbf{B}(t, \mathbf{vt}))] \\ &= \mathbf{d}(t) \times [\mathbf{v} \cdot \nabla \mathbf{B}(t, \mathbf{vt})] + \nabla [\mathbf{d}(t) \cdot (\mathbf{v} \times \mathbf{B}(t, \mathbf{vt}))], \end{aligned} \quad (2.12)$$

where we have used $\nabla \cdot \mathbf{B} = 0$ in the second equality. The third term in Eq. (2.11) can be written as

$$\dot{\mathbf{d}}(t) \times \mathbf{B}(t, \mathbf{vt}) = \frac{d}{dt} [\mathbf{d}(t) \times \mathbf{B}(t, \mathbf{vt})] - \mathbf{d}(t) \times \frac{\partial}{\partial t} \mathbf{B}(t, \mathbf{vt}) - \mathbf{d}(t) \times [\mathbf{v} \cdot \nabla \mathbf{B}(t, \mathbf{vt})], \quad (2.13)$$

where the middle term can be broken into two pieces with the use of Faraday's law,

$$-\mathbf{d}(t) \times \frac{\partial}{\partial t} \mathbf{B}(t, \mathbf{vt}) = \mathbf{d}(t) \times [\nabla \times \mathbf{E}(t, \mathbf{vt})] = \nabla [\mathbf{d}(t) \cdot \mathbf{E}(t, \mathbf{vt})] - \mathbf{d}(t) \cdot \nabla \mathbf{E}(t, \mathbf{vt}). \quad (2.14)$$

When we put Eqs. (2.12)–(2.14) back into Eq. (2.11), several terms cancel and only

²For the study of the fluctuation-induced effects, we will be considering polarizable particles which do not carry intrinsic dipole moments. For these particles, we can ignore the magnetic terms in the polarization sources because the magnetic polarizability is typically several orders of magnitude smaller than the electric polarizability. As a specific comparison, see Ref. [36] for the example of a neon atom.

three terms remain in the expression for the Lorentz force:

$$\mathbf{F}(t) = \nabla [\mathbf{d}(t) \cdot \mathbf{E}(t, \mathbf{vt})] + \nabla [(\mathbf{d}(t) \times \mathbf{v}) \cdot \mathbf{B}(t, \mathbf{vt})] + \frac{d}{dt} [\mathbf{d}(t) \times \mathbf{B}(t, \mathbf{vt})]. \quad (2.15)$$

Now, the total Lorentz force on a moving dipole can be written as a sum of a total spatial derivative and a total time derivative

$$\mathbf{F}(t) = -\nabla \mathcal{F} + \frac{d}{dt} \mathcal{I}, \quad (2.16)$$

where \mathcal{F} is the interaction free energy of the dipole-field system,

$$\mathcal{F} = -\mathbf{d}(t) \cdot \mathbf{E}(t, \mathbf{vt}) - \mathbf{d}(t) \times \mathbf{v} \cdot \mathbf{B}(t, \mathbf{vt}), \quad (2.17)$$

and \mathcal{I} is the Röntgen momentum of the dipole-field system [37],

$$\mathcal{I} = \mathbf{d}(t) \times \mathbf{B}(t, \mathbf{vt}). \quad (2.18)$$

Note in the expression Eq. (2.17) for the free energy, the second term is like the interaction energy of a magnetic dipole in magnetic field if we deem $\boldsymbol{\mu}_v(t) = \mathbf{d}(t) \times \mathbf{v}$ as the magnetic dipole moment induced by the motion of the electric dipole moment carried by the particle, even though we have not considered any intrinsic magnetic dipole moment of the particle. In addition, the total time derivative term in the classical electromagnetic force Eq. (2.16) always drops in the calculation of quantum frictional force, because it is always time independent upon quantization using the fluctuation-dissipation theorem (FDT). We are then left with only the term containing the spatial derivative of the free energy,

$$\mathbf{F}(t) = -\nabla \mathcal{F}, \quad (2.19)$$

which is simply the statement of the principle of virtual work (PVW).

Now we turn to calculate the electromagnetic power or the rate of radiative heat transfer. When the current in Eq. (2.10) is inserted into the JHL Eq. (2.2), we

obtain the power

$$P(t) = \dot{\mathbf{d}}(t) \cdot \mathbf{E}(t, \mathbf{vt}) + [\mathbf{d}(t) \cdot \nabla] [\mathbf{v} \cdot \mathbf{E}(t, \mathbf{vt})], \quad (2.20)$$

where the first term can be rewritten as

$$\dot{\mathbf{d}}(t) \cdot \mathbf{E}(t, \mathbf{vt}) = \frac{d}{dt} [\mathbf{d}(t) \cdot \mathbf{E}(t, \mathbf{vt})] - \mathbf{d}(t) \cdot \frac{\partial}{\partial t} \mathbf{E}(t, \mathbf{vt}) - [\mathbf{v} \cdot \nabla] [\mathbf{d}(t) \cdot \mathbf{E}(t, \mathbf{vt})]. \quad (2.21)$$

Note the second term of Eq. (2.20) and the last term of Eq. (2.21) combine and give

$$\begin{aligned} [\mathbf{d}(t) \cdot \nabla] [\mathbf{v} \cdot \mathbf{E}(t, \mathbf{vt})] - [\mathbf{v} \cdot \nabla] [\mathbf{d}(t) \cdot \mathbf{E}(t, \mathbf{vt})] &= [\mathbf{d}(t) \times \mathbf{v}] \cdot [\nabla \times \mathbf{E}(t, \mathbf{vt})] \\ &= - [\mathbf{d}(t) \times \mathbf{v}] \cdot \frac{\partial}{\partial t} \mathbf{B}(t, \mathbf{vt}), \end{aligned} \quad (2.22)$$

where we have used the Faraday's law in the last equality. As a result, the power is written as

$$P(t) = \frac{d}{dt} [\mathbf{d}(t) \cdot \mathbf{E}(t, \mathbf{vt})] - \mathbf{d}(t) \cdot \frac{\partial}{\partial t} \mathbf{E}(t, \mathbf{vt}) - [\mathbf{d}(t) \times \mathbf{v}] \cdot \frac{\partial}{\partial t} \mathbf{B}(t, \mathbf{vt}). \quad (2.23)$$

The total time derivative term in Eq. (2.23) still will not contribute to the quantum frictional power upon quantization using FDT. The next two terms in Eq. (2.23) each contains a partial time derivative of a term in the interaction free energy in Eq. (2.17). We can then write the power, P , as a time derivative of the free energy, \mathcal{F} , with a special prescription that only the time coordinates in the fields are to be differentiated,

$$P(t) = \frac{\partial}{\partial t} \mathcal{F} = - \frac{\partial}{\partial t_1} [\mathbf{d}(t_0) \cdot \mathbf{E}(t_1, \mathbf{vt}) + \boldsymbol{\mu}_v(t_0) \cdot \mathbf{B}(t_1, \mathbf{vt})] \Big|_{t_0=t_1 \rightarrow t}, \quad (2.24)$$

where, again, we have identified $\mathbf{d}(t) \times \mathbf{v} = \boldsymbol{\mu}_v(t)$ as the magnetic dipole moment induced by the movement of the electric dipole moment. This, perhaps, can be deemed as a PVW, concerning a virtual time displacement rather than a spatial displacement.

We therefore have shown that the quantum frictional force and power can be generated from an interaction free energy in Eq. (2.17) and that the LFL and JHL

can be cast in a form of a PVW for a moving dipolar particle.

2.2 Fluctuation-Dissipation Theorem

We devote this section to an introduction of the fluctuation-dissipation theorem (FDT). The symmetrized correlation function gives a measure to fluctuations. The generalized susceptibility encodes dissipation of a system. The FDT establishes a profound relation between dissipation and fluctuation by connecting the symmetrized correlation function with the generalized susceptibility. Here, we prove the relation by expressing both in terms of the (nonsymmetrized, that is, ordered) correlation function.

The FDT enjoys a happy history of side-by-side efforts between experiment and theory. It starts with Johnson’s observation that the fluctuation of the potential over a conductor is proportional to the resistance and the temperature of the conductor [38]. Nyquist [39] almost simultaneously gave a theoretical explanation of the observation and realized the the direct proportionality to temperature reflects the high temperature limit of the Bose-Einstein distribution factor. Callen and Welton [40] generalized the then “Nyquist relation” to a general dissipative system and provided a more rigorous derivation of the generalized relation based on the perturbation theory of quantum mechanics. They also gave a number of interesting applications, including dipole radiation, which is directly related to the context of this thesis. These generalized Nyquist relations connect the response of a system under a disturbance to the fluctuation within the system in the absence of the disturbanc. Kubo realized that they actually provide an approach to calculate certain quantities, e.g., admittance or kinetic coefficients, in nonequilibrium states, in terms of fluctuations in equilibrium [41]. Therefore, all these relations can be summed up under the name of the fluctuation-dissipation theorem [42].

The FDT is based on the linear response assumption that the system is subject to a perturbation linear to the response operator, x , coupled to an influence function, f ,

$$H = H_0 + H_I(t), \quad H_I(t) = -x(t)f(t), \quad (2.25)$$

where H_0 is the unperturbed Hamiltonian.³ At the initial time, the system is without perturbation, $f(-\infty) = 0$, and is in thermal equilibrium,

$$\rho_0 = \rho(-\infty) = \frac{e^{-\beta H_0}}{Z}, \quad Z = \text{tr} e^{-\beta H_0}, \quad (2.26)$$

where β is the inverse temperature. The presence of the perturbation, however, can drive the system out of equilibrium. It follows from first order perturbation theory that,

$$\rho(t) = \rho_0 + \frac{i}{\hbar} \int_{-\infty}^t dt' f(t') [x(t'), \rho_0]. \quad (2.27)$$

Multiplying the above equation by $x(t)$ and then taking the trace, we find the deviation of the expectation value of the response operator from its equilibrium value to be

$$\langle x(t) \rangle_{\rho(t)} - \langle x(t) \rangle_{\rho_0} = \int_{-\infty}^{\infty} dt' \chi(t-t') f(t'). \quad (2.28)$$

Here, χ is the generalized susceptibility function, which is directly related to the commutator of the response operator at different times:

$$\chi(t-t') = \frac{i}{\hbar} \theta(t-t') \langle [x(t), x(t')] \rangle_{\rho_0}, \quad (2.29)$$

where $\theta(t-t')$ is the Heaviside function. This relation manifestly reflects the fact that the response occurs later than the influence. Note the generalized susceptibility in (space)time coordinates is purely real, which follows from the fact that the commutator of two Hermitian operators is anti-Hermitian.

Now, under the linear response assumption, the response, which describes how the system responds to the perturbation, can be determined by the properties in equilibrium [42]. Let us make one more simplification here by setting $\langle x(t) \rangle_{\rho_0} = 0$. We are allowed to do this because the expectation value of any operator at equilibrium is a known constant, which can always be absorbed in the definition of the operator.⁴ As a result, Eq. (2.29) can be written in a cleaner form in the

³Here, equations of motion are all written in the interaction picture, where the time dependence of the operator is governed by H_0 , $x(t) = e^{iH_0 t/\hbar} x e^{-iH_0 t/\hbar}$, while the state evolve under H_I only, $i\hbar d\rho/dt = [H_I(t), \rho(t)]$. We choose the (Schrödinger, Heisenberg, interaction) pictures to all coincide at $t = 0$. Any conclusion regarding the expectation values, of course, is independent of the picture.

⁴Also, in the context of this thesis, the expectation value of the response operator is in fact always zero, so that the effects are solely given rise from the fluctuations.

frequency domain,

$$\langle x(\omega) \rangle_{\rho_0} = \chi(\omega) f(\omega), \quad (2.30)$$

where $\chi(\omega)$ is the Fourier transform of $\chi(t-t')$ in Eq. (2.29). Suppose we know the spectrum of the unperturbed system, i.e.,

$$H_0 |n\rangle = E_n |n\rangle, \quad (2.31)$$

then, we can derive an explicit expression for the susceptibility in frequency space:

$$\chi(\omega) = -\frac{1}{\hbar} \lim_{\eta \rightarrow 0^+} \sum_{n,m} \frac{(e^{-\beta E_n} - e^{-\beta E_m})}{Z} \frac{|\langle n|x|m\rangle|^2}{\omega + \omega_{nm} + i\eta}, \quad (2.32)$$

where $\omega_{nm} = (E_n - E_m)/\hbar$ is the resonance frequency corresponding to the transition between two internal energy levels of the system. And only at these resonance frequencies,⁵ will the susceptibility develop an imaginary part,

$$\text{Im } \chi(\omega) = \frac{\pi}{\hbar} \sum_{n,m} \frac{(e^{-\beta E_n} - e^{-\beta E_m})}{Z} |\langle n|x|m\rangle|^2 \delta(\omega + \omega_{nm}). \quad (2.33)$$

At other frequencies, the susceptibility is real, and in particular, its static value is

$$\chi(0) = -\sum_{n,m} \frac{(e^{-\beta E_n} - e^{-\beta E_m})}{Z} \frac{|\langle n|x|m\rangle|^2}{E_n - E_m}. \quad (2.34)$$

Now, we turn to quantify the fluctuation. Consider first the (nonsymmetrized, that is, ordered) correlation function of the response operator x at different times

$$C(t, t') = \langle x(t)x(t') \rangle_{\rho_0}. \quad (2.35)$$

The correlation function defined in Eq. (2.35) possesses time-translational invariance,

$$C(t, t') = C(t - t', 0) = C(t - t'), \quad (2.36)$$

which can be easily checked employing the cyclic property of the trace operation.

Another important property of the correlation function concerns the complex con-

⁵Of course, actual resonances have finite width, in which case, the susceptibility develops imaginary part at off-resonant frequencies.

jugate of it,

$$C(\tau)^* = C(-\tau), \quad (2.37)$$

to prove which we have assumed that the response operator x is Hermitian. The most crucial ingredient to the proof of FDT is the Kubo-Martin-Schwinger (KMS) relation [43],

$$\begin{aligned} C(-\tau) &= \frac{1}{Z} \text{tr } x(0)x(\tau)e^{-\beta H_0} = \frac{1}{Z} \text{tr } x(0)e^{iH_0\tau/\hbar}x(0)e^{-iH_0\tau/\hbar}e^{-\beta H_0} \\ &= \frac{1}{Z} \text{tr } x(0)e^{-\beta H_0}x(\tau - i\hbar\beta) = \frac{1}{Z} \text{tr } x(\tau - i\hbar\beta)x(0)e^{-\beta H_0} \\ &= C(\tau - i\hbar\beta). \end{aligned} \quad (2.38)$$

The best measure for fluctuation is, however, the symmetrized correlation function defined as follows,

$$S(t - t') = \frac{1}{2}[C(t - t') + C(t' - t)]. \quad (2.39)$$

Using the KMS relation, the Fourier transform of $S(t - t')$ is connected to the Fourier transform of $C(t - t')$ via

$$S(\omega) = \frac{1}{2}C(\omega)(1 + e^{-\beta\hbar\omega}). \quad (2.40)$$

On the other hand, the generalized susceptibility in Eq. (2.29) can also be expressed in terms of the correlation function,

$$\chi(t - t') = \frac{i}{\hbar}\theta(t - t')[C(t - t') - C(t' - t)] \quad (2.41)$$

With the help of properties Eq. (2.37) and Eq. (2.39), we find the imaginary part of the Fourier transform of $\chi(t - t')$ is

$$\text{Im } \chi(\omega) = \frac{\chi(\omega) - \chi(\omega)^*}{2i} = \frac{1}{2\hbar}C(\omega)(1 - e^{-\beta\hbar\omega}). \quad (2.42)$$

Comparing Eq. (2.40) and Eq. (2.42), we arrive at the FDT in its simplest form:

$$S(\omega) = \hbar \text{Im } \chi(\omega) \coth\left(\frac{\beta\hbar\omega}{2}\right). \quad (2.43)$$

The zero temperature (quantum) and high temperature (thermal, classical) limits of Eq. (2.43) are

$$S(\omega) = \begin{cases} \hbar \operatorname{sgn}(\omega) \operatorname{Im} \chi(\omega), & T \rightarrow 0 \\ \frac{2}{\beta\omega} \operatorname{Im} \chi(\omega), & T \rightarrow \infty. \end{cases} \quad (2.44)$$

Notice $S(\omega)$ is directly proportional to \hbar at zero temperature, while \hbar drops out in the high temperature limit.

In deriving the FDT shown in Eq. (2.43), we have been making several simplifying assumptions. The problems we will explore in later chapters call for at least two generalizations of the simplest scenario already discussed. First, both the response and the influence can be vectors, which then requires a tensor susceptibility,

$$\langle \mathbf{x}(\omega) \rangle_{\rho_0} = \boldsymbol{\chi}(\omega) \cdot \mathbf{f}(\omega). \quad (2.45)$$

Further, the response and the influence can be fields that depend on spatial coordinates, which in general results in a nonlocal susceptibility,

$$\langle \mathbf{x}(\omega; \mathbf{r}) \rangle_{\rho_0} = \int d\mathbf{r}' \boldsymbol{\chi}(\omega; \mathbf{r}, \mathbf{r}') \cdot \mathbf{f}(\omega; \mathbf{r}'). \quad (2.46)$$

We shall now see how the FDT in Eq. (2.42) should be modified for a vector field response. We will still assume that the operator is Hermitian.

The correlation function now becomes tensor which depend on two sets of space-time coordinates. Explicitly, we write out its component as

$$C_{ij}(t, \mathbf{r}; t', \mathbf{r}') = \langle x_i(t, \mathbf{r}) x_j(t', \mathbf{r}') \rangle_{\rho_0}. \quad (2.47)$$

The translational symmetry, the conjugate relation and the KMS relation for the correlation function in Eq. (2.47) now read

$$C_{ij}(t, \mathbf{r}; t', \mathbf{r}') = C_{ij}(t - t'; \mathbf{r}, \mathbf{r}'), \quad (2.48a)$$

$$C_{ij}(t - t'; \mathbf{r}, \mathbf{r}')^* = C_{ji}(t' - t; \mathbf{r}', \mathbf{r}), \quad (2.48b)$$

$$C_{ji}(t' - t; \mathbf{r}', \mathbf{r}) = C_{ij}(t - t' - i\hbar\beta; \mathbf{r}, \mathbf{r}'). \quad (2.48c)$$

The translational symmetry in time again follows from the cyclic property of the trace operation, and is always satisfied. However, we have not invoked the translational symmetry in space, because it is often broken. It is only strictly valid for vacuum and approximately valid for systems that are homogeneous, and without boundaries.⁶ Simple boundaries, like a planar surface or spherical surface, can partially break the spatial translational symmetry in their normal directions, leaving the symmetries in other directions intact.

The symmetrized correlation function is now defined as

$$S_{ij}(t - t'; \mathbf{r}, \mathbf{r}') = \frac{1}{2}[C_{ij}(t - t'; \mathbf{r}, \mathbf{r}') + C_{ji}(t' - t; \mathbf{r}', \mathbf{r})]. \quad (2.49)$$

With the KMS relation, we can verify again its connection with the nonsymmetrized correlation function:

$$S_{ij}(\omega; \mathbf{r}, \mathbf{r}') = \frac{1}{2}C_{ij}(\omega; \mathbf{r}, \mathbf{r}')(1 + e^{-\beta\hbar\omega}). \quad (2.50)$$

The susceptibility also becomes a tensor which is nonlocal in spatial coordinates

$$\chi_{ij}(t - t'; \mathbf{r}, \mathbf{r}') = \frac{i}{\hbar}\theta(t - t')[C_{ij}(t - t'; \mathbf{r}, \mathbf{r}') - C_{ji}(t' - t; \mathbf{r}', \mathbf{r})]. \quad (2.51)$$

Now, we calculate the Fourier transform of its anti-Hermitian part, in contrast to the ordinary imaginary part, and find

$$\Im\chi_{ij}(\omega; \mathbf{r}, \mathbf{r}') = \frac{\chi_{ij}(\omega; \mathbf{r}, \mathbf{r}') - \chi_{ji}(\omega; \mathbf{r}', \mathbf{r})^*}{2i} = \frac{1}{2\hbar}C_{ij}(\omega; \mathbf{r}, \mathbf{r}')(1 - e^{-\beta\hbar\omega}). \quad (2.52)$$

Apparently, a generalized version of the FDT in Eq. (2.43) is still respected between the components of the symmetrized correlation tensor and the anti-Hermitian part of the susceptibility tensor,

$$S_{ij}(\omega; \mathbf{r}, \mathbf{r}') = \hbar\Im\chi_{ij}(\omega; \mathbf{r}, \mathbf{r}') \coth\left(\frac{\beta\hbar\omega}{2}\right). \quad (2.53)$$

⁶It, for example, constitutes a decent approximation for crystals when the required resolution is above the atomic distances within the crystal. [44]

Thus, we obtain the FDT for responses which are vector fields. For a more detailed account, see the Appendixes on FDT in Ref. [45] ⁷.

If there does exist translational symmetry in space, the FDT relation can be further transformed into the momentum space as

$$S_{ij}(\omega, \mathbf{k}) = \hbar \Im \chi_{ij}(\omega, \mathbf{k}) \coth \left(\frac{\beta \hbar \omega}{2} \right). \quad (2.54)$$

More explicitly, the anti-Hermitian part of the susceptibility tensor in frequency-momentum domain is ⁸

$$\Im \chi_{ij}(\omega, \mathbf{k}) = \frac{\chi_{ij}(\omega, \mathbf{k}) - \chi_{ji}(\omega, \mathbf{k})^*}{2i} = \frac{\chi_{ij}(\omega, \mathbf{k}) - \chi_{ji}(-\omega, -\mathbf{k})}{2i}, \quad (2.55)$$

where we have used $\chi(\omega, \mathbf{k})^* = \chi(-\omega, -\mathbf{k})$, a fact which follows from the reality of χ in spacetime domain.

What directly occurs in the calculation we will perform in this thesis is often the correlation between two Fourier components of the response. If we directly Fourier transform both of the two sets of spacetime coordinates in Eq. (2.47), we find

$$\langle x_i(\omega, \mathbf{k}) x_j(\nu, \bar{\mathbf{k}}) \rangle_{\rho_0} = (2\pi)^4 \delta(\omega + \nu) \delta(\mathbf{k} + \bar{\mathbf{k}}) C_{ij}(\omega, \mathbf{k}), \quad (2.56)$$

and a similar relation holds for the symmetrized product of the response. We may then rewrite Eq. (2.54) as

$$\langle S x_i(\omega, \mathbf{k}) x_j(\nu, \bar{\mathbf{k}}) \rangle_{\rho_0} = (2\pi)^4 \delta(\omega + \nu) \delta(\mathbf{k} + \bar{\mathbf{k}}) \hbar \Im \chi_{ij}(\omega, \mathbf{k}) \coth \left(\frac{\beta \hbar \omega}{2} \right), \quad (2.57)$$

where S dictates that the product of the response operators be symmetrically ordered, $\langle S x_i x_j \rangle = \langle x_i x_j + x_j x_i \rangle / 2$.

⁷Note in Ref. [45], the authors did not include $\theta(t - t')$ in the definition of susceptibility.

⁸Note that we have deliberately placed the star symbol after the arguments of the susceptibility. This is to emphasize that the complex conjugate is always taken after the Fourier transform, instead of otherwise.

2.3 Quantization

In Sec. 2.1, we have reviewed the classical formulas for electromagnetic force and power. In Sec. 2.2, we have briefly introduced the FDT. Here, in this section, we will learn how to apply the FDT for dipole and field operators occurring in the expressions for force and power. After applying FDT properly, these formulas are quantized automatically and ready for use in the later calculations.

The system we will consider always consist of a particle and the radiation field. Each of them have their own free Hamiltonian, H_P and H_R . The interaction of the two provides a perturbation term which can be written in a form as

$$H_I(t) = - \int d\mathbf{r} \mathbf{P}(t, \mathbf{r}) \cdot \mathbf{E}(t, \mathbf{r}), \quad (2.58)$$

where \mathbf{P} stands for the polarization field caused by the particle. As a result of the interaction, the particle will respond to the radiation field and vice versa. Recalling Eq. (2.46), the responses are connected to the influence (source) via the corresponding susceptibilities,

$$\begin{aligned} \langle \mathbf{P}(\omega; \mathbf{r}) \rangle &= \int d\mathbf{r}' \chi(\omega; \mathbf{r}, \mathbf{r}') \cdot \mathbf{E}(\omega; \mathbf{r}') \\ \langle \mathbf{E}(\omega; \mathbf{r}) \rangle &= \int d\mathbf{r}' \Gamma(\omega; \mathbf{r}, \mathbf{r}') \cdot \mathbf{P}(\omega; \mathbf{r}'), \end{aligned} \quad (2.59)$$

where we have omitted the subscript ρ_0 for the expectation value. The susceptibility χ will be determined by the internal dynamics of the particles. The electromagnetic Green's tensor, Γ , will be determined only by the boundary conditions, since we have presumed that no other source than the particle exists in the configuration. (These could be hard boundaries like a perfect conductor or soft boundaries given by some macroscopic matter in the configuration.)

Reminiscent of Eq. (2.53), we may write down the FDT which relates the fluctuations of \mathbf{P} and \mathbf{E} fields in equilibrium with the corresponding susceptibilities as follows:

$$\langle S\mathbf{P}'(\omega'; \mathbf{r}')\mathbf{P}'(\nu', \tilde{\mathbf{r}}') \rangle = (2\pi)\delta(\omega' + \nu')\hbar\Im\chi'(\omega'; \mathbf{r}', \tilde{\mathbf{r}}') \coth\left(\frac{\beta_P\hbar\omega'}{2}\right), \quad (2.60a)$$

$$\langle S\mathbf{E}(\omega; \mathbf{r})\mathbf{E}(\nu, \tilde{\mathbf{r}}) \rangle = (2\pi)\delta(\omega + \nu)\hbar\mathfrak{S}\Gamma(\omega; \mathbf{r}, \tilde{\mathbf{r}}) \coth\left(\frac{\beta_{\mathcal{R}}\hbar\omega}{2}\right). \quad (2.60b)$$

Whenever relative motion between the particles and the system is involved, it is important to specify with respect to which frame is the physical quantity measured. Note that all quantities appearing in Eq. (2.60a) refer to the rest frame of the particle, \mathcal{P} , and are denoted with a prime, while those in Eq. (2.60b) refer to the reference frame of the radiation, \mathcal{R} , and are all unprimed. Such notations will be invoked whenever needed throughout the paper.

Now consider a point particle. In its rest frame, the polarization field caused by such a particle located at origin is $\mathbf{P}'(\omega'; \mathbf{r}') = \mathbf{d}'(\omega')\delta(\mathbf{r}')$. When this is plugged into Eq. (2.60a), we find fluctuation of the dipole moments, \mathbf{d} , localized at the position of the particle,

$$\langle S\mathbf{d}'(\omega')\mathbf{d}'(\nu') \rangle = 2\pi\delta(\omega' + \nu')\hbar\mathfrak{S}\alpha'(\omega') \coth\left(\frac{\beta_{\mathcal{P}}'\hbar\omega'}{2}\right), \quad (2.61)$$

where α' is the polarizability of a point particle defined in its rest frame and is connected to χ' via

$$\chi'(\omega'; \mathbf{r}', \tilde{\mathbf{r}}') = \alpha'(\omega')\delta(\mathbf{r}')\delta(\tilde{\mathbf{r}}'). \quad (2.62)$$

As commented earlier, the spatial translational symmetry is not always guaranteed. The translational symmetry could be broken by boundaries or involvement of inhomogeneous materials in the configuration. In fact, in this thesis, apart from the vacuum case, we will often consider planar geometries where only one of the spatial direction, say z , is not translational invariant. This allows us to Fourier transform the transverse coordinates, x and y , but keep the z coordinates in the field operators from being transformed. For example, for the field operators, the FDT relation can be written as

$$\langle S\mathbf{E}(\omega, \mathbf{k}_{\perp}; z)\mathbf{E}(\nu, \bar{\mathbf{k}}_{\perp}; \tilde{z}) \rangle = (2\pi)^3\delta(\omega + \nu)\delta(\mathbf{k}_{\perp} + \bar{\mathbf{k}}_{\perp})\hbar\mathfrak{S}\Gamma(\omega, \mathbf{k}_{\perp}; z, \tilde{z}) \coth\left(\frac{\beta_{\mathcal{R}}\hbar\omega}{2}\right), \quad (2.63)$$

where \perp refers to the transverse directions that possess translational symmetry.

Finally, it is often advantageous to perform calculations in the rest frame of the particle, \mathcal{P} , because the free energy in that frame takes a simpler form. But we have to be careful in applying the FDT for the field in that frame. First of all, the

Green's tensor should be transformed from the rest frame of radiation, \mathcal{R} , to frame \mathcal{P} . Second, the argument of coth factor is no longer isotropic written in terms of frequency and momentum in frame \mathcal{P} . We will always, in this thesis, without loss of generality, assume the particle to be moving in the x direction, with velocity $\mathbf{v} = v\hat{x}$ relative to the radiation. Transforming Eq. (2.63) to frame \mathcal{P} , the FDT now should read

$$\langle S\mathbf{E}'(\omega', \mathbf{k}'_{\perp}; z')\mathbf{E}'(\nu', \bar{\mathbf{k}}'_{\perp}; \bar{z}') \rangle = (2\pi)^4 \delta(\omega' + \nu') \delta(\mathbf{k}'_{\perp} + \bar{\mathbf{k}}'_{\perp}) \hbar \Im \Gamma'(\omega', \mathbf{k}'_{\perp}; z', \bar{z}') \coth\left(\frac{\beta_R \hbar \gamma(\omega' + k'_x v)}{2}\right). \quad (2.64)$$

Note that the Lorentz shifting of the frequency in the thermal factor reflects the fact that the product of inverse temperature and frequency is a Lorentz invariant and the thermal distribution is only isotropic in the natural frame for radiation, \mathcal{R} ,

$$\beta_R^{\mu} k_{\mu} = \beta_R \omega = \beta_R \gamma(\omega' + k'_x v) = \beta'_R \omega' - \beta'_R \cdot \mathbf{k}'. \quad (2.65)$$

The above relation implies that the radiation temperature transformed into the particle's rest frame, \mathcal{P} , becomes a four vector, which reads

$$\beta_R^{\mu'} = (\gamma\beta_R, -\gamma\beta_R \mathbf{v}). \quad (2.66)$$

Of course, there have always been controversies regarding the Lorentz transformation of temperature [46]. Therefore, we shall always try to avoid using this four-temperature and write out the coth factor in terms of β_R .

2.4 Electromagnetic Green's tensor

In this section, we give a detailed account for the electromagnetic Green's tensor. We first discuss the symmetries of the Green's tensor in Sec. 2.4.1, which are, in fact, also valid for other generalized susceptibilities. We then derive in Sec. 2.4.2 a differential equation satisfied by the electromagnetic Green's tensor from the Maxwell equations. Great generality is assumed here, for we have taken into account the magnetic properties, anisotropy, inhomogeneity and nonlocal spatial dispersion.

In Sec. 2.4.3, we give the vacuum Green's tensor, which is the most symmetric and simplest. Finally, in Sec. 2.4.4, we give the form of the Green's tensor in a planar geometry, which will be most useful for the problems that will be discussed in later chapters.

2.4.1 General symmetry properties

The generalized susceptibilities constructed from the commutator of the response operators as in Eq. (2.29) share the common property: they are retarded and real in spacetime. This can also be directly seen by considering the connection between the susceptibility and the correlation function in Eq. (2.51), together with the conjugate relation for the correlation in Eq. (2.48b). From these, it directly follows

$$\chi(t - \tilde{t}; \mathbf{r}, \tilde{\mathbf{r}}) = -\frac{2}{\hbar} \theta(t - \tilde{t}) \text{Im } \mathbf{C}(t - \tilde{t}; \mathbf{r}, \tilde{\mathbf{r}}). \quad (2.67)$$

Notice this is written as a tensorial equation so that the relation is satisfied component by component.

Since the Green's tensor, Γ , is the generalized susceptibility corresponding to the field operators, it must also be real in the spacetime domain. As we shall see, symmetry properties of various Fourier transforms of the Green's tensor can be derived from this simple fact. Considering a planar geometry, where translational symmetry in space is only broken in the z direction, we may write

$$\Gamma(t - \tilde{t}; \mathbf{r}_\perp - \tilde{\mathbf{r}}_\perp, z, \tilde{z}) = \Gamma(t - \tilde{t}; \mathbf{r}_\perp - \tilde{\mathbf{r}}_\perp, z, \tilde{z})^*, \quad (2.68)$$

where $\mathbf{r}_\perp = (x, y)$ denotes the coordinates of the two translational invariant directions. When this is Fourier transformed to frequency space, we find

$$\Gamma(\omega; \mathbf{r}_\perp - \tilde{\mathbf{r}}_\perp, z, \tilde{z}) = \Gamma(-\omega; \mathbf{r}_\perp - \tilde{\mathbf{r}}_\perp, z, \tilde{z})^*. \quad (2.69)$$

It can be further transformed into the momentum space utilizing the translational symmetry in x and y directions,

$$\Gamma(\omega, \mathbf{k}_\perp; z, \tilde{z}) = \Gamma(-\omega, -\mathbf{k}_\perp; z, \tilde{z})^*. \quad (2.70)$$

One could also retain the time coordinate and only take the Fourier transform of Eq. (2.68) into the momentum space, though it is rarely used,

$$\Gamma(t - \tilde{t}; \mathbf{k}_\perp; z, \tilde{z}) = \Gamma(t - \tilde{t}; -\mathbf{k}_\perp; z, \tilde{z})^*. \quad (2.71)$$

Below, we give the symmetry properties for the real and imaginary part of the corresponding Fourier transform of the Green's tensor based on Eq. (2.69) - Eq. (2.71):

$$\begin{aligned} \operatorname{Re} \Gamma(\omega; \mathbf{r}_\perp - \tilde{\mathbf{r}}_\perp, z, \tilde{z}) &= \operatorname{Re} \Gamma(-\omega; \mathbf{r}_\perp - \tilde{\mathbf{r}}_\perp, z, \tilde{z}), \\ \operatorname{Im} \Gamma(\omega; \mathbf{r}_\perp - \tilde{\mathbf{r}}_\perp, z, \tilde{z}) &= -\operatorname{Im} \Gamma(-\omega; \mathbf{r}_\perp - \tilde{\mathbf{r}}_\perp, z, \tilde{z}), \end{aligned} \quad (2.72a)$$

$$\begin{aligned} \operatorname{Re} \Gamma(\omega, \mathbf{k}; z, \tilde{z}) &= \operatorname{Re} \Gamma(-\omega, -\mathbf{k}; z, \tilde{z}), \\ \operatorname{Im} \Gamma(\omega, \mathbf{k}; z, \tilde{z}) &= -\operatorname{Im} \Gamma(-\omega, -\mathbf{k}; z, \tilde{z}), \end{aligned} \quad (2.72b)$$

$$\begin{aligned} \operatorname{Re} \Gamma(t - \tilde{t}; \mathbf{k}_\perp; z, \tilde{z}) &= \operatorname{Re} \Gamma(t - \tilde{t}; -\mathbf{k}_\perp; z, \tilde{z}), \\ \operatorname{Im} \Gamma(t - \tilde{t}; \mathbf{k}_\perp; z, \tilde{z}) &= -\operatorname{Im} \Gamma(t - \tilde{t}; -\mathbf{k}_\perp; z, \tilde{z}). \end{aligned} \quad (2.72c)$$

To sum up, the real part of the Green's tensor is even while the imaginary part of the Green's tensor is odd. But, notice that these symmetry properties only concerns the complete reflection of the Fourier transformed coordinates, i.e., $\operatorname{Im} \Gamma(\omega, \mathbf{k}) \neq -\operatorname{Im} \Gamma(-\omega, \mathbf{k})$, except in special situations.

Finally, let us emphasize that the general symmetry properties discussed here apply to not only the electromagnetic tensor but any generalized susceptibility.

2.4.2 Equations of motion

Let us now derive the equations of motion satisfied by the electromagnetic Green's tensor. The macroscopic Maxwell equations without any free charge or currents reads

$$\nabla \cdot \mathbf{D}(\omega, \mathbf{r}) = 0, \quad (2.73a)$$

$$\nabla \cdot \mathbf{B}(\omega; \mathbf{r}) = 0, \quad (2.73b)$$

$$\nabla \times \mathbf{E}(\omega; \mathbf{r}) = i\omega \mathbf{B}(\omega, \mathbf{r}), \quad (2.73c)$$

$$\nabla \times \mathbf{H}(\omega; \mathbf{r}) = -i\omega \mathbf{D}(\omega; \mathbf{r}). \quad (2.73d)$$

This set of equations is able to describe a system consisting the radiation field and some bulk material. The electric and magnetic responses of the bulk material to the radiation fields is described by the permittivity tensor, ε , and permeability tensor, μ , respectively, through the constitutive relations:

$$\mathbf{D}(\omega; \mathbf{r}) = \int d\mathbf{r}' \varepsilon(\omega; \mathbf{r}, \mathbf{r}') \cdot \mathbf{E}(\omega; \mathbf{r}'), \quad (2.74a)$$

$$\mathbf{B}(\omega; \mathbf{r}) = \int d\mathbf{r}' \mu(\omega; \mathbf{r}, \mathbf{r}') \cdot \mathbf{H}(\omega; \mathbf{r}'). \quad (2.74b)$$

These relations can be inverted as

$$\mathbf{E}(\omega; \mathbf{r}) = \int d\mathbf{r}' \varepsilon^{-1}(\omega; \mathbf{r}, \mathbf{r}') \cdot \mathbf{D}(\omega; \mathbf{r}'), \quad (2.75a)$$

$$\mathbf{H}(\omega; \mathbf{r}) = \int d\mathbf{r}' \mu^{-1}(\omega; \mathbf{r}, \mathbf{r}') \cdot \mathbf{B}(\omega; \mathbf{r}'), \quad (2.75b)$$

where the inverse permittivity, ε^{-1} and inverse permeability, μ^{-1} are to be solved from

$$\int d\mathbf{r}' \varepsilon(\omega; \mathbf{r}, \mathbf{r}') \cdot \varepsilon^{-1}(\omega; \mathbf{r}', \mathbf{r}'') = \mathbf{1}\delta(\mathbf{r} - \mathbf{r}''), \quad (2.76a)$$

$$\int d\mathbf{r}' \mu(\omega; \mathbf{r}, \mathbf{r}') \cdot \mu^{-1}(\omega; \mathbf{r}', \mathbf{r}'') = \mathbf{1}\delta(\mathbf{r} - \mathbf{r}''). \quad (2.76b)$$

We need to introduce external polarization, \mathbf{P} , and the magnetization, \mathbf{M} , into the Maxwell equations by letting ⁹

$$\mathbf{D} \Rightarrow \mathbf{D} + \mathbf{P}, \quad \mathbf{H} \Rightarrow \mathbf{H} - \mathbf{M}. \quad (2.77)$$

As a result, the Maxwell equations in Eq. (2.73) are modified by the additional

⁹In the context of this thesis, a neutral particle interacts with the radiation field and bulk material (if any), and the external polarization and magnetization are precisely due to the neutral particle.

source densities, ρ_s , and \mathbf{j}_s caused by \mathbf{P} and \mathbf{M} .

$$\nabla \cdot \mathbf{D}(\omega; \mathbf{r}) = -\nabla \cdot \mathbf{P}(\omega; \mathbf{r}) = \rho_s(\omega; \mathbf{r}), \quad (2.78a)$$

$$\nabla \cdot \mathbf{B}(\omega; \mathbf{r}) = 0, \quad (2.78b)$$

$$\nabla \times \mathbf{E}(\omega; \mathbf{r}) - i\omega \mathbf{B}(\omega; \mathbf{r}) = 0, \quad (2.78c)$$

$$\nabla \times \mathbf{H}(\omega; \mathbf{r}) + i\omega \mathbf{D}(\omega; \mathbf{r}) = -i\omega \mathbf{P}(\omega; \mathbf{r}) + \nabla \times \mathbf{M}(\omega; \mathbf{r}) = \mathbf{j}_s(\omega; \mathbf{r}). \quad (2.78d)$$

In Eq. (2.78), \mathbf{D} and \mathbf{B} can be eliminated in favor of \mathbf{E} and \mathbf{H} using the constitutive relations and their inverses. The equations of motion for \mathbf{E} and \mathbf{H} can be derived by taking a curl on Eq. (2.78c) and Eq. (2.78d), respectively,

$$\begin{aligned} & \int d\mathbf{r}' \left[\frac{1}{\omega^2} \nabla \times \boldsymbol{\mu}^{-1}(\omega; \mathbf{r}, \mathbf{r}') \cdot \nabla' \times -\boldsymbol{\varepsilon}(\omega; \mathbf{r}, \mathbf{r}') \cdot \right] \mathbf{E}(\omega; \mathbf{r}') \\ &= \int d\mathbf{r}' \mathcal{D}_{\mathbf{E}}(\omega; \mathbf{r}, \mathbf{r}') \mathbf{E}(\omega; \mathbf{r}') \\ &= \mathbf{P}(\omega; \mathbf{r}) + \frac{i}{\omega} \nabla \times \mathbf{M}(\omega; \mathbf{r}), \end{aligned} \quad (2.79a)$$

$$\begin{aligned} & \int d\mathbf{r}' \left[\frac{1}{\omega^2} \nabla \times \boldsymbol{\varepsilon}^{-1}(\omega; \mathbf{r}, \mathbf{r}') \cdot \nabla' \times -\boldsymbol{\mu}(\omega; \mathbf{r}, \mathbf{r}') \cdot \right] \mathbf{H}(\omega; \mathbf{r}') \\ &= \int d\mathbf{r}' \mathcal{D}_{\mathbf{H}}(\omega; \mathbf{r}, \mathbf{r}') \mathbf{H}(\omega; \mathbf{r}') \\ &= \int d\mathbf{r}' \nabla \times \boldsymbol{\varepsilon}^{-1}(\omega; \mathbf{r}, \mathbf{r}') \cdot \left[-\frac{i}{\omega} \mathbf{P}(\omega; \mathbf{r}') + \frac{1}{\omega^2} \nabla' \times \mathbf{M}(\omega; \mathbf{r}') \right]. \end{aligned} \quad (2.79b)$$

Note that the differential operators, $\mathcal{D}_{\mathbf{E}}$ and $\mathcal{D}_{\mathbf{H}}$, are dual under the interchange of the permittivity and permeability, $\boldsymbol{\varepsilon} \leftrightarrow \boldsymbol{\mu}$.

There should be four different kinds of Green's tensors that connect \mathbf{E} and \mathbf{H} to \mathbf{P} and \mathbf{M} :

$$\begin{pmatrix} \mathbf{E}(\omega; \mathbf{r}) \\ \mathbf{H}(\omega; \mathbf{r}) \end{pmatrix} = \int d\mathbf{r}' \begin{pmatrix} \boldsymbol{\Gamma}_{\mathbf{EP}}(\omega; \mathbf{r}, \mathbf{r}') & \boldsymbol{\Gamma}_{\mathbf{EM}}(\omega; \mathbf{r}, \mathbf{r}') \\ \boldsymbol{\Gamma}_{\mathbf{HP}}(\omega; \mathbf{r}, \mathbf{r}') & \boldsymbol{\Gamma}_{\mathbf{HM}}(\omega; \mathbf{r}, \mathbf{r}') \end{pmatrix} \begin{pmatrix} \mathbf{P}(\omega; \mathbf{r}') \\ \mathbf{M}(\omega; \mathbf{r}') \end{pmatrix}. \quad (2.80)$$

The integro-differential equations satisfied by each of the Green's tensors therefore read

$$\int d\mathbf{r}' \mathcal{D}_{\mathbf{E}}(\omega; \mathbf{r}, \mathbf{r}') \cdot \boldsymbol{\Gamma}_{\mathbf{EP}}(\omega; \mathbf{r}', \mathbf{r}'') = \mathbf{1} \delta(\mathbf{r} - \mathbf{r}''), \quad (2.81a)$$

$$\int d\mathbf{r}' \mathcal{D}_{\mathbf{E}}(\omega; \mathbf{r}, \mathbf{r}') \cdot \Gamma_{\text{EM}}(\omega; \mathbf{r}', \mathbf{r}'') = \frac{i}{\omega} \nabla \times \mathbf{1} \delta(\mathbf{r} - \mathbf{r}''), \quad (2.81\text{b})$$

$$\int d\mathbf{r}' \mathcal{D}_{\mathbf{H}}(\omega; \mathbf{r}, \mathbf{r}') \cdot \Gamma_{\text{HP}}(\omega; \mathbf{r}', \mathbf{r}'') = -\frac{i}{\omega} \nabla \times \varepsilon^{-1}(\omega; \mathbf{r}, \mathbf{r}''), \quad (2.81\text{c})$$

$$\int d\mathbf{r}' \mathcal{D}_{\mathbf{H}}(\omega; \mathbf{r}, \mathbf{r}') \cdot \Gamma_{\text{HM}}(\omega; \mathbf{r}', \mathbf{r}'') = -\frac{1}{\omega^2} \nabla \times \varepsilon^{-1}(\omega; \mathbf{r}, \mathbf{r}'') \times \overleftarrow{\nabla}'''. \quad (2.81\text{d})$$

The magnetization effect induced by a particle is typically far smaller than the electric polarization effect. Also, the electric field and magnetic field are not independent, but they are directly related through Eq. (2.78c). These considerations allow us to focus on only the Green's tensor that connects \mathbf{E} to \mathbf{P} , Γ_{EP} . In later chapters, Green's tensor always refer to Γ_{EP} and we shall drop the subscript on it for convenience.

In the above derivation, we have taken into account the spatial nonlocality in the permittivity and permeability tensors. If we can treat them as being local,

$$\varepsilon(\omega; \mathbf{r}, \mathbf{r}') \rightarrow \varepsilon(\omega; \mathbf{r}) \delta(\mathbf{r} - \mathbf{r}'), \quad \mu(\omega; \mathbf{r}, \mathbf{r}') \rightarrow \mu(\omega; \mathbf{r}) \delta(\mathbf{r} - \mathbf{r}'), \quad (2.82)$$

then the integro-differential equation Eq. (2.81a) reduces to a differential equation:

$$\left[\frac{1}{\omega^2} \nabla \times \mu^{-1}(\omega; \mathbf{r}) \cdot \nabla \times -\varepsilon(\omega; \mathbf{r}) \cdot \right] \Gamma(\omega; \mathbf{r}, \tilde{\mathbf{r}}) = \mathbf{1} \delta(\mathbf{r} - \tilde{\mathbf{r}}). \quad (2.83)$$

2.4.3 Vacuum Green's tensor

In vacuum (free space), $\varepsilon = \mu = \mathbf{1}$, and the differential equation, Eq. (2.83) reduces to

$$\left[\frac{1}{\omega^2} \nabla \times \nabla \times -\mathbf{1} \cdot \right] \Gamma(\omega; \mathbf{r}, \tilde{\mathbf{r}}) = \mathbf{1} \delta(\mathbf{r} - \tilde{\mathbf{r}}), \quad (2.84)$$

which is satisfied by the vacuum Green's tensor. If we take the divergence of the above equation, we obtain

$$\nabla \cdot \Gamma(\omega; \mathbf{r}, \tilde{\mathbf{r}}) = -\nabla \cdot \mathbf{1} \delta(\mathbf{r} - \tilde{\mathbf{r}}). \quad (2.85)$$

Let us define the divergenceless part of the Green's tensor to be

$$\mathbf{G}(\omega; \mathbf{r}, \tilde{\mathbf{r}}) = \Gamma(\omega; \mathbf{r}, \tilde{\mathbf{r}}) + \mathbf{1} \delta(\mathbf{r} - \tilde{\mathbf{r}}), \quad (2.86)$$

The retarded solution to Eq. (2.84), in terms of \mathbf{G} is

$$\begin{aligned}\mathbf{G}(\omega; \mathbf{r}, \tilde{\mathbf{r}}) &= \nabla \times \nabla \times \mathbf{1} \frac{e^{i\omega R}}{4\pi R} = (\nabla \nabla - \nabla^2 \mathbf{1}) \frac{e^{i\omega R}}{4\pi R}, \\ &= \left[\hat{\mathbf{R}} \hat{\mathbf{R}} (3 - 3i\omega R - \omega^2 R^2) - \mathbf{1} (1 - i\omega R - \omega^2 R^2) \right] \frac{e^{i\omega R}}{4\pi R^3},\end{aligned}\quad (2.87)$$

where $R = |\mathbf{r} - \tilde{\mathbf{r}}|$ and $\hat{\mathbf{R}} = \frac{\mathbf{R}}{R}$. In the coincident limit, $\mathbf{R} \rightarrow 0$, while $\hat{\mathbf{R}} \hat{\mathbf{R}} \rightarrow 1/3$, upon averaging over all directions, \mathbf{G} becomes

$$\mathbf{G}(\omega; \mathbf{r}, \tilde{\mathbf{r}}) \rightarrow \mathbf{1} \left[\frac{\omega^2}{6\pi R} + i \frac{\omega^3}{6\pi} + \mathcal{O}(R) \right], \quad (2.88)$$

that is, in vacuum, $\text{Re } \mathbf{G}$ becomes divergent in the coincident limit while $\text{Im } \mathbf{G}$ is convergent. We will see in Chapter 3 that it is $\text{Im } \mathbf{G}$ that enters the formula for computing the radiative heat transfer and quantum frictional forces in vacuum.

The Green's tensor \mathbf{G} in Eq. (2.87) can be transformed into (ω, \mathbf{k}) space, since it possesses a full spatial translational symmetry,

$$\mathbf{G}(\omega; \mathbf{R}) = \int \frac{d^3 \mathbf{k}}{(2\pi)^3} e^{i\mathbf{k} \cdot \mathbf{R}} \mathbf{G}(\omega, \mathbf{k}). \quad (2.89)$$

Doing the inverse Fourier transform, we find \mathbf{G} is precisely the usual vacuum photon propagator,

$$G_{ij}(\omega, \mathbf{k}) = \frac{-k_i k_j + k^2 \delta_{ij}}{(\omega + i\eta)^2 - k^2}, \quad (2.90)$$

where η is a small positive parameter which renders the poles of the propagator to be only found in the lower half ω plane. That is, the propagator is retarded.

In the calculations we will perform in later chapters, the Green's function is always evaluated in the limit of coincident spatial coordinates, the particle's position. Therefore, the original Green's tensor, Γ , is divergent due to the delta function in Eq. (2.86). We shall always discard this delta function and only be concerned with the divergenceless Green's tensor, \mathbf{G} . This is, effectively, the point-splitting prescription, which is commonly seen in field theory for regularization purposes.

2.4.4 Green's tensor in planar geometry

When an interface is introduced into the vacuum (free space), the full spatial translational symmetry will be broken. Let us now consider a planar interface, lying at $z = 0$. Above the interface ($z > 0$) is vacuum, below the interface is some medium characterized by an isotropic and homogeneous permittivity, ε , and permeability, μ . The index of refraction of the media is

$$n(\omega) = \sqrt{\varepsilon(\omega)\mu(\omega)}, \quad (2.91)$$

which, in general, can be dispersive in frequency.

The geometry still possesses a spatial translational symmetry in the x - y plane, which permits us to Fourier transform the Green's tensor in these spatial directions,

$$\mathbf{G}(\omega; \mathbf{r}, \tilde{\mathbf{r}}) = \int \frac{d^2 \mathbf{k}_\perp}{(2\pi)^2} e^{i\mathbf{k}_\perp \cdot (\mathbf{r}_\perp - \tilde{\mathbf{r}}_\perp)} \mathbf{G}(\omega, \mathbf{k}_\perp; z, \tilde{z}). \quad (2.92)$$

In this geometry, the Green's tensor evaluated in the vacuum region ($z, \tilde{z} > 0$)¹⁰ takes the following form:

$$\mathbf{G}(\omega, \mathbf{k}_\perp; z, \tilde{z}) = \begin{pmatrix} \frac{k_x^2}{k^2} \partial_z \partial_{\tilde{z}} g^H + \frac{k_y^2}{k^2} \omega^2 g^E & \frac{k_x k_y}{k^2} \partial_z \partial_{\tilde{z}} g^H - \frac{k_x k_y}{k^2} \omega^2 g^E & i k_x \partial_z g^H \\ \frac{k_x k_y}{k^2} \partial_z \partial_{\tilde{z}} g^H - \frac{k_x k_y}{k^2} \omega^2 g^E & \frac{k_y^2}{k^2} \partial_z \partial_{\tilde{z}} g^H + \frac{k_x^2}{k^2} \omega^2 g^E & i k_y \partial_z g^H \\ -i k_x \partial_{\tilde{z}} g^H & -i k_y \partial_{\tilde{z}} g^H & k^2 g^H \end{pmatrix}, \quad (2.93)$$

where $k^2 = k_x^2 + k_y^2$.

As is seen, the Green's tensor above is constructed from the two scalar Green's functions, corresponding to the transverse electric (E) and transverse magnetic (H) modes, respectively. They satisfy the following differential equation,

$$\left(-\frac{\partial^2}{\partial z^2} + k^2 - \omega^2 \right) g^{E,H}(\omega, k; z, \tilde{z}) = \delta(z - \tilde{z}). \quad (2.94)$$

Each of the scalar functions consists of a bulk part and a scattering part,

$$g^{E,H}(\omega, k; z, \tilde{z}) = \frac{1}{2\kappa} e^{-\kappa|z-\tilde{z}|} + \frac{r^{E,H}}{2\kappa} e^{-\kappa(z+\tilde{z})}, \quad (2.95)$$

¹⁰In this thesis, the Green's tensor is always evaluated at the position of the particle, which is moving in the vacuum region.

where κ is the propagation wave number corresponding to the vacuum,

$$\kappa^2 = k^2 - \omega^2. \quad (2.96)$$

with the reflection coefficients,

$$r^E = \frac{\kappa - \kappa_n/\mu}{\kappa + \kappa_n/\mu}, \quad r^H = \frac{\kappa - \kappa_n/\varepsilon}{\kappa + \kappa_n/\varepsilon}. \quad (2.97)$$

and κ_n is the propagation wave number associated with the medium,

$$\kappa_n^2 = k^2 - \omega^2\varepsilon\mu = k^2 - \omega^2n^2. \quad (2.98)$$

In certain regions of ω and \mathbf{k}_\perp , κ and κ_n will develop imaginary parts.¹¹ In those regions, the branch is so chosen that the Green's tensor is guaranteed to be retarded,

$$\kappa \rightarrow -i\text{sgn}(\omega)\sqrt{\omega^2 - k^2}, \quad \omega^2 > k^2; \quad \kappa_n \rightarrow -i\text{sgn}(\omega)\sqrt{\omega^2\varepsilon\mu - k^2}, \quad \omega^2\varepsilon\mu > k^2. \quad (2.99)$$

Note that κ and κ_n become odd in ω in the regions where they develop imaginary parts.

If we now take the vacuum limit, $\varepsilon = \mu = 1$, for the planar Green's tensor in Eq. (2.93), $\kappa_n = \kappa$, and the reflection coefficients vanish, $r^E = r^H = 0$. There is no interface in the geometry and the Green's tensor only has a bulk contribution, which reads

$$\mathbf{G}^0(\omega, \mathbf{k}_\perp; z, \tilde{z}) = \frac{1}{2\kappa} e^{-\kappa|z-\tilde{z}|} \begin{pmatrix} \omega^2 - k_x^2 & -k_x k_y & -ik_x \kappa \text{sgn}(z - \tilde{z}) \\ -k_x k_y & \omega^2 - k_y^2 & -ik_y \kappa \text{sgn}(z - \tilde{z}) \\ ik_x \kappa \text{sgn}(\tilde{z} - z) & ik_y \kappa \text{sgn}(\tilde{z} - z) & k^2 \end{pmatrix}. \quad (2.100)$$

Obviously, the vacuum Green's tensor is a symmetric matrix, which reflects the reciprocity of the vacuum.

Another limit to take is to assume the interface to be a perfectly conducting

¹¹It is precisely these modes that give rise to the quantum frictional effects that we will be discussing.

boundary for which the permittivity, ε , and permeability, μ , take the extreme values,¹²

$$\varepsilon \rightarrow \infty, \quad \mu \rightarrow 0 \quad (2.101)$$

so that the reflection coefficients simplify to be

$$r^{E,H} = \mp 1. \quad (2.102)$$

The Green's tensor in the presence of a perfectly conducting plate therefore has both a bulk contribution and a scattering contribution,

$$\mathbf{G}^{\text{PC}} = \mathbf{G}^0 + \mathbf{G}^{\text{SC}}, \quad (2.103)$$

where the bulk part \mathbf{G}^0 is identical to the vacuum Green's tensor in Eq. (2.100) while the scattering part is

$$\mathbf{G}^{\text{SC}}(\omega, \mathbf{k}_\perp; z, \tilde{z}) = \frac{1}{2\kappa} e^{-\kappa(z+\tilde{z})} \begin{pmatrix} -(\omega^2 - k_x^2) & k_x k_y & -i k_x \kappa \\ k_x k_y & -(\omega^2 - k_y^2) & -i k_y \kappa \\ i k_x \kappa & i k_y \kappa & k^2 \end{pmatrix}. \quad (2.104)$$

The vacuum Green's tensor and the Green's tensor in the presence of a perfectly conducting plate are special in that they evaluate the same in frame \mathcal{P} as in frame \mathcal{R} ,

$$\mathbf{G}'(\omega', \mathbf{k}'_\perp; z, \tilde{z}) = \mathbf{G}(\omega', \mathbf{k}'_\perp; z, \tilde{z}). \quad (2.105)$$

This can be checked explicitly using the Lorentz transformations for Green's tensors listed in Appendix A. The quantization in frame \mathcal{P} therefore becomes easier in these geometries, since we do not need to worry about Lorentz transforming the Green's tensor.

Finally, let us consider an interface lying at $z = 0$, which separates two different isotropic and homogeneous materials (which could be dispersive) characterized by

¹²To mimic a perfectly conducting boundary, materials with impedance $Z = \sqrt{\frac{\mu}{\varepsilon}} \rightarrow 0$ is desirable. The index of refraction $n = \sqrt{\varepsilon\mu}$ does not have to remain unity but should be finite [47].

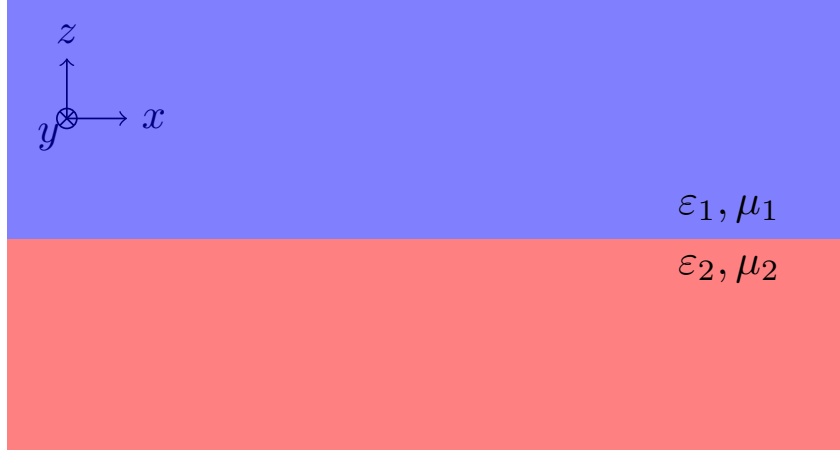


Figure 2.1: Illustration of the two-layer geometry.

permittivity and permeability ε_1, μ_1 and ε_2, μ_2 , respectively. This two-layer geometry is illustrated in Figure 2.1. The Green's tensor in region 1 is now modified to be

$$\mathbf{G}(\omega, \mathbf{k}_\perp; z, \tilde{z}) = \begin{pmatrix} \frac{k_x^2}{k^2} \partial_z \partial_{\tilde{z}} \frac{g^H}{\varepsilon_1^2} + \frac{k_y^2}{k^2} \omega^2 g^E & \frac{k_x k_y}{k^2} \partial_z \partial_{\tilde{z}} \frac{g^H}{\varepsilon_1^2} - \frac{k_x k_y}{k^2} \omega^2 g^E & i k_x \partial_z \frac{g^H}{\varepsilon_1^2} \\ \frac{k_x k_y}{k^2} \partial_z \partial_{\tilde{z}} \frac{g^H}{\varepsilon_1^2} - \frac{k_x k_y}{k^2} \omega^2 g^E & \frac{k_y^2}{k^2} \partial_z \partial_{\tilde{z}} \frac{g^H}{\varepsilon_1^2} + \frac{k_x^2}{k^2} \omega^2 g^E & i k_y \partial_z \frac{g^H}{\varepsilon_1^2} \\ -i k_x \partial_z \frac{g^H}{\varepsilon_1^2} & -i k_y \partial_z \frac{g^H}{\varepsilon_1^2} & k^2 \frac{g^H}{\varepsilon_1^2} \end{pmatrix}, \quad (2.106)$$

Note μ_1 does not explicitly enter the Green's tensor but implicitly through the two scalar Green's functions, which now satisfy different differential equations:

$$\begin{cases} \left(-\frac{\partial^2}{\partial z^2} + k^2 - \omega^2 \varepsilon_1 \mu_1 \right) g^E(\omega, k; z, \tilde{z}) = \varepsilon_1 \delta(z - \tilde{z}), \\ \left(-\frac{\partial^2}{\partial z^2} + k^2 - \omega^2 \varepsilon_1 \mu_1 \right) g^H(\omega, k; z, \tilde{z}) = \mu_1 \delta(z - \tilde{z}). \end{cases} \quad (2.107)$$

Now, they read

$$\begin{cases} g^E(\omega, k; z, \tilde{z}) = \varepsilon_1 \left[\frac{1}{2\kappa_1} e^{-\kappa_1 |z - \tilde{z}|} + \frac{r^E}{2\kappa_1} e^{-\kappa_1 (z + \tilde{z})} \right], \\ g^H(\omega, k; z, \tilde{z}) = \mu_1 \left[\frac{1}{2\kappa_1} e^{-\kappa_1 |z - \tilde{z}|} + \frac{r^H}{2\kappa_1} e^{-\kappa_1 (z + \tilde{z})} \right]. \end{cases} \quad (2.108)$$

The reflection coefficients are

$$r^E = \frac{\kappa_1 / \mu_1 - \kappa_2 / \mu_2}{\kappa_1 / \mu_1 + \kappa_2 / \mu_2}, \quad r^H = \frac{\kappa_1 / \varepsilon_1 - \kappa_2 / \varepsilon_2}{\kappa_1 / \varepsilon_1 + \kappa_2 / \varepsilon_2}, \quad (2.109)$$

where

$$\kappa_1 = k^2 - \omega^2 \varepsilon_1 \mu_1, \quad \kappa_2 = k^2 - \omega^2 \varepsilon_2 \mu_2. \quad (2.110)$$

2.5 Polarizability Tensor

In this section, we discuss another important susceptibility, the polarizability tensor. Unlike the Green's tensor, which is fully determined by the macroscopic boundary conditions, the polarizability should in principle be derived from the atomic and molecular properties of the materials. However, we will not go deeply in the atomic or condensed matter consideration of the subject. Rather, the emphasis here is to introduce some decent models for the polarizability, both for a nanoparticle in Sec. 2.5.1 and for an atom in Sec. 2.5.2, so that we could use them to estimate the fluctuation-induced effects that will be discussed in later chapters.

2.5.1 Polarizability of a nanoparticle

The expressions in Eq. (2.31) and Eq. (2.32) are only practically useful to calculate the susceptibility of a system with a small number of energy levels. For a macroscopic particle, on the contrary, its energy spectrum becomes so dense that its susceptibility, effectively, becomes a continuous function in frequency. In that case, instead of deriving the susceptibility from the information about the microscopic energy spectrum (which will be enormous), one usually relies on some empirical model for the susceptibility which only uses a few parameters of the macroscopic material as input.

If we assume the nanoparticle is isotropic and made of homogeneous material, its polarizability, $\alpha(\omega)$, can then be expressed in terms of its volume, V , and the permittivity of the material, $\varepsilon(\omega)$, through the Lorenz-Lorentz relation

$$\alpha(\omega) = 3V \frac{\varepsilon(\omega) - 1}{\varepsilon(\omega) + 2}. \quad (2.111)$$

An introduction of the Lorenz-Lorentz relation can be found in Refs. [48]. The relation takes into account the distinction between fields acting on the atoms in a medium and the actual applied field [49]. In the "dilute" limit, $\varepsilon(\omega) \rightarrow 1$, where

such distinction is not important, the Lorenz-Lorentz relation reduces to a volume summation of the local susceptibility

$$\alpha(\omega) \sim V [\varepsilon(\omega) - 1] = V\chi(\omega), \quad (2.112)$$

which can be easily extended for a particle made of inhomogeneous material,

$$\alpha(\omega) = \int d\mathbf{r} \chi(\omega; \mathbf{r}). \quad (2.113)$$

The permittivity of the material, $\varepsilon(\omega)$, can often be modeled by a series of resonant-damped oscillators [50]

$$\varepsilon(\omega) = 1 + \sum_i \frac{\omega_{p,i}^2}{\omega_{0,i}^2 - \omega^2 - i\omega\nu_i}, \quad (2.114)$$

where $\omega_{0,i}$, $\omega_{p,i}$ and ν_i are the resonant frequency, plasma frequency, and damping frequency corresponding to each oscillator. For metals, however, it is usually a good approximation, to just keep one term with zero resonance frequency:

$$\varepsilon(\omega) = 1 - \frac{\omega_p^2}{\omega^2 + i\omega\nu}. \quad (2.115)$$

In later chapters, we will often use gold as a concrete example. The nominal value for its plasma frequency and damping parameter are: $\omega_p = 9.00 \text{ eV}$ and $\nu = 0.0350 \text{ eV}$ [51].

Combining Eq. (2.111) and Eq. (2.115), we find the polarizability of a nanoparticle made of metal to be

$$\alpha(\omega) = V \frac{\omega_p^2}{\omega_1^2 - \omega^2 - i\omega\nu}, \quad (2.116)$$

where through the Lorenz-Lorentz relation, the free oscillator term have now acquired a resonance frequency $\omega_1 = \omega_p/\sqrt{3}$.¹³ The real part and the imaginary part

¹³If we were to consider a nanoparticle made of an insulator, we would, similarly, see a shift of the old resonance frequency, $\omega_0^2 \rightarrow \omega_0^2 + \omega_p^2/3$.

of the polarizability in Eq. (2.116) can be readily found,

$$\operatorname{Re} \alpha(\omega) = V \frac{\omega_p^2(\omega_1^2 - \omega^2)}{(\omega_1^2 - \omega^2)^2 + \omega^2 \nu^2}, \quad \operatorname{Im} \alpha(\omega) = V \frac{\omega_p^2 \omega \nu}{(\omega_1^2 - \omega^2)^2 + \omega^2 \nu^2}. \quad (2.117)$$

Notice $\operatorname{Re} \alpha(\omega)$ is even in ω and $\operatorname{Im} \alpha(\omega)$ is odd in ω , which is just the symmetry property of a spatially local generalized susceptibility.

The polarizability in Eq. (2.116) is temperature independent if all the parameters involved are constant. However, in reality, even though the plasma parameter, ω_p , has very weak temperature dependence, the damping parameter, ν , is usually more sensitive to variation of temperatures. It is therefore more realistic to adopt a temperature dependent model for the damping parameter. Damping of a simple metal is mainly due to the scattering of electrons by phonons and can be well described by the Bloch-Grüneisen (BG) model [52, 53],

$$\nu(T) = \nu_0 \left(\frac{T}{\theta} \right)^5 \int_0^{\frac{\theta}{T}} dx \frac{x^5 e^x}{(e^x - 1)^2}. \quad (2.118)$$

For gold, the Bloch-Grüneisen temperature θ is 175 K. And the constant ν_0 in Eq. (2.118) can be determined to be 0.0832 eV from the room temperature (300 K) value of the damping parameter $\nu = 0.0350$ eV given in Refs. [51, 54, 55].¹⁴ The low and high temperature limits of the Bloch-Grüneisen damping can be easily worked out,

$$\nu(T) \rightarrow \begin{cases} 5\Gamma(5)\zeta(5)\nu_0 \left(\frac{T}{\theta}\right)^5, & T \ll \theta, \\ \frac{\nu_0}{4} \left(\frac{T}{\theta}\right), & T \gg \theta. \end{cases} \quad (2.119)$$

In Fig. 2.2, we plot the Bloch-Grüneisen damping parameter for gold as a function of temperature. The transition between the low and high temperature behavior of ν is seen to occur at a rather low temperature around $T = 40$ K.

¹⁴The value for ν_0 we use is slightly different than that in Appendix D of [51] where the room temperature is taken to be 295 K. There is, of course, no definite consensus on the meaning of the room temperature. Nonetheless, taking it to be 300 K is more consistent with the source of the raw data in [55].

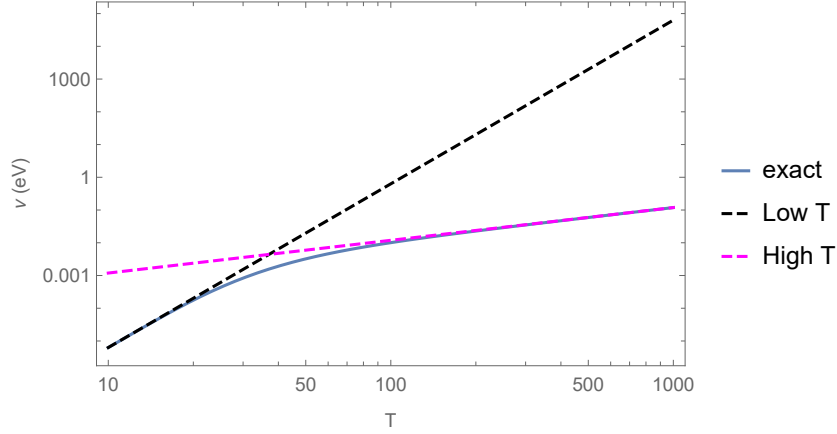


Figure 2.2: The temperature-dependent damping parameter ν in Eq. (2.118) is illustrated for gold with $\theta = 175$ K and $\nu_0 = 0.0832$ eV.

2.5.2 Polarizability of an atom

Thanks to the development of the atomic precision experiments and spectroscopy, physicists have accumulated a good knowledge about the energy spectrum of most common atoms. A convenient resource for finding such data is [56]. These data, in principle, enables us to compute the polarizability of an atom using Eq. (2.32)

$$\alpha(\omega) = -\frac{1}{\hbar} \lim_{\eta \rightarrow 0^+} \sum_{n,m} \frac{\sigma_{nm}}{\omega + \omega_{nm} + i\eta}. \quad (2.120)$$

Here, σ_{nm} is a tensorial oscillator strength determined by relevant energy levels and the dipole transition matrix elements,

$$\sigma_{nm} = \frac{(e^{-\beta E_n} - e^{-\beta E_m})}{Z} \langle n | \mathbf{d} | m \rangle \langle m | \mathbf{d} | n \rangle, \quad (2.121)$$

which possesses the obvious symmetry

$$\sigma_{nm} = -\sigma_{mn}. \quad (2.122)$$

If Eq. (2.120) were strictly true, $\alpha(\omega)$ would be purely real and even at all off-resonant frequencies,

$$\alpha(\omega) = -\frac{1}{\hbar} \sum_{n,m} \frac{\sigma_{nm}}{\omega + \omega_{nm}} = \frac{2}{\hbar} \sum_{n,m < n} \frac{\sigma_{nm} \omega_{nm}}{\omega^2 - \omega_{nm}^2}, \quad \omega \neq -\omega_{nm}, \quad (2.123)$$

and the imaginary part of the polarizability could only arise at resonances

$$\text{Im } \alpha(\omega) = -\frac{\pi}{\hbar} \sum_{n,m} \sigma_{nm} \delta(\omega + \omega_{nm}) = -\frac{\pi}{\hbar} \sum_{n,m < n} \sigma_{nm} [\delta(\omega - \omega_{nm}) - \delta(\omega + \omega_{nm})], \quad (2.124)$$

which is manifestly odd.

More realistically, instead of being infinitely thin, each resonance should have a finite width, $\eta_{nm}(\omega)$, which could also be a function of frequency. Then, Eq. (2.120) is replaced with

$$\alpha(\omega) = -\frac{1}{\hbar} \sum_{n,m} \frac{\sigma_{nm}}{\omega + \omega_{nm} + i\eta_{nm}(\omega)}, \quad (2.125)$$

where the width could be linear in ω or behave as ω^3 , depending on whether the velocity gauge or length gauge is employed [57]. Considering the finite width, the polarizability develops an imaginary part at off-resonant frequencies as well.

Even though all frequency modes will contribute to the fluctuation-induced effects, the contributions from frequency modes much higher than the corresponding temperature, $\hbar\omega \gg k_B T$ are suppressed due to an ever-present Bose-Einstein factor in the expressions for these effects. In other words, at temperatures lower than that corresponding to the first excited energy of the atom, $T < T_1$, all resonance contributions will be suppressed. It is therefore a decent approximation to treat the polarizability as being purely real and even replace the dynamic polarizability with the static polarizability for these sufficiently low temperatures. In this case, we will see that the various fluctuation-induced effects will be of second order in the intrinsic polarizability of the atom. For temperatures higher than T_1 , the resonance modes become important in the evaluation of the fluctuation-induced effects and these effects will be of first order to the polarizability. But, for the discussion of fluctuation-induced effects, we should not consider temperatures exceeding the ionization temperature of the atom, T_i , beyond which the atom will be ionized and cannot stay neutral anymore. That is, at such high temperatures, all of the fluctuation-induced effects will be completely flooded by the classical charged effects.

Chapter 3

Quantum Vacuum Frictional Effects (QVF)

What is the simplest setting for quantum frictional effects, i.e., forces and heat transfer, to occur on a neutral but polarizable particle? Surprisingly, a particle moving uniformly in free space, not in contact with or close to any other objects, can experience a force, parallel to its motion, originating from the vacuum fluctuations. We will call such a frictional force quantum vacuum friction (QVF). In the case of an intrinsically dissipative particle, the fluctuations can also induce a radiative heat transfer so that the particle will either absorb energy from or release energy to the surrounding blackbody radiation, which we can name as quantum vacuum radiative heat transfer (QVRHT).

In this chapter, we explore these vacuum effects. In Sec. 3.1, we study QVF and QVRHT for an intrinsically dissipative nanoparticle. In Sec. 3.2, we investigate the quantum vacuum frictional effects for a nondissipative atom. They have to be treated differently. For the former, quantum vacuum frictional effects are induced by both the electromagnetic field fluctuations and intrinsic dipole fluctuations. For the latter, the only dissipation mechanism for the particle is through its interaction with the surrounding blackbody radiation. As a result, a nondissipative atom will always be found in the nonequilibrium steady state (NESS), where it never loses or gains internal energy. On the contrary, a dissipative nanoparticle can be out of NESS and therefore has its own temperature independent of the radiation. The separate treatments for the two different kinds of particle are still needed for the

discussion of quantum frictional effects in other more complicated scenarios than vacuum. So, what we discuss in this chapter provides a paradigm for the discussions in the following chapters.

The nonrelativistic discussion of frictional force on particles moving in free space filled with only blackbody radiation can be traced back to the works of Mkrtchian et al. [16] or even Einstein and Hopf [3]. Ever since, there has been considerable interest in the subject of blackbody friction/quantum vacuum friction (QVF) [58, 17, 59, 60]. Recently, we have also investigated such quantum vacuum frictional effects on a particle moving with relativistic velocities, be it a nondissipative atom [21] or an intrinsically dissipative nanoparticle [22].

In this chapter, we will set the universal constants, $c = k_B = 1$ in the analytic expressions. SI units, however, are reinstated in the numerical evaluations. Primes will be used on physical quantities that are referring to the rest frame of the particle, \mathcal{P} . Since the inverse temperature of the radiation, β_R , and that of the particle, β'_P , are always defined in their respective rest frames, we omit the subscript on these symbols throughout the chapter. That is, starting from this chapter, we will use the following shorthand notation for the two temperatures, $\beta_R \rightarrow \beta$ and $\beta'_P \rightarrow \beta'$.

3.1 Quantum Vacuum Frictional Effects on a Dissipative Nanoparticle

In this section, we will consider a neutral but polarizable nanoparticle which is intrinsically dissipative, that is, its polarizability is complex in frequency space. For simplicity, we will also assume that the polarizability is isotropic and only dispersive in frequency, that is

$$\boldsymbol{\alpha}(\omega) = \alpha(\omega)\mathbf{1} = [\text{Re } \alpha(\omega) + i \text{Im } \alpha(\omega)] \mathbf{1}. \quad (3.1)$$

It then immediately follows that $\text{Re } \alpha(\omega)$ is even in frequency while $\text{Im } \alpha(\omega)$ is odd.

The particle is dissipative intrinsically so that it can exchange energy with the environment. This indicates that the particle has its own temperature, T' , independent of the temperature of the radiation, T , and it does not have to be in thermal

equilibrium or nonequilibrium steady state (NESS) with the environment filled with blackbody radiation.

3.1.1 Radiative heat transfer of a particle at rest

Even if the atom is at rest in free space, there will be radiative heat transfer between the atom and the environment induced by the fluctuations when they are not in thermal equilibrium. In Chapter 2, we have found that the radiative power on a moving electric dipole could be obtained by differentiating a free energy as follows:

$$P(t) = \frac{\partial}{\partial t} \mathcal{F} = -\frac{\partial}{\partial t_1} [\mathbf{d}(t_0) \cdot \mathbf{E}(t_1, \mathbf{v}t) + \boldsymbol{\mu}_v(t_0) \cdot \mathbf{B}(t_1, \mathbf{v}t)] |_{t_0=t_1 \rightarrow t}, \quad (3.2)$$

where $\boldsymbol{\mu}_v(t) = \mathbf{d}(t) \times \mathbf{v}$ is the magnetic dipole moment induced by the motion of the electric dipole. For $\mathbf{v} = \mathbf{0}$, this reduces to

$$\begin{aligned} P(t) &= -\frac{\partial}{\partial t_1} \mathbf{d}(t_0) \cdot \mathbf{E}(t_1, \mathbf{0}) |_{t_0=t_1 \rightarrow t} \\ &= \int \frac{d\omega}{2\pi} e^{-i\omega t} \mathbf{d}(\omega) \cdot \int \frac{d\nu}{2\pi} e^{-i\nu t} i\nu \mathbf{E}(\nu; \mathbf{0}), \end{aligned} \quad (3.3)$$

where we have assumed that the dipole is stationary at position $\mathbf{r} = \mathbf{0}$. The expression in Eq. (3.3) involves the dipole moment and the electric field. But, the nanoparticle does not carry any intrinsic dipole moment. Neither is there any external field present in the configuration. That is, the expectation value of both operators are zero for the particle-radiation system. However, a radiative heat transfer can still be induced because of the nonvanishing expectation value of the product of these operators, that is, due to the fluctuations.

Two types of fluctuations exist in the system: field fluctuation (EE) and dipole fluctuation (dd). Expanding the dipole in Eq. (3.3) through the polarizability of the particle,

$$\mathbf{d}(\omega) = \boldsymbol{\alpha}(\omega) \cdot \mathbf{E}(\omega; \mathbf{0}), \quad (3.4)$$

we find the radiative power induced by the field fluctuation,

$$\mathcal{P}_{EE}(t) = \int \frac{d\omega}{2\pi} e^{-i\omega t} \int \frac{d\nu}{2\pi} e^{-i\nu t} i\nu \langle S\mathbf{E}(\nu; \mathbf{0}) \cdot \boldsymbol{\alpha}(\omega) \cdot \mathbf{E}(\omega; \mathbf{0}) \rangle, \quad (3.5)$$

where S refers to the symmetrization of the field operators. The field in Eq. (3.3) can also be expanded through the Green's tensor in vacuum,

$$\mathbf{E}(\nu; \mathbf{0}) = \int d\mathbf{r} \mathbf{G}(\nu; \mathbf{0}, \mathbf{r}) \cdot \mathbf{P}(\nu; \mathbf{r}), \quad (3.6)$$

where \mathbf{P} is the polarization field caused by a particle at rest,

$$\mathbf{P}(\nu; \mathbf{r}) = \mathbf{d}(\nu) \delta(\mathbf{r}). \quad (3.7)$$

The radiative power induced by the dipole fluctuation is,

$$\mathcal{P}_{dd}(t) = \int \frac{d\omega}{2\pi} e^{-i\omega t} \int \frac{d\nu}{2\pi} e^{-i\nu t} i\nu \langle S\mathbf{d}(\omega) \cdot \mathbf{G}(\nu; \mathbf{0}, \mathbf{0}) \cdot \mathbf{d}(\nu) \rangle. \quad (3.8)$$

Now we use the appropriate forms of FDT to quantize P_{EE} and P_{dd} , respectively:

$$\langle S\mathbf{E}(\omega; \mathbf{0})\mathbf{E}(\nu, \mathbf{0}) \rangle = (2\pi)\delta(\omega + \nu) \text{Im} \mathbf{G}(\omega; \mathbf{0}, \mathbf{0}) \coth\left(\frac{\beta\omega}{2}\right), \quad (3.9a)$$

$$\langle S\mathbf{d}(\omega)\mathbf{d}(\nu) \rangle = 2\pi\delta(\omega + \nu) \text{Im} \boldsymbol{\alpha}(\omega) \coth\left(\frac{\beta'\omega}{2}\right). \quad (3.9b)$$

Note that the anti-Hermitian parts of the corresponding susceptibilities tensor reduce to their ordinary imaginary part. This is possible for the polarizability, $\boldsymbol{\alpha}$ because we have assumed that it is isotropic. It is also allowed for the Green's tensor because it is reciprocal (invariant under interchange of spatial indices and coordinates) in vacuum. As a result, we find the total radiative heat transfer is time independent

$$P = \int \frac{d\omega}{2\pi} \omega \text{Im} \alpha(\omega) \text{tr} \text{Im} \mathbf{G}(\omega; \mathbf{0}, \mathbf{0}) \left[\coth\left(\frac{\beta\omega}{2}\right) - \coth\left(\frac{\beta'\omega}{2}\right) \right], \quad (3.10)$$

for which we have utilized the symmetry properties of the susceptibilities and the integrand. The vacuum Green's tensor, in the coincident limit, is isotropic and has a finite imaginary part as recorded in Eq. (2.88)

$$\text{Im} \mathbf{G}(\omega; \mathbf{0}, \mathbf{0}) = \frac{\omega^3}{6\pi} \mathbf{1}. \quad (3.11)$$

When this is plugged back into Eq. (3.10), we find

$$\begin{aligned}
P &= \frac{1}{4\pi^2} \int d\omega \omega^4 \operatorname{Im} \alpha(\omega) \left[\coth\left(\frac{\beta\omega}{2}\right) - \coth\left(\frac{\beta'\omega}{2}\right) \right] \\
&= \frac{1}{\pi^2} \int_0^\infty d\omega \omega^4 \operatorname{Im} \alpha(\omega) \left[\frac{1}{e^{\beta\omega} - 1} - \frac{1}{e^{\beta'\omega} - 1} \right].
\end{aligned} \tag{3.12}$$

This radiative heat transfer on a particle at rest is nonzero so long as the particle is not in thermal equilibrium with the radiation background, $T' \neq T$.

How long will it take for the nanoparticle at rest come to equilibrium with the radiation? Suppose the heat capacity of the particle, C_V , is a known function of the particle's temperature. To find out the time for the particle to reach thermal equilibrium with the blackbody radiation at temperature T from an initial temperature, T_0 , we have

$$C_V(T')dT' = P(T, T')dt \implies \Delta t = \int_{T_0}^T dT' \frac{C_V(T')}{P(T, T')} \tag{3.13}$$

A suitable model to use for the heat capacity might be the Debye model for a crystalline:

$$C_V(T') = \left. \frac{\partial U}{\partial T'} \right|_V, \quad U = 3VnD_3(x), \quad x = \frac{\theta}{T'}, \tag{3.14}$$

where U is the internal energy, V and n are the volume and number density (number/volume) of the solid, θ is the Debye temperature of the solid, and D_3 is the Debye function (of order 3) defined as

$$D_3(x) = \frac{3}{x^3} \int_0^x dt \frac{t^3}{e^t - 1}. \tag{3.15}$$

A discussion of the cooling of a nanoparticle utilizing the Debye model for its heat capacity can be found in our recent work Ref. [61].

3.1.2 Radiative heat transfer of a uniformly moving particle and the nonequilibrium steady state (NESS)

Now, let us consider what will happen to a nanoparticle moving at constant velocity, \mathbf{v} , with respect to the blackbody background. Physical quantities now become frame dependent. If we perform a Lorentz transformation from the rest frame of the

radiation, \mathcal{R} , to the rest frame of the particle, \mathcal{P} , where the velocity of the particle becomes $\mathbf{v}' = \mathbf{0}$, the derivations above can still be used to calculate the radiative heat transfer in frame \mathcal{P} . We just need to keep in mind that every physical quantity involved is defined in frame \mathcal{P} , and we shall denote those with primes,

$$\mathcal{P}'_{EE}(t') = \int \frac{d\omega}{2\pi} e^{-i\omega t'} \int \frac{d\nu}{2\pi} e^{-i\nu t'} i\nu \langle S\mathbf{E}'(\nu; \mathbf{0}) \cdot \boldsymbol{\alpha}'(\omega) \cdot \mathbf{E}'(\omega; \mathbf{0}) \rangle, \quad (3.16a)$$

$$\mathcal{P}'_{dd}(t) = \int \frac{d\omega}{2\pi} e^{-i\omega t} \int \frac{d\nu}{2\pi} e^{-i\nu t} i\nu \langle S\mathbf{d}'(\omega) \cdot \mathbf{G}'(\nu; \mathbf{0}, \mathbf{0}) \cdot \mathbf{d}'(\nu) \rangle, \quad (3.16b)$$

To quantize the equations in Eq. (3.16), we must apply the FDTs in frame \mathcal{P} . For the field fluctuations, we recall Eq. (2.64)

$$\langle S\mathbf{E}'(\omega, \mathbf{k}_\perp; z) \mathbf{E}'(\nu, \bar{\mathbf{k}}_\perp; \bar{z}) \rangle = (2\pi)^4 \delta(\omega + \nu) \delta(\mathbf{k}_\perp + \bar{\mathbf{k}}_\perp) \Im \mathbf{G}'(\omega, \mathbf{k}_\perp; z, \bar{z}) \coth \left(\frac{\beta \hbar \gamma (\omega + k_x v)}{2} \right) \quad (3.17)$$

and find

$$P'_{EE} = \int \frac{d\omega}{2\pi} \frac{d^2 \mathbf{k}_\perp}{(2\pi)^2} \omega \text{Im } \alpha'(\omega) \text{tr } \text{Im } \mathbf{G}'(\omega, \mathbf{k}_\perp; 0, 0) \coth \left(\frac{\beta \gamma (\omega + k_x v)}{2} \right). \quad (3.18)$$

Notice it is the motion of the particle that breaks the complete translational symmetry of the particle-radiation system and compels us to apply FDT in momentum space. And, we deliberately leave the z coordinates not transformed, so that the equations derived here for vacuum can be readily extended to planar geometries.

For the dipole fluctuations, we use Eq. (2.61)

$$\langle S\mathbf{d}'(\omega) \mathbf{d}'(\nu) \rangle = 2\pi \delta(\omega + \nu) \text{Im } \boldsymbol{\alpha}'(\omega) \coth \left(\frac{\beta' \omega}{2} \right). \quad (3.19)$$

and find

$$P'_{dd} = - \int \frac{d\omega}{2\pi} \frac{d^2 \mathbf{k}_\perp}{(2\pi)^2} \omega \text{Im } \alpha'(\omega) \text{tr } \text{Im } \mathbf{G}'(\omega, \mathbf{k}_\perp; 0, 0) \coth \left(\frac{\beta' \omega}{2} \right). \quad (3.20)$$

The total radiative heat transfer is therefore

$$P' = \int \frac{d\omega}{2\pi} \frac{d^2 \mathbf{k}_\perp}{(2\pi)^2} \omega \text{Im } \alpha'(\omega) \cdot \text{tr } \text{Im } \mathbf{G}'(\omega, \mathbf{k}_\perp; 0, 0) \left\{ \coth \left[\frac{\beta}{2} \gamma (\omega + k_x v) \right] - \coth \left(\frac{\beta' \omega}{2} \right) \right\}. \quad (3.21)$$

For the vacuum background, the Green's tensor is happily invariant in different frames,

$$\begin{aligned} \mathbf{G}'(\omega, \mathbf{k}_\perp; z, \tilde{z}) &= \mathbf{G}(\omega, \mathbf{k}_\perp; z, \tilde{z}) \\ &= \frac{1}{2\kappa} e^{-\kappa|z-\tilde{z}|} \begin{pmatrix} \omega^2 - k_x^2 & -k_x k_y & -ik_x \kappa \text{sgn}(z - \tilde{z}) \\ -k_x k_y & \omega^2 - k_y^2 & -ik_y \kappa \text{sgn}(z - \tilde{z}) \\ ik_x \kappa \text{sgn}(\tilde{z} - z) & ik_y \kappa \text{sgn}(\tilde{z} - z) & k^2 \end{pmatrix}, \end{aligned} \quad (3.22)$$

where $\kappa = \sqrt{k^2 - \omega^2}$. The trace of the Green's tensor evaluated in the coincident limit is therefore

$$\text{tr } \mathbf{G}'(\omega, \mathbf{k}_\perp; z = \tilde{z}) = \frac{\omega^2}{\kappa}. \quad (3.23)$$

Its imaginary part can only arise from κ for $\omega^2 > k^2$,

$$\kappa \Rightarrow -i \text{sgn}(\omega) \sqrt{\omega^2 - k^2}, \quad \omega^2 > k^2, \quad (3.24)$$

where the branch is chosen so that the Green's tensor is retarded. Inserting these into Eq. (3.21), the integration on k_y can be performed. Further, with the change of variable, $k_x = \omega u$ and $y = \gamma(1 + uv)$ the power in Eq. (3.21) can be written as

$$\begin{aligned} P' &= \frac{1}{2\pi^2 \gamma v} \int_0^\infty d\omega \text{Im } \alpha(\omega) \omega^4 \int_{y_-}^{y_+} dy \left[\frac{1}{e^{\beta \omega y} - 1} - \frac{1}{e^{\beta' \omega} - 1} \right], \\ &= \frac{1}{2\pi^2 \gamma v} \int_0^\infty d\omega \text{Im } \alpha(\omega) \omega^4 \left[\frac{1}{\beta \omega} \ln \left(\frac{1 - e^{-\beta \omega y_-}}{1 - e^{-\beta \omega y_+}} \right) - \frac{2\gamma v}{e^{\beta' \omega} - 1} \right] \end{aligned} \quad (3.25)$$

where the integral limits on y are $y_- = \gamma(1 - v)$ and $y_+ = \gamma(1 + v)$. Note we have taken advantage of the integrand's evenness in ω and the cancellation of the divergent piece in the coth factors.

It can be seen that, for nonzero velocity, $P' \neq 0$ when the temperature of the particle is equal to the temperature of the radiation, $\beta' = \beta$. But, for a fixed velocity, there exists a temperature, $\tilde{\beta}$, at which the particle reaches a nonequilibrium steady state (NESS) where there is no net flow of energy between the particle and the background [62]. Therefore, the NESS temperature, $\tilde{\beta}$, can be found as a function

of velocity and the radiation temperature by solving the implicit equation

$$P'(v, \beta, \beta' = \tilde{\beta}) = 0. \quad (3.26)$$

This equation shall be referred to as the NESS condition for the moving particle.

For ease of discussion of the NESS condition, let us define a function

$$I(\xi) = \int_0^\infty d\omega \operatorname{Im} \alpha(\omega) \omega^4 \frac{1}{e^{\xi\omega} - 1}. \quad (3.27)$$

The NESS condition $P' = 0$ can then be written as

$$\int_{y_-}^{y_+} dy I(\tilde{\beta}) = \int_{y_-}^{y_+} dy I(\beta y). \quad (3.28)$$

Using the above, we can eliminate β in Eq. (3.25) and rewrite P' as

$$P' = \frac{1}{\pi^2} [I(\tilde{\beta}) - I(\beta')]. \quad (3.29)$$

Because $I(\xi)$ is a decreasing function, the sign of P' (the direction of the radiative heat transfer) is determined by the deviation of the temperature of the particle from its NESS temperature as below,

$$\begin{cases} T' < \tilde{T} \Rightarrow P' > 0, \\ T' = \tilde{T} \Rightarrow P' = 0, \\ T' > \tilde{T} \Rightarrow P' < 0. \end{cases} \quad (3.30)$$

Imagine the particle slightly deviating from NESS with a temperature lower than the NESS temperature, $T' < \tilde{T}$. According to Eq. (3.30), the particle will absorb net energy thereafter, which will in turn raise the temperature of the particle T' ¹ so that it becomes closer to the NESS temperature \tilde{T} . Likewise, the particle will be cooled down to the NESS temperature if it is initially hotter, $T' > \tilde{T}$. Therefore, the particle would tend to return to NESS after deviating from it.

¹Here, we assume the change of the particle's temperature is adiabatic so that it still has a well-defined temperature while it is away from NESS.

To determine the NESS temperature as a function of the radiation temperature and the velocity, $\tilde{\beta} = \tilde{\beta}(\beta, v)$, requires a specific model for $\text{Im } \alpha(\omega)$. But we may also discuss some general features of the NESS temperature independent of $\text{Im } \alpha(\omega)$.

First of all, in the low velocity limit, $v \ll 1$, the deviation of the NESS temperature from the radiation temperature starts with a quadratic term. There is no linear correction in the velocity,

$$\tilde{\beta} \sim \beta + \mathcal{O}(v^2), \quad v \rightarrow 0. \quad (3.31)$$

In fact, this is not just true for the vacuum case but is general because it directly follows from the v -reflection invariance of the general expression for the radiative heat transfer, P' , in Eq. (3.21). As is seen there, changing the sign of v does not alter P' because the integrand is even under the combined reflection of ω and \mathbf{k}_\perp . So, the NESS inverse temperature, $\tilde{\beta}$, obtained by requiring $P' = 0$, must also be even in v .

Second, independent of the model for $\text{Im } \alpha(\omega)$, the vacuum NESS temperature, \tilde{T} , must be greater than the Planck-Einstein transformed temperature of the blackbody radiation T/γ [63]. We need the following assumptions to prove this theorem:

$$\text{Im } \alpha(\omega) \geq 0 \quad \text{and} \quad \lim_{\omega \rightarrow 0} \omega^4 \text{Im } \alpha(\omega) = 0. \quad (3.32)$$

The first assumption is usually satisfied by a realistic particle made of ordinary lossy materials [64]. The second assumption is to avoid an infrared divergence in Eq. (3.25). Noting γ is the midpoint of the interval $[y_-, y_+]$ and $I(\xi)$ is a decreasing and convex function, that is, $I'(\xi) < 0$ and $I''(\xi) > 0$, the following inequality follows,

$$\int_{y_-}^{y_+} dy I(\beta y) > \int_{y_-}^{y_+} dy I(\beta \gamma). \quad (3.33)$$

Combining Eq. (3.33) and Eq. (3.28), we find

$$\int_{y_-}^{y_+} dy I(\tilde{\beta}) > \int_{y_-}^{y_+} dy I(\beta \gamma). \quad (3.34)$$

Since both $I(\tilde{\beta})$ and $I(\beta \gamma)$ are independent of y , they can be taken out of the

integral. It then follows that $I(\tilde{\beta}) > I(\beta\gamma)$. Recalling $I(\xi)$ is a decreasing function, we conclude

$$\tilde{\beta} < \beta\gamma \Rightarrow \tilde{T} > \frac{T}{\gamma}. \quad (3.35)$$

The theorem therefore predicts the Planck-Einstein temperature is a lower bound for the NESS temperature of a particle moving in vacuum. In proving this, we used the NESS condition for an isotropic particle. However, this conclusion also applies to particles with a nonisotropic but diagonal polarizability. The more general proof for this theorem can be found in Ref. [22].

3.1.3 Quantum vacuum friction in the rest frame of the particle

We now turn to the calculation of the frictional force caused by electromagnetic radiation in the rest frame of the particle, \mathcal{P} . According to Chapter 2, the force can be obtained by differentiating the free energy with respect to the spatial coordinates in the field operator. We are interested in finding the force parallel to the motion of the particle, which we assume to be the x direction. It can therefore be written out as ²

$$\begin{aligned} F'(t') &= -\frac{\partial}{\partial x'} \mathcal{F}'(t') = \frac{\partial}{\partial x'} \mathbf{d}'(t') \cdot \mathbf{E}'(t', \mathbf{r}')|_{\mathbf{r}' \rightarrow \mathbf{0}} \\ &= -\int \frac{d\omega}{2\pi} \int \frac{d\nu}{2\pi} \int \frac{d^2 \mathbf{k}_\perp}{(2\pi)^2} e^{-i(\omega+\nu)t'} (ik_x) \mathfrak{F}'(\omega, \nu, \mathbf{k}_\perp; 0), \end{aligned} \quad (3.36)$$

where \mathfrak{F}' is the Fourier transform of the free energy, \mathcal{F}' ,

$$\mathfrak{F}'(\omega, \nu, \mathbf{k}_\perp; 0) = -\mathbf{d}'(\omega) \cdot \mathbf{E}'(\nu, \mathbf{k}_\perp; z' = 0). \quad (3.37)$$

Expanding the dipole operator as

$$\mathbf{d}'(\omega) = \boldsymbol{\alpha}'(\omega) \cdot \mathbf{E}'(\omega; \tilde{\mathbf{r}}' = \mathbf{0}) = \boldsymbol{\alpha}'(\omega) \cdot \int \frac{d^2 \bar{\mathbf{k}}_\perp}{(2\pi)^2} \mathbf{E}'(\omega, \bar{\mathbf{k}}_\perp; \tilde{z}' = 0), \quad (3.38)$$

²We will drop the subscript x on the frictional force throughout the thesis.

we obtain the contribution from the field fluctuations to be

$$F'_{EE}(t') = \int \frac{d\omega}{2\pi} \frac{d\nu}{2\pi} \frac{d^2\mathbf{k}_\perp}{(2\pi)^2} \frac{d^2\bar{\mathbf{k}}_\perp}{(2\pi)^2} e^{-i(\omega+\nu)t'} (ik_x) \langle S\mathbf{E}'(\nu, \mathbf{k}_\perp; z' = 0) \cdot \boldsymbol{\alpha}'(\omega) \cdot \mathbf{E}'(\omega, \bar{\mathbf{k}}_\perp; \tilde{z}' = 0) \rangle, \quad (3.39)$$

Upon quantization using Eq. (2.64), it becomes

$$F'_{EE} = \int \frac{d\nu}{2\pi} \frac{d^2\mathbf{k}_\perp}{(2\pi)^2} k_x \text{Im } \boldsymbol{\alpha}'(\nu) \cdot \text{Im } \mathbf{G}'(\nu, \mathbf{k}_\perp; 0, 0) \coth \left[\frac{\beta}{2} \gamma(\nu + k_x v) \right], \quad (3.40)$$

where we have used the symmetry property, $\text{Im } \boldsymbol{\alpha}'(-\nu) = -\text{Im } \boldsymbol{\alpha}'(\nu)$.

If we expand the field operator in Eq. (3.36),

$$\mathbf{E}'(\nu, \mathbf{k}_\perp; z' = 0) = \int d\tilde{z}' \mathbf{G}'(\nu, \mathbf{k}_\perp; 0, \tilde{z}') \cdot \mathbf{P}'(\nu, \mathbf{k}; \tilde{z}') = \mathbf{G}'(\nu, \mathbf{k}_\perp; 0, 0) \cdot \mathbf{d}'(\nu), \quad (3.41)$$

where $\mathbf{P}'(\nu, \mathbf{k}; \tilde{z}') = \mathbf{d}'(\nu) \delta(\tilde{z}')$, we obtain the contribution to the force from the dipole fluctuations,

$$F'_{dd}(t') = \int \frac{d\omega}{2\pi} \int \frac{d\nu}{2\pi} \int \frac{d^2\mathbf{k}_\perp}{(2\pi)^2} e^{-i(\omega+\nu)t'} ik_x \langle S\mathbf{d}'(\omega) \cdot \mathbf{G}'(\nu, \mathbf{k}_\perp; 0, 0) \cdot \mathbf{d}'(\nu) \rangle. \quad (3.42)$$

Quantizing it with Eq. (2.61), we find

$$F'_{dd} = - \int \frac{d\omega}{2\pi} \frac{d^2\mathbf{k}_\perp}{(2\pi)^2} k_x \text{Im } \boldsymbol{\alpha}'(\omega) \cdot \text{Im } \mathbf{G}'(\omega, \mathbf{k}_\perp; 0, 0) \coth \left(\frac{\beta'\omega}{2} \right). \quad (3.43)$$

The two contributions combine to give the total frictional force in frame \mathcal{P} ,

$$F' = \int \frac{d\omega}{2\pi} \frac{d^2\mathbf{k}_\perp}{(2\pi)^2} k_x \text{Im } \boldsymbol{\alpha}'(\omega) \cdot \text{Im } \mathbf{G}'(\omega, \mathbf{k}_\perp; 0, 0) \left\{ \coth \left[\frac{\beta}{2} \gamma(\omega + k_x v) \right] - \coth \left(\frac{\beta'\omega}{2} \right) \right\}, \quad (3.44)$$

which is a general expression for F' and can be applied to different configurations.

Note that all the components of the vacuum Green's tensor in Eq. (3.22) are even in k_x , except for G_{xz} and G_{zx} , which are vanishing in the coincident spatial limit. As a result, when we specify the background to be vacuum, the second term in Eq. (3.44), originating from the dd fluctuations, will not contribute because of its oddness in k_x . The QVF in frame \mathcal{P} is therefore only originates from the field fluctuations and only depends on the radiation temperature. For an isotropic

particle, we find

$$\begin{aligned}
F' &= \frac{1}{2\pi^2\gamma^2v^2} \int_0^\infty d\omega \omega^4 \operatorname{Im} \alpha'(\omega) \int_{y_-}^{y_+} dy \frac{(y - \gamma)}{e^{\beta\omega y} - 1} \\
&= \frac{1}{2\pi^2\gamma^2v^2} \int_{y_-}^{y_+} dy (y - \gamma) I(\beta y),
\end{aligned} \tag{3.45}$$

where $I(\xi)$ is already defined in Eq. (3.27). If the $I(\beta y)$ factor were not present, the integral in Eq. (3.45) would be zero. Recalling that $I(\xi)$ monotonically decreases, we can conclude that F' is negative definite. That is, it is a true drag. This has an important physical implication: to maintain the particle's relative motion through the blackbody background, an external force in the direction of the motion,

$$F'_{ext} = -F' \tag{3.46}$$

is required.

3.1.4 Quantum vacuum frictional force in the rest frame of radiation

The frictional force we derive in Sec. 3.1.3 is the friction observed in frame \mathcal{P} , which balances the external force needed to keep the particle moving relative to the surrounding blackbody radiation. But, what does the frictional force look like in the rest frame of radiation, \mathcal{R} ? Will it still be negative definite? There are two ways of approaching this. We will defer the quick but slick approach to Sec. 3.1.5. In this section, let us perform an honest calculation again by applying the principle of virtual work in frame \mathcal{R} .

In Chapter 2.1, we have derived the force on a moving dipole to be

$$\mathbf{F}(t) = -\nabla\mathcal{F}(t), \quad \mathcal{F}(t) = -\mathbf{d}(t) \cdot \mathbf{E}(t, \mathbf{vt}) - \mathbf{d}(t) \times \mathbf{v} \cdot \mathbf{B}(t, \mathbf{vt}), \tag{3.47}$$

where we have ignored the total time derivative of the Röntgen momentum, $\mathbf{d}(t) \times \mathbf{B}(t, \mathbf{vt})$ since it does not contribute to the frictional force upon quantization using FDT.

We will assume the particle moves in the following trajectory:

$$\mathbf{r}(t) = (x = vt, y = 0, z = a), \tag{3.48}$$

where we deliberately keep the z coordinate nonzero so that the derivation below can be easily generalized to the problems with a planar interface lying at $z = 0$. Of course, this makes no difference to the vacuum case discussed here, for it shall be independent of the position of the particle. The frictional force (the x component of the quantized Lorentz force) therefore is,

$$F(t) = \partial_x \{ \mathbf{d}(t) \cdot \mathbf{E}(t, \mathbf{r}) + v [d_z(t)B_y(t, \mathbf{r}) - d_y(t)B_z(t, \mathbf{r})] \} |_{\mathbf{r}=\mathbf{r}(t)}. \quad (3.49)$$

Let us Fourier transform Eq. (3.49) in time and two transverse spatial directions (again, to keep our discussion readily extensible to planar geometry):

$$F(t) = - \int \frac{d\omega}{2\pi} \frac{d\nu}{2\pi} \frac{d^2\mathbf{k}_\perp}{(2\pi)^2} e^{-i(\omega+\nu-k_x v)t} (ik_x) \mathfrak{F}(\omega, \nu, \mathbf{k}_\perp; a),$$

where $\mathfrak{F}(\omega, \nu, \mathbf{k}_\perp; a) = -\mathbf{d}(\omega) \cdot \mathbf{E}(\nu, \mathbf{k}_\perp; a) - v [d_z(\omega)B_y(\nu, \mathbf{k}_\perp; a) - d_y(\omega)B_z(\nu, \mathbf{k}_\perp; a)]$.

$$(3.50)$$

Here, \mathfrak{F} is precisely the Fourier transform of the free energy expressed in terms of the dipole and fields in frame \mathcal{R} . Using the Faraday's law

$$i\nu\mathbf{B}(\nu; \mathbf{r}) = \nabla \times \mathbf{E}(\nu; \mathbf{r}) \quad (3.51)$$

we can eliminate the magnetic fields in \mathfrak{F} and obtain

$$\begin{aligned} \mathfrak{F}(\omega, \nu, \mathbf{k}_\perp; a) &= -\mathbf{d}(\omega) \cdot \mathbf{E}(\nu, \mathbf{k}_\perp; a) \\ &- \frac{v}{i\nu} \{ d_z(\omega) [ik_z E_x(\nu, \mathbf{k}_\perp; a) - ik_x E_z(\nu, \mathbf{k}_\perp; a)] - d_y(\omega) [ik_x E_y(\nu, \mathbf{k}_\perp; a) - ik_y E_x(\nu, \mathbf{k}_\perp; a)] \}. \end{aligned} \quad (3.52)$$

Ideally, we want to quantize the frictional force Eq. (3.50) in frame \mathcal{P} . Let us then try to express it in terms of the dipole and fields in frame \mathcal{P} . To do that, we need the proper Lorentz transformations for dipole moment and field operators in Appendix A. It is then convenient to use the frequency and momentum attached to frame \mathcal{P} (denoted by primes) as new integration variables,

$$\omega' = \gamma\omega, \quad \nu' = \gamma(\nu - k_x v), \quad k'_x = \gamma(k_x - \nu v), \quad k'_y = k_y, \quad (3.53)$$

After the Lorentz transformation, the frictional force becomes

$$F(t) = - \int \frac{d\omega'}{2\pi} \frac{d\nu'}{2\pi} \frac{d^2\mathbf{k}'_{\perp}}{(2\pi)^2} e^{-i(\omega'+\nu')\frac{t}{\gamma}} [i\gamma(k'_x + \nu'v)] \mathfrak{F}(\omega', \nu', \mathbf{k}'_{\perp}; a), \quad (3.54)$$

where

$$\begin{aligned} \mathfrak{F}(\omega', \nu', \mathbf{k}'_{\perp}; a) = & -\frac{1}{\gamma} \left(d'_x(\omega') E'_x(\nu', \mathbf{k}'_{\perp}; a) \right. \\ & + \frac{d'_y(\omega')}{\nu' + k'_x v} \left\{ \nu' [E'_y(\nu', \mathbf{k}'_{\perp}; a) + v B'_z(\nu', \mathbf{k}'_{\perp}; a)] + k'_y v E'_x(\nu', \mathbf{k}'_{\perp}; a) \right\} \\ & \left. + \frac{d'_z(\omega')}{\nu' + k'_x v} \left\{ \nu' [E'_z(\nu', \mathbf{k}'_{\perp}; a) - v B'_y(\nu', \mathbf{k}'_{\perp}; a)] - i v \partial_z E'_x(\nu', \mathbf{k}'_{\perp}; a) \right\} \right). \end{aligned} \quad (3.55)$$

Notice the Lorentz transformations reintroduce the magnetic fields in Eq. (3.55). Once again, we should express them in terms of electric fields using Faraday's law in momentum space,

$$\begin{aligned} i\nu' B'_y(\nu', \mathbf{k}'_{\perp}; a) &= \partial_z E'_x(\nu', \mathbf{k}'_{\perp}; a) - i k'_x E'_z(\nu', \mathbf{k}'_{\perp}; a) \\ i\nu' B'_z(\nu', \mathbf{k}'_{\perp}; a) &= i k'_x E'_y(\nu', \mathbf{k}'_{\perp}; a) - i k'_y E'_x(\nu', \mathbf{k}'_{\perp}; a). \end{aligned} \quad (3.56)$$

Inserting Eq. (3.56) into Eq. (3.55) and reorganizing the terms, we find, miraculously,

$$\mathfrak{F}(\omega', \nu', \mathbf{k}'_{\perp}; a) = -\frac{1}{\gamma} \mathbf{d}'(\omega') \cdot \mathbf{E}'(\nu', \mathbf{k}'_{\perp}; a). \quad (3.57)$$

When it is compared with Eq. (3.37), we find a simple relationship between the free energies in the two frames,

$$\mathfrak{F} = \frac{1}{\gamma} \mathfrak{F} \quad \Rightarrow \quad \mathcal{F} = \frac{1}{\gamma} \mathcal{F} \quad (3.58)$$

Back to Eq. (3.54), the frictional force therefore reads

$$F(t) = \int \frac{d\omega'}{2\pi} \frac{d\nu'}{2\pi} \frac{d^2\mathbf{k}'_{\perp}}{(2\pi)^2} e^{-i(\omega'+\nu')\frac{t}{\gamma}} [i(k'_x + \nu'v)] \mathbf{d}'(\omega') \cdot \mathbf{E}'(\nu', \mathbf{k}'_{\perp}; a). \quad (3.59)$$

Comparing Eq. (3.59) for F with Eq. (3.36) for F' , the main differences are the shift in the momentum factor, $k'_x \rightarrow k'_x + \nu'v$, and the slightly different time argument

on the exponential, t/γ , where the latter can be recognized as the proper time attached to the particle. So, we can follow the same quantization procedure outlined in Sec. 3.1.3 to quantize Eq. (3.124). Adding the contributions from the field fluctuations and the dipole fluctuations, we obtain

$$F = \int \frac{d\nu'}{2\pi} \frac{d^2\mathbf{k}'}{(2\pi)^3} (k'_x + \nu'v) \text{Im } \boldsymbol{\alpha}'(\nu') \cdot \text{Im } \mathbf{G}'(\nu', \mathbf{k}'_{\perp}; a, a) \left\{ \coth \left[\frac{\beta}{2} \gamma (\nu' + k'_x v) \right] - \coth \left(\frac{\beta \nu'}{2} \right) \right\}. \quad (3.60)$$

Apparently, F can be written as

$$F = F' + P'v, \quad (3.61)$$

where P' is the radiative heat transfer in Eq. (3.21) and F' is the quantum friction in Eq. (3.44). If we further impose the NESS condition, $P' = 0$, the frictional force in \mathcal{R} becomes identical to that in \mathcal{P} . That is, for a particle in NESS, the frictional force on the particle is

$$\tilde{F} = F'. \quad (3.62)$$

It is negative definite and should be balanced by the external force, F_{ext} , so that the total force on the particle is zero,

$$\tilde{F}_{tot} = \tilde{F} + F_{ext} = 0 \quad (3.63)$$

In general, the particle can be out of NESS, $P' \neq 0$. In particular, the sign of P' can be positive for $T' < \tilde{T}$. The particle can absorb energy when it is cooler than the NESS temperature. In this case, the positive non-NESS contribution to the force, vP' , could overcome the negative definite contribution, F' , and could render F positive. That is, the frictional force induced by fluctuations appears to be a push instead of a drag in the rest frame of radiation!

In addition, when the particle is out of NESS, the total force on it will be nonzero. In the rest frame of radiation, \mathcal{R} , applying the Newton's second law to the moving particle, we have

$$F_{tot} = F + F_{ext} = \frac{d}{dt} \gamma m v. \quad (3.64)$$

Here, m is the rest mass of the particle, which varies when the particle absorbs or emits net energy. Since the particle is moving with constant velocity, the rate of change of the particle's momentum is only due to its mass change,

$$\frac{d}{dt}\gamma mv = \frac{dm}{dt'}v = P'v, \quad (3.65)$$

where we have used the time dilation relation, $dt = \gamma dt'$ and identified the rate of change in the particle's mass with rate of change in internal energy of the particle through the radiative heat transfer. The relations Eq. (3.61)–Eq. (3.65), leads to

$$F_{ext} = -F'. \quad (3.66)$$

Recalling again Eq. (3.46), we find the same amount of external force is needed whichever frame we are viewing the interplay between the particle and radiation fields,

$$F_{ext} = -F' = F'_{ext}. \quad (3.67)$$

All of the above remarks are general. But, let us now use Eq. (3.60) to evaluate the quantum frictional force that an isotropic particle feels in vacuum. After inserting the vacuum Green's tensor, we find

$$F = \frac{1}{2\pi^2\gamma^2v^2} \int_0^\infty d\omega \omega^4 \text{Im} \alpha(\omega) \int_{y_-}^{y_+} dy \left(y - \frac{1}{\gamma} \right) \left[\frac{1}{e^{\beta\omega y} - 1} - \frac{1}{e^{\beta'\omega} - 1} \right]. \quad (3.68)$$

Some numerical results regarding to both the NESS temperature and NESS frictional force for a gold nanosphere is given in Ref. [22].

3.1.5 Interrelations between the powers and forces in different frames

We have calculated P' in Sec. 3.1.2. It tells us the rate that the particle emits or absorbs energy. Now, we turn to the calculation of the power in frame \mathcal{R} , P , which tells us the rate that the radiation field is doing work on the particle.

Exactly parallel to the discussion in Sec. 3.59 for the frictional force, let us write

down from the first principle:

$$\mathbf{P}(t) = \frac{\partial}{\partial t} \mathcal{F}(t), \quad \mathcal{F}(t) = -\mathbf{d}(t) \cdot \mathbf{E}(t, \mathbf{v}t) - \mathbf{d}(t) \times \mathbf{v} \cdot \mathbf{B}(t, \mathbf{v}t). \quad (3.69)$$

This can be Fourier transformed to yield

$$P(t) = \int \frac{d\omega}{2\pi} \frac{d\nu}{2\pi} \frac{d^2 \mathbf{k}_\perp}{(2\pi)^2} e^{-i(\omega+\nu-k_x v)t} (i\nu) \mathfrak{F}(\omega, \nu, \mathbf{k}_\perp; a), \quad (3.70)$$

where $\mathfrak{F}(\omega, \nu, \mathbf{k}_\perp; a)$ is still the Fourier transformed free energy as defined in Eq. (3.50).

With the coordinate transformation in Eq. (3.53), \mathfrak{F} can be rewritten in terms of the dipole and field operator in frame \mathcal{P} as

$$\mathfrak{F}(\omega', \nu', \mathbf{k}'_\perp; a) = -\frac{1}{\gamma} \mathbf{d}'(\omega') \cdot \mathbf{E}'(\nu', \mathbf{k}'_\perp; a). \quad (3.71)$$

As a result, the radiation power reads

$$P(t) = \int \frac{d\omega'}{2\pi} \frac{d\nu'}{2\pi} \frac{d^2 \mathbf{k}'_\perp}{(2\pi)^2} e^{-i(\omega'+\nu')\frac{t}{\gamma}} [i(\nu' + k'_x v)] \mathbf{d}'(\omega') \cdot \mathbf{E}'(\nu', \mathbf{k}'_\perp; a). \quad (3.72)$$

After quantization using FDT, we obtain

$$P = \int \frac{d\omega'}{2\pi} \frac{d\nu'}{2\pi} \frac{d^3 \mathbf{k}'}{(2\pi)^3} (\nu' + k'_x v) \text{Im } \boldsymbol{\alpha}'(\nu') \cdot \text{Im } \mathbf{G}'(\nu', \mathbf{k}') \left(\coth \frac{\beta\gamma(\nu' + k'_x v)}{2} - \coth \frac{\beta\nu'}{2} \right). \quad (3.73)$$

Specifying the background to be vacuum and the particle to be isotropic leads to

$$P = \frac{1}{2\pi^2 \gamma^2 v} \int_0^\infty d\omega \text{Im } \alpha(\omega) \omega^4 \int_{y_-}^{y_+} dy y \left(\frac{1}{e^{\beta\omega y} - 1} - \frac{1}{e^{\beta'\omega} - 1} \right). \quad (3.74)$$

This expression agrees with the time component of the four-force that Pieplow and Henkel derive for blackbody friction in Ref. [65] using a fully covariant formulation, and with the thermal radiation power (a different sign convention is used there, though) obtained by Dedkov and Kyasov in Ref. [66].

Just as in Eq. (3.61) for F , P can be expressed in terms of P' and $F'v$ as well:

$$P = P' + F'v. \quad (3.75)$$

Even if the particle is in NESS, $P' = 0$, the rate of work done on the particle

$$\tilde{P} = F'v \quad (3.76)$$

is nonzero unless the particle is stationary relative to the radiation background.

The relations, Eq. (3.61) and Eq. (3.75), which express F and P in terms of F' and P' , are general and hold whether the particle is in or out of NESS. We will benefit from these interrelations because the calculations for F' and P' are easier.

We arrive at these relations by examining the results derived from first principles. One might wonder if these relations follow, from a simpler explanation. We attempt to give one by assuming the existence of an effective static action describing the interaction between the particle and radiation. Of course, the action should be Lorentz invariant,

$$W = -\mathcal{F}\mathcal{T} = -\mathcal{F}'\mathcal{T}', \quad (3.77)$$

where \mathcal{F} and \mathcal{F}' are the interacting free energies and \mathcal{T} and \mathcal{T}' are the duration of the configuration. The latter two are related by the time dilation relation, $\mathcal{T} = \gamma\mathcal{T}'$, which then leads to

$$\mathcal{F} = \frac{1}{\gamma}\mathcal{F}', \quad (3.78)$$

which is confirmed in Eq. (3.58) by a detailed calculation of the free energies. Utilizing the transformation of the free energy, one can derive the transformations for power and force between the two frames, \mathcal{R} and \mathcal{P} symbolically as below:

$$P = \frac{\partial}{\partial t}\mathcal{F} = \gamma \left(\frac{\partial}{\partial t'} - v\frac{\partial}{\partial x'} \right) \frac{1}{\gamma}\mathcal{F}' = \left(\frac{\partial}{\partial t'} - v\frac{\partial}{\partial x'} \right) \mathcal{F}' = P' + vF', \quad (3.79a)$$

$$F = -\frac{\partial}{\partial x}\mathcal{F} = -\gamma \left(\frac{\partial}{\partial x'} - v\frac{\partial}{\partial t'} \right) \frac{1}{\gamma}\mathcal{F}' = - \left(\frac{\partial}{\partial x'} - v\frac{\partial}{\partial t'} \right) \mathcal{F}' = F' + vP'. \quad (3.79b)$$

This derivation is rather formal, because the derivatives involved are to be understood as only differentiating the field operators in the free energy. (The free energy is, otherwise, independent of time and spatial coordinates.) Nonetheless, the transformation of the derivatives here essentially carries out the Lorentz transformation of the frequency and momentum in the Fourier space. As a result, it does leads to the right interrelations for both the power and force.

3.2 Quantum Vacuum Frictional Effects on a Nondissipative Particle in Vacuum

Continuing our previous investigations, let us now consider a particle whose polarizability is purely real before it is dressed by radiation. The particle is then guaranteed to be in the nonequilibrium steady state (NESS), where it absorbs and emits energy at the same rate, $P' = 0$. In NESS, the quantum vacuum frictional force, $F = F'$, is shown to be a true drag, independent of the model for polarizability and the polarization state of the particle. And the electromagnetic work done on the particle in frame \mathcal{R} is precisely given by $P = Fv$. Finally we also give an estimate of the quantum vacuum friction on a gold atom and comment on the feasibility of detecting such quantum vacuum frictional effects.

3.2.1 Second order in polarizability

For a nondissipative particle, $\text{Im } \alpha(\omega) = 0$, therefore, the quantum frictional power and forces derived in Sec. 3.1 would all vanish. However, quantum frictional effects can still arise, if these expressions are expanded to the second order in the real polarizability, $\alpha(\omega)$.

We have learned that P' , F' , F and P can all be derived from the free energy in frame \mathcal{P} ,

$$\mathcal{F}'(t') = - \int \frac{d\omega}{2\pi} e^{-i\omega t'} \mathbf{d}'(\omega) \cdot \int \frac{d\nu}{2\pi} \int \frac{d^2\mathbf{k}_\perp}{(2\pi)^2} e^{-i\nu t'} \mathbf{E}'(\nu, \mathbf{k}_\perp; a). \quad (3.80)$$

Their interrelations in Eq. (3.79) is still true for a nondissipative particle. Through these relations, we will know all four quantities with the knowledge of any two of them.

Let us first try to calculate the radiative heat transfer, P' , which can be obtained by taking the time derivative of the field operator in the expression for free energy,

$$P'(t') = \int \frac{d\omega}{2\pi} e^{-i(\omega+\nu)t'} \int \frac{d\nu}{2\pi} \int \frac{d^2\mathbf{k}_\perp}{(2\pi)^2} (i\nu) \mathbf{d}'(\omega) \cdot \mathbf{E}'(\nu, \mathbf{k}_\perp; a) \quad (3.81)$$

If we only expand the expression to first order in $\alpha(\omega)$ as in Eq. (3.16), we find

both the EE and dd contributions will vanish because $\alpha(\omega)$ only has a real part, which is even in ω . Therefore, we have to at least expand Eq. (3.81) to second order in α . There exist two routes for the expansion, which corresponds to the contribution from direct field fluctuation and that from the induced dipole fluctuation, respectively.

The first route is to expand only the dipole operator to second order in α as

$$\begin{aligned}
\mathbf{d}'(\omega) &= \alpha'(\omega) \cdot \int \frac{d^2 \bar{\mathbf{k}}_{\perp}}{(2\pi)^2} \mathbf{E}'(\omega, \bar{\mathbf{k}}_{\perp}; a) \\
&= \alpha'(\omega) \cdot \int \frac{d^2 \bar{\mathbf{k}}_{\perp}}{(2\pi)^2} \mathbf{G}'(\omega, \bar{\mathbf{k}}_{\perp}; a, a) \cdot \mathbf{d}'(\omega) \\
&= \alpha'(\omega) \cdot \int \frac{d^2 \bar{\mathbf{k}}_{\perp}}{(2\pi)^2} \mathbf{G}'(\omega, \bar{\mathbf{k}}_{\perp}; a, a) \cdot \alpha'(\omega) \cdot \int \frac{d^2 \tilde{\mathbf{k}}_{\perp}}{(2\pi)^2} \mathbf{E}'(\omega, \tilde{\mathbf{k}}_{\perp}; a). \tag{3.82}
\end{aligned}$$

Replacing the dipole operator in Eq. (3.81) with Eq. (3.82) gives the contribution from direct field fluctuation

$$\begin{aligned}
P'_{EE}(t') &= \int \frac{d\omega}{2\pi} \frac{d\nu}{2\pi} \frac{d^2 \mathbf{k}_{\perp}}{(2\pi)^2} \frac{d^2 \bar{\mathbf{k}}_{\perp}}{(2\pi)^2} \frac{d^2 \tilde{\mathbf{k}}_{\perp}}{(2\pi)^2} e^{i(\omega+\nu)t'} (i\nu) \\
&\quad \times \mathbf{E}'(\nu, \mathbf{k}_{\perp}; a) \cdot \alpha'(\omega) \cdot \mathbf{G}'(\omega, \bar{\mathbf{k}}_{\perp}; a, a) \cdot \alpha'(\omega) \cdot \mathbf{E}'(\omega, \tilde{\mathbf{k}}_{\perp}; a). \tag{3.83}
\end{aligned}$$

Using the FDT in Eq. (2.64) for the product of the two \mathbf{E} operators in frame \mathcal{P} , we obtain

$$\begin{aligned}
P'_{EE} &= \int \frac{d\nu}{2\pi} \frac{d^2 \mathbf{k}_{\perp}}{(2\pi)^2} \frac{d^2 \bar{\mathbf{k}}_{\perp}}{(2\pi)^2} (i\nu) \alpha'(-\nu) \cdot \mathbf{G}'(-\nu, \bar{\mathbf{k}}_{\perp}; a, a) \cdot \alpha'(-\nu) \cdot \text{Im} \mathbf{G}'(\nu, \mathbf{k}_{\perp}; a, a) \\
&\quad \times \coth \frac{\beta\gamma(\nu + k_x v)}{2}. \tag{3.84}
\end{aligned}$$

Considering the symmetry properties of the polarizability and the Green's tensor, it is the imaginary part of the first Green's tensor that will be picked up and P'_{EE} can be rewritten as

$$\begin{aligned}
P'_{EE} &= \int \frac{d\nu}{2\pi} \frac{d^2 \mathbf{k}_{\perp}}{(2\pi)^2} \frac{d^2 \bar{\mathbf{k}}_{\perp}}{(2\pi)^2} \nu \alpha'(\nu) \cdot \text{Im} \mathbf{G}'(\nu, \bar{\mathbf{k}}_{\perp}; a, a) \cdot \alpha'(\nu) \cdot \text{Im} \mathbf{G}'(\nu, \mathbf{k}_{\perp}; a, a) \\
&\quad \times \coth \frac{\beta\gamma(\nu + k_x v)}{2}. \tag{3.85}
\end{aligned}$$

The second route is to expand both the dipole operator and the field operator

in Eq. (3.81) to first order in the polarizability so that their product is still second order in α :

$$\begin{aligned} \mathbf{d}'(\omega) &= \boldsymbol{\alpha}'(\omega) \cdot \int \frac{d^2 \bar{\mathbf{k}}_{\perp}}{(2\pi)^2} \mathbf{E}'(\nu, \bar{\mathbf{k}}_{\perp}; a) \\ \mathbf{E}'(\nu, \mathbf{k}_{\perp}; a) &= \mathbf{G}'(\nu, \mathbf{k}_{\perp}; a, a) \cdot \mathbf{d}'(\nu) = \mathbf{G}'(\nu, \mathbf{k}_{\perp}; a, a) \cdot \boldsymbol{\alpha}'(\nu) \cdot \int \frac{d^2 \tilde{\mathbf{k}}_{\perp}}{(2\pi)^2} \mathbf{E}'(\nu, \tilde{\mathbf{k}}_{\perp}; a). \end{aligned} \quad (3.86)$$

Notice both dipole operators in Eq. (3.86) are induced by the field through the polarizability. No intrinsic dipole fluctuation exists in the nondissipative particle. However, we may say that this expansion results in a contribution from the induced dipole fluctuation due to field fluctuations,

$$\begin{aligned} P'_{dd}(t') &= \int \frac{d\omega}{2\pi} \frac{d\nu}{2\pi} \frac{d^2 \mathbf{k}_{\perp}}{(2\pi)^2} \frac{d^2 \bar{\mathbf{k}}_{\perp}}{(2\pi)^2} \frac{d^2 \tilde{\mathbf{k}}_{\perp}}{(2\pi)^2} e^{i(\omega+\nu)t'} (i\nu) \\ &\quad \times \boldsymbol{\alpha}'(\omega) \cdot \mathbf{E}'(\omega, \bar{\mathbf{k}}_{\perp}; a) \cdot \mathbf{G}'(\nu, \mathbf{k}_{\perp}; a, a) \cdot \boldsymbol{\alpha}'(\nu) \cdot \mathbf{E}'(\nu, \tilde{\mathbf{k}}_{\perp}; a). \end{aligned} \quad (3.87)$$

Upon quantization using FDT and considering the symmetry properties, we find

$$\begin{aligned} P'_{dd} &= - \int \frac{d\nu}{2\pi} \frac{d^2 \mathbf{k}_{\perp}}{(2\pi)^2} \frac{d^2 \tilde{\mathbf{k}}_{\perp}}{(2\pi)^2} \nu \boldsymbol{\alpha}'(\nu) \cdot \text{Im} \mathbf{G}'(\nu, \tilde{\mathbf{k}}_{\perp}; a, a) \cdot \boldsymbol{\alpha}'(\nu) \cdot \text{Im} \mathbf{G}'(\nu, \mathbf{k}_{\perp}; a, a) \\ &\quad \times \coth \frac{\beta\gamma(\nu + \tilde{k}_x v)}{2}. \end{aligned} \quad (3.88)$$

Adding the two contributions in Eq. (3.85) and Eq. (3.88), we find the total radiative heat transfer for the nondissipative particle vanishes,

$$P' = 0. \quad (3.89)$$

That is, the nondissipative particle is guaranteed to be in NESS while it interacts with the surrounding radiation fields. The explanation for this can be both intuitive and profound. Intuitively, a nondissipative particle with a purely real intrinsic polarizability, $\text{Im} \alpha(\omega) = 0$, can only act as an energy bookkeeper precisely because of its lack of ability to either store or release net energy. More profoundly, this relates to the fact that its effective polarizability (that is, the polarizability after dressing by the radiation), $\hat{\alpha}(\omega)$, satisfies the optical theorem, $\text{Im} \hat{\alpha}(\omega) = \text{Im} \Gamma'(\omega) |\hat{\alpha}(\omega)|^2$

[67, 21].

Next, let us calculate the quantum friction in frame \mathcal{P} , F' , which can be obtained by taking the spatial derivative (with a minus sign) of the field operator in the free energy,

$$F'(t') = \int \frac{d\omega}{2\pi} e^{-i(\omega+\nu)t'} \int \frac{d\nu}{2\pi} \int \frac{d^2\mathbf{k}_\perp}{(2\pi)^2} (ik_x) \mathbf{d}'(\omega) \cdot \mathbf{E}'(\nu, \mathbf{k}_\perp; a). \quad (3.90)$$

Comparing F' in Eq. (3.90) with P' in Eq. (3.81), it is apparent that F' can be obtained from P' by the replacement, $\nu \rightarrow k_x$. We then find, immediately,

$$F'_{EE} = \int \frac{d\nu}{2\pi} \frac{d^2\mathbf{k}_\perp}{(2\pi)^2} \frac{d^2\bar{\mathbf{k}}_\perp}{(2\pi)^2} k_x \boldsymbol{\alpha}'(\nu) \cdot \text{Im } \mathbf{G}'(\nu, \bar{\mathbf{k}}_\perp; a, a) \cdot \boldsymbol{\alpha}'(\nu) \cdot \text{Im } \mathbf{G}'(\nu, \mathbf{k}_\perp; a, a) \\ \times \coth \frac{\beta\gamma(\nu + k_x v)}{2}. \quad (3.91a)$$

$$F'_{dd} = - \int \frac{d\nu}{2\pi} \frac{d^2\mathbf{k}_\perp}{(2\pi)^2} \frac{d^2\tilde{\mathbf{k}}_\perp}{(2\pi)^2} k_x \boldsymbol{\alpha}'(\nu) \cdot \text{Im } \mathbf{G}'(\nu, \tilde{\mathbf{k}}_\perp; a, a) \cdot \boldsymbol{\alpha}'(\nu) \cdot \text{Im } \mathbf{G}'(\nu, \mathbf{k}_\perp; a, a) \\ \times \coth \frac{\beta\gamma(\nu + \tilde{k}_x v)}{2}. \quad (3.91b)$$

Notice k_x appears in the Doppler shift of the thermal factor for F'_{EE} but not F'_{dd} . As a result, when the two terms are added, the total friction is nonzero and can be written as

$$F' = \int \frac{d\nu}{2\pi} \frac{d^2\mathbf{k}_\perp}{(2\pi)^2} \frac{d^2\bar{\mathbf{k}}_\perp}{(2\pi)^2} (k_x - \bar{k}_x) \boldsymbol{\alpha}'(\nu) \cdot \text{Im } \mathbf{G}'(\nu, \bar{\mathbf{k}}_\perp; a, a) \cdot \boldsymbol{\alpha}'(\nu) \cdot \text{Im } \mathbf{G}'(\nu, \mathbf{k}_\perp; a, a) \\ \times \coth \frac{\beta\gamma(\nu + k_x v)}{2}. \quad (3.92)$$

Therefore, though an energy bookkeeper, the particle acts as a momentum converter. Due to the relative motion between the particle and the blackbody radiation, the radiation carries a momentum bias and causes a blackbody wind blowing on the particle. It is precisely this momentum bias that is transferred to the particle and gives rise to the quantum vacuum friction on the particle.

Since the particle is in NESS, $P' = 0$, according to the interrelation Eq. (3.79), we find the quantum friction is the same in frame \mathcal{R} as in frame \mathcal{P}

$$F = F', \quad (3.93)$$

and the frictional power in frame \mathcal{R} relates to the force simply through

$$P = F'v. \quad (3.94)$$

Then, the only independent quantity to evaluate is F' . If we now specify the Green's tensor to be the vacuum Green's tensor in Eq. (2.100), only the diagonal components of the Green's tensor can contribute to the frictional force on an isotropic particle because the off-diagonal components are either odd in k_y or evaluate to zero in the coincident limit. Further considering the diagonal components of the Green's tensor are all even in k_x , we find F'_{dd} actually vanishes. The surviving contribution, F'_{EE} , is found to be

$$F = F_{EE} = \frac{1}{12\pi^3\gamma^2v^2} \int_0^\infty d\omega \alpha^2(\omega) \omega^7 \int_{y_-}^{y_+} dy (y - \gamma) \frac{1}{e^{\beta\omega y} - 1}. \quad (3.95)$$

where we use again the definition introduced in Sec. 3.1, $y_- = \gamma(1 - v)$ and $y_+ = \gamma(1 + v)$.

The frictional force shown in Eq. (3.95) is clearly negative definite, indicating that it is a true drag on the particle, opposing its motion. An external driving force $F_{\text{ext}} = -F' = -F$ is needed to balance the quantum friction caused by radiation whether we view the situation in frame \mathcal{P} or in frame \mathcal{R} . The energetics are different, though. In frame \mathcal{R} , the quantum friction does negative work on the moving particle and causes it to lose energy to the electromagnetic vacuum in the rate of $P = F'v = Fv$. In the meantime, the external force, which keeps the particle moving in constant velocity, does positive work on the particle and causes it to gain energy exactly in the same rate as the loss, $P_{\text{ext}} = F_{\text{ext}}v = -Fv$. Overall, the internal energy of the neutral particle is conserved. In frame \mathcal{P} , neither the quantum friction nor the external force do any work on the particle, and, as a result, the particle's internal energy is conserved too. Or, in other words, the particle is guaranteed to be in NESS.

In the nonrelativistic limit, Eq. (3.95) reduces to

$$F \sim -\frac{v}{72\pi^3} \int_0^\infty d\omega \alpha^2(\omega) \omega^7 \frac{\beta\omega}{\sinh^2(\beta\omega/2)}. \quad (3.96)$$

The spectrum of the frictional force here reminds us of the Einstein-Hopf drag [3]. Indeed, if we introduce an effective polarizability, denoted by $\hat{\alpha}(\omega)$,

$$\text{Im } \hat{\alpha}(\omega) = \frac{\omega^3}{6\pi} \alpha^2(\omega), \quad (3.97)$$

the quantum friction in Eq. (3.96) can be rewritten as

$$F = -\frac{v}{12\pi^2} \int_0^\infty d\omega \text{Im } \hat{\alpha}(\omega) \omega^4 \frac{\beta\omega}{\sinh^2(\beta\omega/2)}. \quad (3.98)$$

This is precisely the form of the Einstein-Hopf drag on a neutral atom written in various modern papers [16, 20, 68]. A detailed account for the connection between the formula Eq. (3.98) and the original Einstein-Hopf drag can be found in [17].

Let us observe that $\hat{\alpha}$ in Eq. (3.97) does have the correct dimension for a polarizability. In fact, Eq. (3.97) only shows the second order in α approximation for the imaginary part of the full effective polarizability, that is, the polarizability of the particle dressed by radiation. This is the lowest order term in $\text{Im } \hat{\alpha}$, when the particle is nondissipative, as will be seen more clearly in the next section.

3.2.2 Effective polarizability

In the end of last section, we are able to recast the correct nonrelativistic QVF using the effective polarizability. It therefore seems possible that there exists another, more convenient, viewpoint for the frictional effects on a nondissipative atom, which avoids performing calculations to second order in the particle's intrinsic polarizability.

An effective polarizability must account for the dressing of the particle by the radiation fields. In frame \mathcal{P} , the total dipole moment of a particle is

$$\mathbf{d}'(\omega) = \boldsymbol{\alpha}'(\omega) \cdot \mathbf{E}'(\omega; \mathbf{R}_0), \quad (3.99)$$

where \mathbf{R}_0 is the fixed position of the particle in its rest frame. In the following, let us suppress the frequency and position arguments whenever no ambiguity arises.

In a space free from any external field, the total field, \mathbf{E} can be split into two parts,

$$\mathbf{E}' = \mathbf{E}'_f + \mathbf{E}'_i = \mathbf{E}'_f + \mathbf{G}' \cdot \mathbf{d}' = \mathbf{E}'_f + \mathbf{G}' \cdot \boldsymbol{\alpha}' \cdot \mathbf{E}' \quad (3.100)$$

Here, \mathbf{E}'_f is the fluctuating field in space without any reference to the particle. On the other hand, \mathbf{E}'_i is the induced field due to the presence of the particle, which is itself expressed in terms of the total field, \mathbf{E}' . The above relation can be inverted as

$$\mathbf{E}' = \frac{1}{1 - \mathbf{G}' \cdot \boldsymbol{\alpha}'} \mathbf{E}'_f, \quad (3.101)$$

expressing the total field, \mathbf{E}' , in terms of the fluctuating field, \mathbf{E}'_f . Apparently, all scattering effects of the particle are encoded in the prefactor.

Using Eq. (3.101), the dipole moment at the position of the particle is written as

$$\mathbf{d}' = \boldsymbol{\alpha}' \cdot \frac{1}{1 - \mathbf{G}' \cdot \boldsymbol{\alpha}'} \mathbf{E}'_f. \quad (3.102)$$

Now, if we define the effective polarizability as

$$\hat{\boldsymbol{\alpha}}' = \boldsymbol{\alpha}' \cdot \frac{1}{1 - \mathbf{G}' \cdot \boldsymbol{\alpha}'}, \quad (3.103)$$

the dipole moment can be reexpressed in terms of the fluctuating field, \mathbf{E}'_f , instead of the total field \mathbf{E}' ,

$$\mathbf{d}' = \hat{\boldsymbol{\alpha}}' \cdot \mathbf{E}'_f. \quad (3.104)$$

In Eq. (3.99), the scattering effects by the particle are included in the total field, \mathbf{E}' . In Eq. (3.104), however, they are now hidden in the effective polarizability, $\hat{\boldsymbol{\alpha}}'$.

In the regime where the scattering contribution is subdominant, we can expand Eq. (3.103) perturbatively,

$$\hat{\boldsymbol{\alpha}}'(\omega) = \boldsymbol{\alpha}'(\omega) + \boldsymbol{\alpha}'(\omega) \cdot \mathbf{G}'(\omega; \mathbf{R}_0, \mathbf{R}_0) \cdot \boldsymbol{\alpha}'(\omega) + \dots \quad (3.105)$$

Now, as we take the imaginary part of the effective polarizability, we find, for a dissipative particle, the leading term is first order in the intrinsic polarizability, $\boldsymbol{\alpha}'$

$$\text{Im } \hat{\boldsymbol{\alpha}}'^{(1)}(\omega) \sim \text{Im } \boldsymbol{\alpha}'(\omega), \quad (3.106)$$

while for a nondissipative particle, the leading term is second order in the intrinsic polarizability,

$$\text{Im } \hat{\alpha}'^{(2)}(\omega) \sim \boldsymbol{\alpha}'(\omega) \cdot \text{Im } \mathbf{G}'(\omega; \mathbf{R}_0, \mathbf{R}_0) \cdot \boldsymbol{\alpha}'(\omega). \quad (3.107)$$

That is why the leading quantum frictional effects are first order in $\boldsymbol{\alpha}'$ for an intrinsically dissipative particle, but second order in $\boldsymbol{\alpha}'$ for a nondissipative particle.

Now, with the effective polarizability, we try to rewrite the second-order quantum vacuum friction on a nondissipative particle in Eq. (3.91). For the direct field fluctuation contribution, F'_{EE} , this is straightforward,

$$\begin{aligned} F'_{EE} &= \int \frac{d\nu}{2\pi} \frac{d^2 \mathbf{k}_\perp}{(2\pi)^2} k_x \boldsymbol{\alpha}'(\nu) \cdot \text{Im } \mathbf{G}'(\nu; \mathbf{R}_0, \mathbf{R}_0) \cdot \boldsymbol{\alpha}'(\nu) \cdot \text{Im } \mathbf{G}'(\nu, \mathbf{k}_\perp; a, a) \coth \frac{\beta\gamma(\nu + k_x v)}{2} \\ &= \int \frac{d\nu}{2\pi} \frac{d^2 \mathbf{k}_\perp}{(2\pi)^2} k_x \text{Im } \hat{\alpha}'^{(2)}(\nu) \cdot \text{Im } \mathbf{G}'(\nu, \mathbf{k}_\perp; a, a) \coth \frac{\beta\gamma(\nu + k_x v)}{2}, \end{aligned} \quad (3.108)$$

where the effective polarizability here is

$$\text{Im } \hat{\alpha}'^{(2)}(\nu) = \boldsymbol{\alpha}'(\nu) \cdot \text{Im } \mathbf{G}'(\nu; \mathbf{R}_0, \mathbf{R}_0) \cdot \boldsymbol{\alpha}'(\nu). \quad (3.109)$$

However, such a replacement cannot be done for the induced dipole fluctuation contribution, F'_{dd} , because the two Green's tensors appearing in Eq. (3.91b) are entangled with the k_x factor and the coth factor respectively. As a result, they can not be directly integrated to yield $\text{Im } \mathbf{G}'(\nu; \mathbf{R}_0, \mathbf{R}_0)$. But, we can still introduce a spatially dispersive effective polarizability³ as

$$\text{Im } \hat{\alpha}'^{(2)}(\nu, \tilde{\mathbf{k}}_\perp) = \boldsymbol{\alpha}'(\nu) \cdot \text{Im } \mathbf{G}'(\nu, \tilde{\mathbf{k}}_\perp; a, a) \cdot \boldsymbol{\alpha}'(\nu), \quad (3.110)$$

which enables us to rewrite F'_{dd} as

$$F'_{dd} = - \int \frac{d\nu}{2\pi} \frac{d^2 \mathbf{k}_\perp}{(2\pi)^2} \frac{d^2 \tilde{\mathbf{k}}_\perp}{(2\pi)^2} k_x \text{Im } \hat{\alpha}'^{(2)}(\nu, \tilde{\mathbf{k}}_\perp) \cdot \text{Im } \mathbf{G}'(\nu, \mathbf{k}_\perp; a, a) \coth \left[\frac{\beta}{2} \gamma(\nu + \tilde{k}_x v) \right]. \quad (3.111)$$

In the coincident limit, the imaginary part of the vacuum Green's tensor is (See

³This indicates that the effective polarizability is spatially translationally invariant inherited from the geometry.

Eq. (2.88).)

$$\text{Im } \mathbf{G} = \frac{\omega^3}{6\pi} \mathbf{1}. \quad (3.112)$$

As a result, only the diagonal components of the intrinsic polarizability will be picked up. For an isotropic, nondissipative particle in vacuum, the second-order effective polarizability will also be isotropic, being precisely the form in Eq. (3.97),

$$\text{Im } \hat{\alpha}'^{(2)}(\omega) = \frac{\omega^3}{6\pi} \alpha'^2(\omega). \quad (3.113)$$

In addition, F'_{dd} vanishes for the vacuum background. The remaining contribution, F'_{EE} , can be recast into the following form using the effective polarizability in Eq. (3.111),

$$F' = F'_{EE} = \frac{1}{2\pi^2 \gamma^2 v^2} \int_0^\infty d\omega \omega^4 \text{Im } \hat{\alpha}'^{(2)}(\omega) \int_{y_-}^{y_+} dy \frac{(y - \gamma)}{e^{\beta\omega y} - 1}, \quad (3.114)$$

which is a relativistic extension of the nonrelativistic Einstein-Hopf formula in Eq. (3.98). This now also has the same form as the quantum friction for an intrinsically dissipative particle in Eq. (3.95). Such a resemblance only exists if F'_{dd} vanishes.

In principle, we can extend the calculation for the QVF to all orders in α' (the intrinsic polarizability) by replacing the second order effective polarizability with the full effective polarizability in Eq. (3.103), which includes the contribution of scattering process to arbitrary orders. However, we find ourselves immediately running into problems when we try to expand $\text{Im } \hat{\alpha}'$ beyond second order in α' . For example,

$$\text{Im } \hat{\alpha}'^{(3)}(\omega) = 2\alpha'(\omega) \cdot \text{Im } \mathbf{G}'(\omega; \mathbf{R}_0, \mathbf{R}_0) \cdot \alpha'(\omega) \cdot \text{Re } \mathbf{G}'(\omega; \mathbf{R}_0, \mathbf{R}_0) \cdot \alpha'(\omega). \quad (3.115)$$

Apparently, higher order contributions to $\text{Im } \hat{\alpha}'$ involve the real part of the Green's tensor, which is divergent in the coincident limit according to Eq. (2.88).

In order to obtain finite results, we effect a renormalization of the bare intrinsic polarizability, α' by absorbing $\text{Re } \mathbf{G}'(\omega; \mathbf{R}'_0, \mathbf{R}'_0)$ into the definition of a renormalized

polarizability, α'_R . We now proceed to formalize this prescription:

$$\begin{aligned}
\hat{\alpha}' &= \alpha' (\mathbf{1} - \mathbf{G}' \cdot \alpha')^{-1} = \alpha' (\mathbf{1} - \text{Re } \mathbf{G}' \cdot \alpha' - i \text{Im } \mathbf{G}' \cdot \alpha')^{-1} \\
&= \alpha' \left\{ \left[\mathbf{1} - i \text{Im } \mathbf{G}' \cdot \alpha' (\mathbf{1} - \text{Re } \mathbf{G}' \cdot \alpha')^{-1} \right] (\mathbf{1} - \text{Re } \mathbf{G}' \cdot \alpha') \right\}^{-1} \\
&= \alpha' (\mathbf{1} - \text{Re } \mathbf{G}' \cdot \alpha')^{-1} \left[\mathbf{1} - i \text{Im } \mathbf{G}' \cdot \alpha' (\mathbf{1} - \text{Re } \mathbf{G}' \cdot \alpha')^{-1} \right]^{-1} \\
&= \alpha'_R (\mathbf{1} - i \text{Im } \mathbf{G}' \cdot \alpha'_R)^{-1}, \tag{3.116}
\end{aligned}$$

where we have dropped all of the obvious arguments and the renormalized polarizability, α'_R reads

$$\alpha'_R(\omega) \equiv \alpha'(\omega) \frac{1}{\mathbf{1} - \text{Re } \mathbf{G}'(\omega; \mathbf{R}_0, \mathbf{R}_0) \alpha'(\omega)} \tag{3.117}$$

is the renormalized intrinsic polarizability, which clearly inherits from the bare intrinsic polarizability the properties of being real and symmetric.

In vacuum, the full effective polarizability may therefore be written, using α'_R as

$$\hat{\alpha}'(\omega) = \alpha'_R(\omega) \frac{1}{\mathbf{1} - i \text{Im } \mathbf{G}'(\omega; \mathbf{R}_0, \mathbf{R}_0) \cdot \alpha'_R(\omega)} = \alpha'_R(\omega) \frac{1}{\mathbf{1} - i \frac{\omega^3}{6\pi} \alpha'_R(\omega)}, \tag{3.118}$$

which agrees with the functional form of the atomic polarizability obtained in Ref. [68] by a perturbative analysis on the energy shift. The imaginary part of the full effective polarizability now reads

$$\text{Im } \hat{\alpha}'(\omega) = \frac{\omega^3}{6\pi} \alpha'^2_R(\omega) \frac{1}{\mathbf{1} + \left(\frac{\omega^3}{6\pi}\right)^2 \alpha'^2_R(\omega)}. \tag{3.119}$$

In general, $\alpha'^2_R(\omega) = \alpha'_R(\omega) \cdot \alpha'_R(\omega)$, while, for an isotropic particle, $\alpha'^2_R(\omega) = \alpha'^2(\omega)$.

The quantum vacuum friction in Eq. (3.114) can now be extended to all orders in the intrinsic polarizability by replacing $\text{Im } \hat{\alpha}'^{(2)}$ with the full effective polarizability in Eq. (3.119),

$$F' = \frac{1}{2\pi^2 \gamma^2 v^2} \int_0^\infty d\omega \omega^4 \text{Im } \hat{\alpha}'(\omega) \int_{y_-}^{y_+} dy \frac{(y - \gamma)}{e^{\beta \omega y} - 1}, \tag{3.120}$$

Since it is the renormalized polarizability that is measured in a lab, the intrinsic polarizability which enters all previous formulas as an input should have been un-

derstood as the renormalized polarizability. But, for simplicity, we shall drop the subscript R on the renormalized polarizability, that is, $\alpha'_R \rightarrow \alpha'$.

3.2.3 Numerical estimates of the quantum vacuum friction for a gold atom

How big is quantum vacuum friction on a nondissipative atom? Will it be accessible to experiments? To answer these questions, in this section let us obtain an estimate for the quantum friction on an atom moving uniformly in vacuum. We will assume the renormalized intrinsic polarizability of the atom is isotropic⁴. Further, let us also assume the atom stays in its ground state and that we can approximate its polarizability at different frequencies with its static value

$$\alpha'(\omega) \sim \alpha_0 \mathbf{1}. \quad (3.121)$$

These assumptions break down when the environment temperature is higher than the temperature corresponding to the atom's first excitation energy, T_1 . For such high temperatures, the thermal agitation is able to excite the atom to its excited states and we would have to use the dynamical polarizability then. For much lower temperatures, it is safe to use the static value for the atom's intrinsic polarizability. In this static approximation, the effective polarizability in Eq. (3.119) becomes

$$\text{Im } \hat{\alpha}'(\omega) = \frac{\omega^3}{6\pi} \alpha_0^2 \frac{\mathbf{1}}{1 + (\frac{\omega^3}{6\pi})^2 \alpha_0^2}. \quad (3.122)$$

For a gold atom, the static polarizability is $5.33 \times 10^{-24} \text{cm}^3$ according to Ref. [69]. For low frequencies, the higher order correction to the effective polarizability is negligible and $\text{Im } \hat{\alpha}'(\omega)$ reduces to the well-known radiation reaction model [71], $\frac{\omega^3}{6\pi} \alpha_0^2$. For high frequencies, however, $\text{Im } \hat{\alpha}'(\omega)$ becomes $\frac{6\pi}{\omega^3}$, which is independent of the value for the static polarizability.

⁴Atoms are usually quite isotropic. That is, their anisotropy is typically small compared to the isotropic part of the polarizability. Closed-shell atoms are almost exactly isotropic [69]. Within a single period in the chemical table, the anisotropy is largest when the first p electron is added [70].

Plugging Eq. (3.122) into the formula for quantum friction Eq. (3.120), we obtain

$$F = F' = \frac{\alpha_0^2}{12\pi^3} \int_0^\infty d\omega \frac{\omega^7}{1 + (\frac{\omega^3}{6\pi})^2 \alpha_0^2} \int_{y_-}^{y_+} \frac{dy}{\gamma^2 v^2} \frac{y - \gamma}{e^{\beta\omega y} - 1}. \quad (3.123)$$

For ease of numerical evaluation, let us introduce a dimensionless frequency $x = \frac{\beta\omega}{2}$ and a dimensionless temperature $\lambda = (\frac{\alpha_0}{6\pi})^{1/3} \frac{2}{\beta}$. Then Eq. (3.123) can be rewritten as

$$F = F_0 \int_0^\infty dx \frac{\lambda^8 x^7}{1 + \lambda^6 x^6} \int_{y_-}^{y_+} \frac{dy}{\gamma^2 v^2} \frac{y - \gamma}{e^{2xy} - 1}, \quad F_0 = \frac{(6\pi)^{8/3}}{12\pi^3} \alpha_0^{-2/3}. \quad (3.124)$$

For a gold atom, the dimensional factor F_0 in Eq. (3.124), which is independent of temperature and velocity, evaluates to $F_0 = 6.99 \times 10^{-6}$ N, after converting to SI units. The remaining factor in Eq. (3.124) is a dimensionless function of velocity v and rescaled temperature λ . The integral in Eq. (3.124) is dominated by the low-frequency contributions in the low-temperature limit ($\lambda \ll 1$) and the high-frequency contributions in the high-temperature limit ($\lambda \gg 1$). Therefore, the behavior of the QVF on the atom depends on the value of λ .

For the gold atom, $\lambda = 1$ corresponds to a temperature of 1.74×10^7 K. This far exceeds the ionization temperature of the gold atom, $T_i = 107\,000$ K [72], let alone the first excitation temperature, $T_1 = 13\,100$ K [73]. Therefore, the atom would have been ionized and no longer stay neutral long before it reaches the temperature for the higher order corrections to become important. Effectively, when evaluating the frictional force on the gold atom, we can use the low frequency approximation for $\text{Im } \hat{\alpha}'(\omega)$ and find

$$F_{\lambda \ll 1} = F_0 \int_0^\infty dx \lambda^8 x^7 \int_{y_-}^{y_+} \frac{dy}{\gamma^2 v^2} \frac{y - \gamma}{e^{2xy} - 1} = -\frac{4\pi^5 \alpha_0^2 \gamma^6}{45\beta^8} \left(\frac{8}{3}v + \frac{16}{3}v^3 + \frac{8}{7}v^5 \right). \quad (3.125)$$

Here, we note the nonrelativistic limit of the low-temperature blackbody friction agrees exactly with Eq. (15) in Ref. [71].

Suppose there exist some atom (nondissipative particle) which could stay neutral at very high temperatures so that the corresponding $\lambda \gg 1$. Then at such high temperatures, we should take the opposite limit and use the high frequency

approximation for the effective polarizability. The QVF becomes

$$F_{\lambda \gg 1} = F_0 \int_0^\infty dx \lambda^2 x \int_{y_-}^{y_+} \frac{dy}{\gamma^2 v^2} \frac{y - \gamma}{e^{2xy} - 1} = \frac{\pi}{2\gamma^2 v^2 \beta^2} \left[\ln \left(\frac{1+v}{1-v} \right) - 2\gamma^2 v \right]. \quad (3.126)$$

We see that the high temperature behavior of QVF is independent of the actual value of the intrinsic polarizability of the particle.

For the sake of attracting the attention of experimentalists, let us comment on the possibility of detecting the quantum vacuum friction on a gold atom. Presumably, such a friction will cause the gold atom to decelerate when the external driving force is removed. To make a rough estimate of the time taken for the atom to decelerate by a noticeable amount, we assume the gold atom would be in a “quasi nonequilibrium steady state” where the friction on it could still be calculated using the NESS formulas derived here. For all realistic purposes, we can use the low temperature approximation for the force in Eq. (3.125). In addition, since it is hard, experimentally, to accelerate a neutral particle to relativistic velocities, we should also be content with a nonrelativistic discussion, where we can safely apply Newton’s second law together with the lowest order (in v) approximation of the frictional force shown in Eq. (3.125):

$$F(v) = -\frac{32\pi^5 \alpha_0^2}{135\beta^8} v = m \frac{dv}{dt}. \quad (3.127)$$

The time taken for the gold atom to decelerate from an initial velocity v_i to a final velocity v_f is then found to be

$$\Delta t = -\tau \ln \frac{v_f}{v_i}, \quad \tau = \frac{135m\beta^8}{32\pi^5 \alpha_0^2}, \quad (3.128)$$

where τ is evaluated to be 1.72×10^{25} s at room temperature $T = 300$ K.⁵

For example, the time taken for the velocity of to be reducing by 10% is $\Delta t = 1.81 \times 10^{24}$ s. It then seems hopeless to detect the quantum vacuum frictional effect at room temperature. However, if the experiment could be performed at $T = 30,000$ K, Δt would be 16 orders of magnitude shorter, being 1.81×10^8 s = 5.91 yrs.

⁵The mass of a gold atom is $197u = 1.84 \times 10^{11}$ eV. The conversion factors used in the estimate are $k_B = 8.62 \times 10^{-5}$ eV/K, $\hbar c = 1.97 \times 10^{-5}$ eV · cm and $c = 3.00 \times 10^{10}$ cm/s.

Chapter 4

Quantum Friction in the Presence of a Perfectly Conducting Plate (QFPC)

It is well known that, when a neutral but polarizable particle sits near a perfectly conducting (PC) plate, it feels a force normal to the surface, pulling it towards the plate. This attractive force is often named after Casimir and Polder, who predicted it back in 1948 [7]. And the Casimir-Polder force was first experimentally confirmed by measuring the deflection of a sodium atom beam passing through a gold cavity [9]. There have been many experiments confirming the existence of the Casimir-Polder force ever since. Another ingenious method, which is suitable for detecting the thermal effects at larger atom-surface separation, is through the measurement of the center-of-mass oscillation frequencies of a rubidium atom Bose-Einstein condensate [74, 75].

In this chapter, we ask and answer this question: will a force parallel to the surface of the PC plate arise when the particle moves parallel to a PC plate?

Even though the subject of quantum friction (QF) with a dielectric surface has been much discussed in the literature, this more idealized case involving a PC plate seems to have been largely ignored. The lack of discussion of this case may be due to an incorrect intuition arising from the image particle picture. One might think that the interaction between the particle and the PC plate can be entirely mimicked by the particle's interaction with its image. As the particle moves above the plate, the image moves below the plate. Because the plate is perfectly conducting, the image keeps up with the particle and is always located at the mirror position of

the particle. Consequently, any interaction between the two would only lie in the direction normal to the surface of the plate and no force in the transverse directions could possibly arise. This reasoning sounds convincing except that it ignores one important aspect: the particle interacts with the blackbody radiation surrounding it even when the plate is taken away, resulting in the quantum vacuum friction (QVF) which we have just discussed in Chapter 3. Now, when a PC plate is added into the configuration, the vacuum field (electromagnetic field fluctuations) in the vicinity of the plate will be different from that of the vacuum. We therefore expect the QVF to be modified and become spatially varying in the normal direction. For convenience of presentation, we will refer to this new quantum frictional force on a neutral particle passing above a PC plate as QFPC.

Throughout this chapter, we set $k_B = c = \hbar = 1$ in the analytic expressions. SI units are reinstated in the numerical evaluations.

In this section, we will explore QFPC on a nondissipative atom. Much of the discussion is based on our paper [23].

The physical situation we consider is illustrated in Fig. 4.1. A PC plate lies in the x - y plane. An atom is at a distance a from the plate and moves in the x direction with constant velocity v . The polarizability of the atom is $\alpha(\omega)$, which could be dispersive in frequency and have different components corresponding to different polarization states of the atom. Since the atom we consider is intrinsically nondissipative, $\alpha(\omega)$ is a real quantity. The radiation background is at finite temperature T . We assume the PC plate is in thermal equilibrium with the radiation background. Due to its motion, the atom is not in equilibrium with the radiation. However, it is guaranteed to be in the nonequilibrium steady state (NESS) because we assume the atom is nondissipative and cannot change its internal energy.

The quantum friction on an intrinsically nondissipative particle moving in a

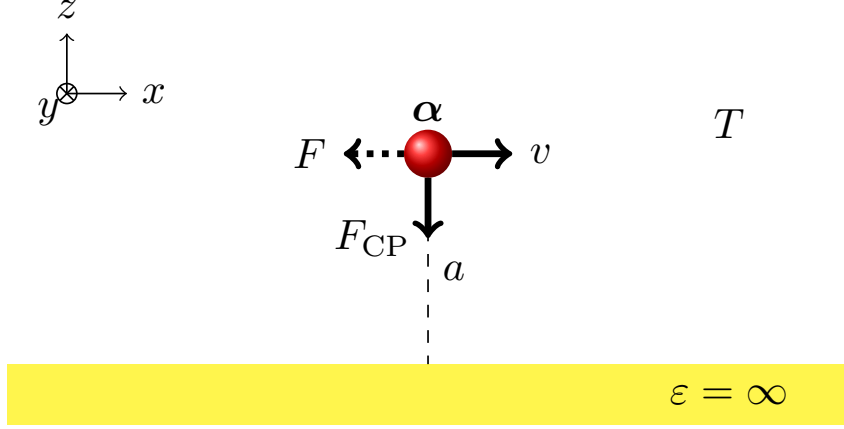


Figure 4.1: Illustration of an atom flying above a PC plate.

planar background can be obtained by generalizing Eq. (3.92) as¹

$$F = \int \frac{d\omega}{2\pi} \frac{d^2\mathbf{k}_\perp}{(2\pi)^2} \frac{d^2\bar{\mathbf{k}}_\perp}{(2\pi)^2} (\bar{k}_x - k_x) \text{tr } \boldsymbol{\alpha}'(\omega) \cdot \Im \mathbf{G}'(\omega, \mathbf{k}_\perp; a, a) \cdot \boldsymbol{\alpha}'(\omega) \cdot \Im \mathbf{G}'(\omega, \bar{\mathbf{k}}_\perp; a, a) \times \coth \frac{\beta\gamma(\omega + \bar{k}_x v)}{2}, \quad (4.1)$$

where the ordinary imaginary parts of the Green's tensor, $\text{Im } G$, are replaced by the anti-Hermitian parts of the Green's tensor, $\Im G$, defined as

$$\begin{aligned} (\Im \mathbf{G})_{ij}(\omega, \mathbf{k}_\perp; z, \tilde{z}) &= \frac{G_{ij}(\omega, \mathbf{k}_\perp; z, \tilde{z}) - G_{ji}^*(\omega, \mathbf{k}_\perp; \tilde{z}, z)}{2i} \\ &= \frac{G_{ij}(\omega, \mathbf{k}_\perp; z, \tilde{z}) - G_{ji}(-\omega, -\mathbf{k}_\perp; \tilde{z}, z)}{2i}. \end{aligned} \quad (4.2)$$

Note the frequencies and momenta being integrated over in Eq. (4.1) are intrinsic to the rest frame of the particle, \mathcal{P} , but we are not keeping the primes on these integration variables because doing so will not cause confusions here.

The quantum friction in Eq. (4.1) is again just the x component of the Lorentz force on a moving dipole quantized using the fluctuation-dissipation theorem (FDT). Because the atom is intrinsically nondissipative, the frictional force is second order in α like that discussed in Sec. 3.2. There are two contributions to the force: the \bar{k}_x term comes from the field fluctuations directly while the k_x term comes from the induced dipole fluctuations. Although entering the friction formula with different

¹This frictional force has also been calculated in Ref. [21] and tabulated for different polarization states in Appendix D therein. The formulas there are equivalent to Eq. (4.1) here when we take into account the transformations in Appendix A.

signs, these two contributions do not cancel each other due to the Doppler shifting of the frequency in the \coth factor. Even at zero temperature, the quantum friction does not vanish in general. But we have learned from the previous chapters that if the background is just free space, the resultant QVF does vanish at zero temperature [21, 22]. This is also the case when a PC plate is added into the configuration. That is, no QFPC arises at zero temperature. In Appendix B, we prove that the zero temperature QF is absent not only for the vacuum case and the PC case, but also for the broader class of diaphanous materials.

In general, to calculate the frictional force, we need first express \mathbf{G}' in terms of \mathbf{G} using the transformations recorded in Appendix A. For the special background of the PC plate, \mathbf{G} reads, according to Eq. (2.103) and Eq. (2.104),

$$\mathbf{G}^{\text{PC}}(\omega, \mathbf{k}_\perp; a, a) = \begin{pmatrix} \frac{\omega^2 - k_x^2}{2\kappa}(1 - e^{-2\kappa a}) & -\frac{k_x k_y}{2\kappa}(1 - e^{-2\kappa a}) & -\frac{i}{2}k_x e^{-2\kappa a} \\ -\frac{k_x k_y}{2\kappa}(1 - e^{-2\kappa a}) & \frac{\omega^2 - k_y^2}{2\kappa}(1 - e^{-2\kappa a}) & -\frac{i}{2}k_y e^{-2\kappa a} \\ +\frac{i}{2}k_x e^{-2\kappa a} & +\frac{i}{2}k_y e^{-2\kappa a} & \frac{k^2}{2\kappa}(1 + e^{-2\kappa a}) \end{pmatrix} \quad (4.3)$$

with $\kappa = \sqrt{k^2 - \omega^2}$. When we apply the transformations in Appendix A to the tensor above, we find

$$\mathbf{G}'^{\text{PC}}(\omega, \mathbf{k}_\perp; a, a) = \mathbf{G}^{\text{PC}}(\omega, \mathbf{k}_\perp; a, a), \quad (4.4)$$

similar to the vacuum situation. In addition, the off-diagonal components $g_{xy} = g_{yx}$ and $g_{yz} = -g_{zy}$ will not contribute to the friction due to their oddness in k_y .

We see from the starting formula Eq. (4.1) that each contribution to the frictional force is proportional to the product of two nonvanishing components of the polarizability tensor. The matrix structure under the trace in the integrand is still complicated because of many contributing terms that mixes the different components of the polarizability. Let us now assume that the polarizability is diagonal. Then there are only four nonvanishing contributions left. They are proportional to α_{xx}^2 , α_{yy}^2 , α_{zz}^2 , $\alpha_{xx}\alpha_{zz}$ and will be denoted as F^{XX} , F^{YY} , F^{ZZ} and F^{XZ} , respectively.

Among them, the only contribution to the friction involving the off-diagonal components of the Green's tensor, which mixes different components of the polarizability tensor is

$$F^{\text{XZ}} = 2 \int \frac{d\omega}{2\pi} \frac{d^2 \mathbf{k}_\perp}{(2\pi)^2} \frac{d^2 \bar{\mathbf{k}}_\perp}{(2\pi)^2} (\bar{k}_x - k_x) \alpha_{xx}(\omega) (\Im \mathbf{G})_{xz}^{\text{PC}}(\omega, \mathbf{k}_\perp; a, a) \\ \times \alpha_{zz}(\omega) (\Im \mathbf{G})_{zx}^{\text{PC}}(\omega, \bar{\mathbf{k}}_\perp; a, a) \coth \left[\frac{\beta}{2} \gamma(\omega + \bar{k}_x v) \right]. \quad (4.5)$$

In fact, F^{XZ} turns out to be the most interesting contribution to the frictional force, because it actually corresponds to a push instead of a drag.

Crucial to the calculation is finding the anti-Hermitian part of the relevant components of \mathbf{G}^{PC} . It can be seen from Eq. (2.104) that $\Im \mathbf{G}^{\text{PC}} = \mathbf{0}$ unless the propagation wave number κ develops an imaginary part. Since the integrand in Eq. (4.1) involves the product of two Green's tensors evaluated at $(\omega, \mathbf{k}_\perp)$ and $(\omega, \bar{\mathbf{k}}_\perp)$, respectively, the integration is restricted to regions where the propagation wave numbers associated with both Green's tensors become imaginary,

$$\kappa \rightarrow -i \text{sgn}(\omega) \sqrt{\omega^2 - k^2}, \quad k^2 < \omega^2, \quad \bar{\kappa} \rightarrow -i \text{sgn}(\omega) \sqrt{\omega^2 - \bar{k}^2}, \quad \bar{k}^2 < \omega^2. \quad (4.6)$$

The branches need to be chosen so that the Green's tensor is retarded. The anti-Hermitian parts of the relevant components of the Green's tensor therefore read

$$(\Im \mathbf{G})_{xx}(\omega, \mathbf{k}_\perp; a, a) = \text{Im } G_{xx}(\omega, \mathbf{k}_\perp; a, a) = \text{sgn}(\omega) \frac{\omega^2 - k_x^2}{2\sqrt{\omega^2 - k^2}} \left[1 - \cos\left(2\sqrt{\omega^2 - k^2}a\right) \right], \quad (4.7a)$$

$$(\Im \mathbf{G})_{yy}(\omega, \mathbf{k}_\perp; a, a) = \text{Im } G_{yy}(\omega, \mathbf{k}_\perp; a, a) = \text{sgn}(\omega) \frac{\omega^2 - k_y^2}{2\sqrt{\omega^2 - k^2}} \left[1 - \cos\left(2\sqrt{\omega^2 - k^2}a\right) \right], \quad (4.7b)$$

$$(\Im \mathbf{G})_{zz}(\omega, \mathbf{k}_\perp; a, a) = \text{Im } G_{zz}(\omega, \mathbf{k}_\perp; a, a) = \text{sgn}(\omega) \frac{k^2}{2\sqrt{\omega^2 - k^2}} \left[1 + \cos\left(2\sqrt{\omega^2 - k^2}a\right) \right], \quad (4.7c)$$

$$(\Im \mathbf{G})_{xz}(\omega, \mathbf{k}_\perp; a, a) = -(\Im \mathbf{G})_{zx}(\omega, \mathbf{k}_\perp; a, a) = -i \text{sgn}(\omega) \frac{k_x}{2} \sin\left(2\sqrt{\omega^2 - k^2}a\right). \quad (4.7d)$$

The off-diagonal components of $\Im \mathbf{G}$ are different from the diagonal components in several respects. First of all, they are purely imaginary. Second, they are odd in k_x . As a result, in Eq. (4.1), F^{XZ} contributes to the total friction through the $-k_x$

term, while F^{XX} , F^{YY} and F^{ZZ} all contribute through the \bar{k}_x term. It is precisely the minus sign in the $-k_x$ term that renders F^{XZ} positive, corresponding to a push instead of a drag.² Third, they do not contain terms independent of the atom-plate separation, a , as those in the diagonal components. These terms reflect the vacuum contributions. So, the off-diagonal components do not contribute to the QVF.

Without any further assumptions, we insert Eq. (4.7) into Eq. (4.1) and integrate k_x , k_y and \bar{k}_y analytically. With a further change of variable, $\bar{k}_x = \omega u$, we find the contribution to the QFPC from the PQ polarization states can be written as

$$F^{\text{PQ}} = \frac{1}{32\pi^3} \int_0^\infty d\omega \alpha_{pp}(\omega) \alpha_{qq}(\omega) \omega^7 \mathcal{F}^{\text{PQ}}(x, v, z), \quad (4.8)$$

and for each contribution, \mathcal{F}^{PQ} reads

$$\begin{aligned} \mathcal{F}^{\text{XX}}(x, v, z) &= \left\{ \frac{4}{3} - \frac{2}{x^3} [x \cos x + (x^2 - 1) \sin x] \right\} \\ &\times \int_{-1}^1 du u (1 - u^2) \left[1 - J_0(x\sqrt{1 - u^2}) \right] \frac{1}{e^{x\gamma(1+uv)z} - 1}, \end{aligned} \quad (4.9a)$$

$$\begin{aligned} \mathcal{F}^{\text{YY}}(x, v, z) &= \left\{ \frac{4}{3} - \frac{2}{x^3} [x \cos x + (x^2 - 1) \sin x] \right\} \\ &\times \int_{-1}^1 du u \left[\frac{1}{2}(1 + u^2) - J_0(x\sqrt{1 - u^2}) + \frac{\sqrt{1 - u^2}}{x} J_1(x\sqrt{1 - u^2}) \right] \frac{1}{e^{x\gamma(1+uv)z} - 1}, \end{aligned} \quad (4.9b)$$

$$\begin{aligned} \mathcal{F}^{\text{ZZ}}(x, v, z) &= \left\{ \frac{4}{3} - \frac{4}{x^3} [x \cos x - \sin x] \right\} \\ &\times \int_{-1}^1 du u \left[\frac{1}{2}(1 + u^2) + u^2 J_0(x\sqrt{1 - u^2}) + \frac{\sqrt{1 - u^2}}{x} J_1(x\sqrt{1 - u^2}) \right] \frac{1}{e^{x\gamma(1+uv)z} - 1}, \end{aligned} \quad (4.9c)$$

²Physically, the $-k_x$ term comes from the induced dipole fluctuations, while the \bar{k}_x term comes from the direct field fluctuations. In the QVF case, only the direct field fluctuation contributes to the QVF on an atom as discussed in Chapter 3.

$$\mathcal{F}^{\text{XZ}} = -2 \left\{ \frac{2}{x^4} [-3x \cos x - (x^2 - 3) \sin x] \right\} \times \int_{-1}^1 du u \sqrt{1-u^2} J_1(x\sqrt{1-u^2}) \frac{1}{e^{x\gamma(1+uv)z} - 1}. \quad (4.9d)$$

Here, we have introduced a dimensionless frequency scaled by the distance a ,

$$x = 2\omega a, \quad (4.10)$$

as well as a dimensionless inverse temperature also scaled by a ,

$$z = \frac{\beta}{2a} = \frac{1}{2aT}. \quad (4.11)$$

So far, the expressions we have for QFPC in Eq. (4.9) are exact and involve the dynamical polarizability of the atom. For frequencies smaller than the lowest excitation energy of the atom, the dynamical polarizability, $\alpha(\omega)$, can be replaced by the static polarizability [70], $\alpha(0)$. Due to the common exponential factors in Eq. (4.9a)–(4.9d), the high frequency modes with $\beta\omega = xz \gg 1$ will be cut off and do not significantly contribute to the ω integral. Therefore, so long as the temperature is not high enough to excite the atom to its higher energy states, we can work in the static limit, where we substitute the polarizability with its static value. This allows us to take the product of the polarizabilities out of the ω integral in Eq. (4.8):

$$F^{\text{PQ}} = \frac{\alpha_{pp}(0)\alpha_{qq}(0)}{32\pi^3(2a)^8} f^{\text{PQ}}(v, z), \quad f^{\text{PQ}}(v, z) = \int_0^\infty dx x^7 \mathcal{F}^{\text{PQ}}(x, v, z), \quad (4.12)$$

where the dimensionless functions f^{PQ} now characterize contributions to QFPC from different polarization states.

Note the magnitude of z determines the dominating modes of the x integral in Eq. (4.12). For $z \ll 1$, it is dominated by the large x modes, where the complicated x dependences in the integrands become subdominant and drop out, except for the common factor of $\frac{x^7}{e^{x\gamma(1+uv)z} - 1}$. As a result, the diagonal contributions F^{XX} , F^{YY} and F^{ZZ} become distance independent and proportional to T^8 . Indeed, for $z \ll 1$, the diagonal contributions of QFPC precisely reduce to the corresponding contributions of QVF in Ref. [21]. On the other hand, F^{XZ} , which is proportional to T^4/a^4 , becomes completely negligible in comparison to the diagonal contributions.

To sum up, the contributions to QFPC in the small z limit read

$$F_{z \ll 1}^{\text{PQ}} = \frac{\alpha_{pp}^2(0)}{32\pi^3(2a)^8} f_{z \ll 1}^{\text{PQ}}(v, z), \quad (4.13a)$$

$$f_{z \ll 1}^{\text{PQ}}(v, z) = \begin{cases} -\frac{4\Gamma(8)\zeta(8)}{3z^8} \frac{32}{105} \gamma^4 v (7 + 3v^2), & \text{PQ} = \text{XX} \\ -\frac{4\Gamma(8)\zeta(8)}{3z^8} \frac{32}{105} \gamma^6 v (14 + 37v^2 + 9v^4), & \text{PQ} = \text{YY}, \text{ZZ} \\ \frac{16\Gamma(4)\zeta(4)}{z^4} \frac{v}{\gamma^4}, & \text{PQ} = \text{XZ}. \end{cases} \quad (4.13b)$$

As is shown in Eq. (4.13), unlike the diagonal contributions which monotonically increase with velocity, we find F^{XZ} vanishes when the velocity approaches the speed of light.

It is not so surprising that the small z limit of QFPC coincides with QVF. Small z values correspond to large distances or high temperatures. When the atom is far away from the PC plate, it is obvious that QFPC should reduce to QVF. In the case of high temperatures (but not so high to ionize the atom), the atom interacts with photons of very high frequency. It therefore mainly probes the very short distances around it and, effectively, does not feel the PC plate. That is, in the high temperature limit, the distribution of energy eigenvalues of photons interacting with the atom is insensitive to the presence of the plate.

Since quantum vacuum friction has been explored for a nondissipative atom in Chapter 3, the new physics really lies in the large z limit, the short-distance or low-temperature behavior of QFPC. For $z \gg 1$, the small x modes dominate the integrals. We can therefore expand the integrands in powers of x before carrying out the integrals. Quite interestingly, the integrands for various polarization states exhibit different leading power behaviors in x , which determine the distance and temperature dependences of their contributions to QFPC. After expansion in x , both the x and u integrals can be done exactly if we keep only the leading in z terms. For $z \gg 1$, the resultant QFPC is found to be

$$F_{z \gg 1}^{\text{PQ}} = \frac{\alpha_{pp}(0)\alpha_{qq}(0)}{32\pi^3(2a)^8} f_{z \gg 1}^{\text{PQ}}(v, z), \quad (4.14a)$$

$$f_{z \gg 1}^{\text{PQ}}(v, z) = \begin{cases} -\frac{\Gamma(12)\zeta(12)}{15z^{12}} \frac{64}{3465} \gamma^6 v (99 + 110v^2 + 15v^4), & \text{PQ} = \text{XX} \\ -\frac{\Gamma(12)\zeta(12)}{15z^{12}} \frac{32}{3465} \gamma^8 v (297 + 1034v^2 + 625v^4 + 60v^6), & \text{PQ} = \text{YY} \\ -\frac{8\Gamma(8)\zeta(8)}{3z^8} \frac{64}{105} \gamma^6 v (14 + 37v^2 + 9v^4), & \text{PQ} = \text{ZZ} \\ 2\frac{\Gamma(10)\zeta(10)}{15z^{10}} \frac{8}{63} \gamma^6 v (21 + 30v^2 + 5v^4), & \text{PQ} = \text{XZ}. \end{cases} \quad (4.14\text{b})$$

Since the results shown in Eq. (4.14) are for the large z limit, it is apparent that F^{ZZ} dominates over the contributions from the other polarizations. In this limit, F^{ZZ} is independent of distance a and proportional to T^8 , just as is the case for QVF. In fact, we find F^{ZZ} is precisely four times the corresponding QVF contribution shown in Eq. (4.13). The next leading contribution, F^{XZ} , is proportional to $a^2 T^{10}$ with an overall positive sign, suggesting that this particular contribution corresponds to a push instead of a drag. The smallest contributions, F^{XX} and F^{YY} , are both proportional to $a^4 T^{12}$. On closer examination of Eq. (4.14), we also observe that f^{YY} is always greater than f^{XX} , for arbitrary velocities.

Interestingly, these behaviors of QFPC may be easily understood from the image particle picture criticized in the beginning of this chapter. In fact, there is nothing wrong with replacing the PC plate by an image particle moving synchronously with the actual particle. We only need to keep in mind that both particles would interact with the surrounding photon bath, so that a frictional force does indeed arise. Following this line of reasoning, the image particle would double the normal component of the fluctuation-induced field, E_z , but eliminate the tangential components, E_x and E_y , at the surface of the PC plate. Since these fluctuation-induced frictional forces are proportional to the product of the relevant fields, F^{ZZ} is therefore quadrupled while the other contributions are all suppressed when the distance between the particle and the PC plate approaches zero.

The physics here is analogous to a classical situation in hydrodynamics. For example, Krüger and Rauscher [76] studied colloidal particles driven through a suspension of mutually noninteracting Brownian particles and the corresponding frictional force induced by the nonequilibrium fluid structure. (The flow field comoving

with the colloidal particles is not in equilibrium with the Brownian particles.) They found that the frictional force on a single colloidal particle traveling along a wall (analogous to the PC plate in our case) is precisely the same as that on two colloidal particles driven side by side. The authors also found an enhancement of the friction due to the wall or image colloidal particle in comparison to the friction on an isolated colloidal particle. From the density plot of the solute Brownian particles, they interpret this increase in friction as the result of more Brownian particles aggregating in front of the colloidal particles when the wall or image particle is present. An analogous interpretation applies to what we see here for QFPC. That is, the electromagnetic energy density is stronger near the PC plate.

So far, both the small z results in Eq. (4.13) and the large z results in Eq. (4.14) are exact in velocity. Another meaningful limit to take is the nonrelativistic (NR) limit without assuming anything about z . It turns out that all contributions to QFPC start with a term linear in v in the NR limit. In Appendix C, we use F^{XZ} to illustrate how to obtain the small z limit, the large z limit as well as the non-relativistic limit analytically. The approach listed there will work for contributions from other polarizations as well.

As one of the contributions, F^{XZ} , is positive (a push), while the others are all negative (a drag), a natural question arises: could the overall “frictional” force on an atom ever flip sign and therefore become a push? Of course, from Eq. (4.13) and Eq. (4.14), we can already conclude that the overall QFPC is negative definite in both the small z (vacuum/high-temperature) limit and large z (short-distance/low-temperature) limit. But, there is no convincing argument just from the analytic results suggesting that QFPC cannot switch sign in the intermediate z regime. Therefore, we resort to numerical methods to ascertain the sign of QFPC.

We will therefore consider atoms in their ground states, the polarizability of which is normally quite isotropic and can be well approximated by its static value, $\alpha(\omega) = \alpha(0)\mathbf{1}$. For such isotropic atoms, the sign of the QFPC is determined by the sum of the dimensionless functions introduced in Eq. (4.12):

$$F^{\text{ISO}} = \frac{\alpha^2(0)}{32\pi^3(2a)^8} f^{\text{ISO}}(v, z), \quad f^{\text{ISO}}(v, z) = f^{\text{XX}}(v, z) + f^{\text{YY}}(v, z) + f^{\text{ZZ}}(v, z) + f^{\text{XZ}}(v, z). \quad (4.15)$$

We show the absolute value of these dimensionless functions across their transition region in Fig. 4.2. Starting from small z values, the total frictional force on the isotropic particle is dominated almost evenly between the ZZ and YY contributions. But as z grows larger, the weight of the YY contribution decays so that the ZZ contribution solely dominates the entire frictional force. As for the unique positive contribution from the XZ polarization, it is completely negligible when z is small but it eventually surpasses the contributions from the XX and YY polarizations for large z . Nonetheless, it never dominates the ZZ polarization. The asymptotic (in z) expressions in Eq. (4.13) and Eq. (4.14) are consistent with these behaviors and the agreement with the numerical data in their supposedly valid regimes are also clearly illustrated in the figure. So, we can conclude that the total QFPC on an isotropic atom *is always a drag*, since it *cannot* change sign even in the intermediate z regime.

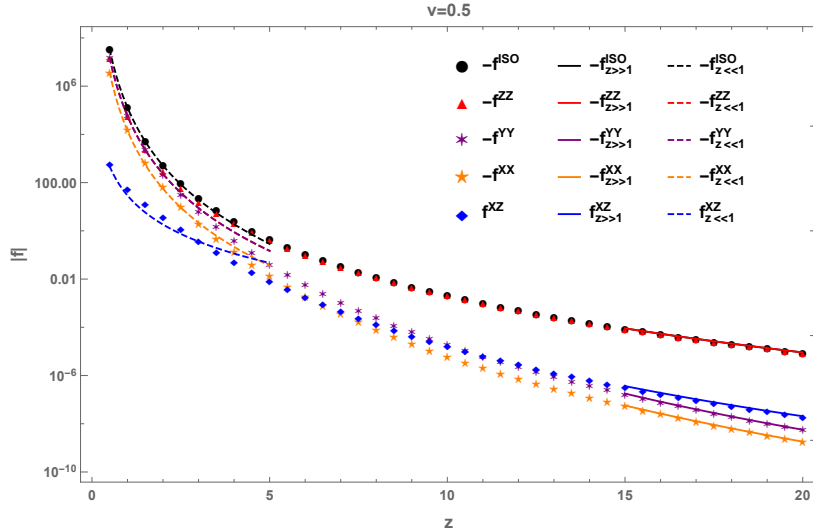


Figure 4.2: The absolute values of the dimensionless functions f^{PQ} in Eq. (4.15) are shown as functions of z for fixed velocity ($v = 0.5$). The numerical results are computed directly using Eq. (4.9) and Eq. (4.12). Their small z and large z approximations are obtained from Eq. (4.13) and Eq. (4.14), respectively. Since the small z approximation for f^{ZZ} and f^{YY} is identical, the dashed purple line overlaps with the dashed red line. As is seen, the small z approximation of F^{XZ} cannot give a good description of the numerical data beyond $z = 1$. A further detailed plot is provided in Appendix C, where the agreement between the analytic approximation and the numerical data for F^{XZ} is more clearly demonstrated for smaller z values.

Another interesting aspect of the force is, of course, its magnitude. Fluctuation induced forces are typically small. But, is the QFPC possibly accessible to experiment? Here, we estimate QFPC on a cesium (Cs) atom, which has the

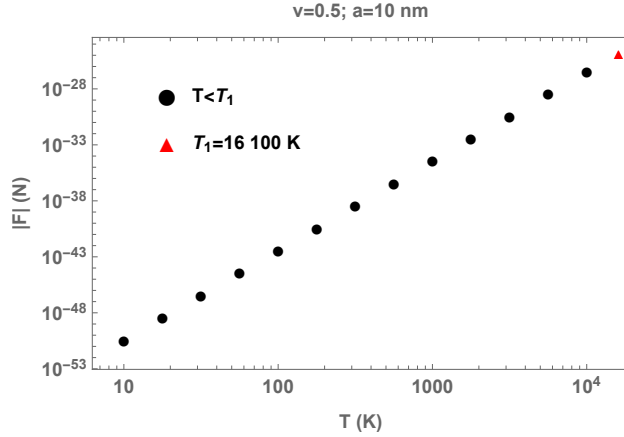


Figure 4.3: The magnitude of the total frictional force on a Cs atom moving at $v = 0.5$ and at a distance $a = 10$ nm from the PC plate is plotted as a function of temperature. The friction at the first excited temperature is indicated by the red triangle, with a magnitude of 1.30×10^{-25} N.

largest static polarizability,³ according to Ref. [69], $\alpha_{\text{Cs}}(0) = 59.3 \text{ \AA}^3$. Because the expression (4.12) we use for numerical calculation is obtained in the static limit, the corresponding numerical results are only expected to be appropriate when the atom is in its ground state, that is, up to the temperature that corresponds to the *first excitation energy* of the Cs atom, $T_1 = 16\,100$ K,⁴ beyond which a model for its dynamical polarizability is needed. In Fig. 4.3, we show the magnitude of the total frictional force on a Cs atom up to T_1 , fixing velocity and distance. The friction clearly exhibits a power-law dependence on temperature. This is no surprise because we already know that the frictional force should behave as T^8 in both the large z (low T) and small z (high T) regimes.

Of course, QFPC also depends on the distance between the atom and the plate, distinguishing it from QVF. Considering the size of the Cs atom⁵, we should keep the distance greater than 1 nm to avoid additional surface effects. We therefore show the magnitude of QFPC for a Cs atom as a function of distance in Fig. 4.4, from 1 nm to 1 μm , fixing the velocity at $v = 0.5$ and temperature at $T = T_1$. It is seen that the total friction is only doubled when the distance is reduced from 1 μm to

³Within a period, the alkali metal atoms generally have the biggest polarizabilities. They are also supposed to have very tiny anisotropy because their valence electrons are in s states [70]. Cs has the largest polarizability among the alkali metal atoms.

⁴This temperature and the ionization temperature used later are obtained from the first excitation energy of Cs listed in Ref. [77].

⁵Cesium also has the largest covalent radius (244 pm) among the nonradioactive atoms according to Ref. [78].

1 nm. This can be well understood from the asymptotic behavior of the dominant contributions: the ZZ contribution quadruples, yet the YY contribution vanishes at small distances, which is also clearly illustrated in the figure.

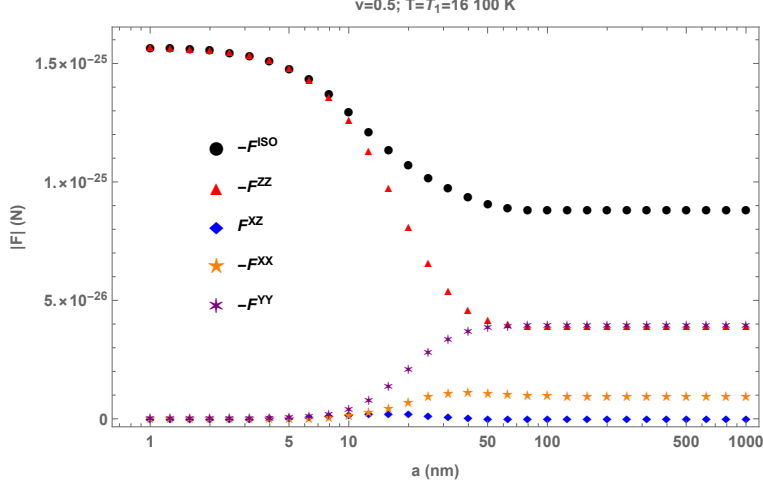


Figure 4.4: The magnitude of the total frictional force, along with its contributions from different polarizations, on a Cs atom moving at $v = 0.5$ and at its first excited temperature $T = 16\,100$ K is plotted as a function of distance. The largest magnitude of the total friction shown by the black dots is for $a = 1$ nm, being 1.57×10^{-25} N.

Finally, QFPC depends on the velocity of the atom. As is shown in Fig. 4.5a, the magnitude of the frictional force is linear in v for very small velocities; however, the velocity dependence becomes more prominent for larger velocities. In Fig. 4.5b, we not only plot the total frictional force at the first excitation temperature, $T_1 = 16\,100$ K, but also extrapolate our numerical results to the ionization temperature of the cesium atom, $T_i = 45\,100$ K [77]. Above T_i , the outermost electron will be stripped off the atom so that the cesium atom cannot stay neutral. It is therefore not feasible experimentally to detect the quantum friction on an atom above its ionization temperature. In between T_1 and T_i , the atom can be excited, though not ionized. Now, the frequencies corresponding to the transition of the atom's internal energy levels become important in evaluating QFPC. At these frequencies, the polarizability of the atom develops an imaginary part [57], which results in a QFPC that is first order in the polarizability. This effect is not included in the results we show for $T = T_i$. In addition, by employing the static value for the polarizability, we underestimate the magnitude of the second order QFPC,

because atoms in excited states, e.g., Rydberg atoms,⁶ tend to have much larger polarizabilities.

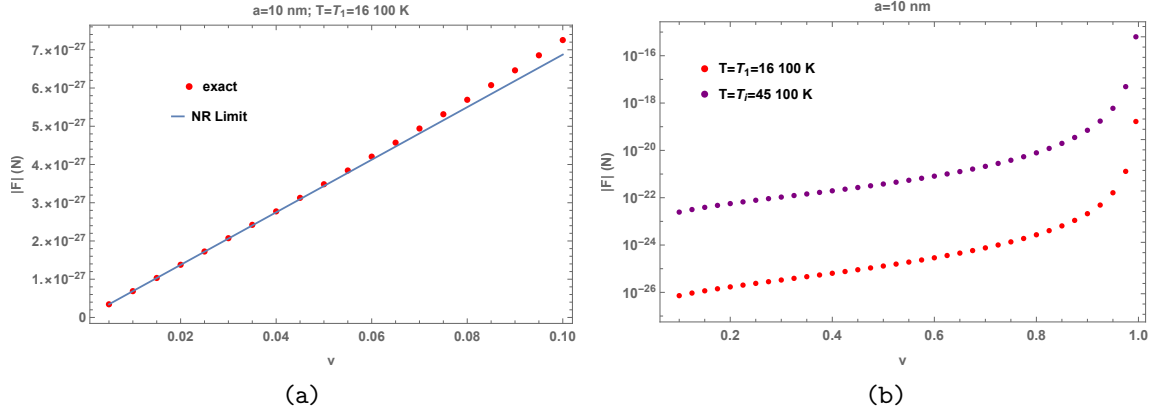


Figure 4.5: The velocity dependence of the magnitude of the total frictional force on a cesium atom at a distance of $a = 10$ nm away from the PC plate. (a) At the first excitation temperature, $T_1 = 16\,100$ K, the frictional force is plotted as a function of velocity for velocities, $v \in [0.005, 0.100]$. The red dots show the exact numerical results based on Eq. (4.12) and Eq. (4.9). The blue solid line shows the term linear in v obtained using the nonrelativistic approximation detailed in Appendix C. (b) In the more relativistic regime, $v \in [0.100, 0.995]$, the red dots show the total frictional force at the first excitation temperature, $T_1 = 16\,100$ K, while the purple dots show the numerical results extrapolated to the ionization temperature, $T_i = 45\,100$ K. For the maximum velocity shown in the figure, $v = 0.995$, the magnitude of the total friction is 1.66×10^{-19} N at T_1 and 6.30×10^{-16} N at T_i .

⁶Even though Rydberg atoms possess much larger polarizabilities, which presumably will enhance the resulting frictional effect, we are unsure whether they could be appropriate candidates for experimental consideration, because blackbody radiation induces transitions to lower n states and reduces the lifetime of the Rydberg states. Even at room temperature, transitions induced by blackbody radiation can contribute more to the decay rate than the spontaneous transitions [79]. At higher temperatures, the transition rate induced by blackbody radiation is even larger.

Chapter 5

Induced Cherenkov Friction (ICF)

We have discussed the two simplest backgrounds for quantum frictional effects to occur, the vacuum whose permittivity is 1 and the perfectly conducting plate whose permittivity is infinite. The next logical step is, of course, to consider the presence of a medium with a finite permittivity different than unity or infinity. Here, for simplicity, we will ignore the permeability of the medium and assume the permittivity is isotropic, which also results in a finite index of refraction, $\varepsilon = n^2$.

What has been known for almost a century as the Vavilov-Cherenkov effect [80, 81, 82] states that a charged particle moving faster than the speed of light of the surrounding medium emits radiation. For pedagogical discussions, see, for example [49, 48]. Similar effects have also been investigated for moving dipoles [83, 84, 85, 20]. The frictional force which accompanies the energy loss of the moving particle can be referred to as Cherenkov friction. Such a force will slow down a fast-moving particle in a medium even if the collision between the charged particle and the medium particles could be ignored. In this chapter, however, we will illustrate that an induced Cherenkov friction (ICF) can also occur for fast-moving particles in a vacuum region above the medium, even for a neutral but polarizable particle which does not carry an intrinsic dipole moment. Emphasis will be placed on how the usual Cherenkov condition, $v > 1/n$, arises in these situations.

We examine ICF on charged particles in Sec. 5.1. Dispersion of the medium is ignored in Sec. 5.1.1, which allows us to derive the frictional force analytically. Dispersion is taken into account in Sec. 5.2, where we obtain the expressions of ICF ready for numerical evaluation. Quantum Cherenkov friction resulting from fluctu-

ations is discussed in Sec. 5.2. We obtain the expression for ICF on a dissipative nanoparticle and give some numerical estimates of the force for a gold nanosphere. Of course, quantum Cherenkov friction could also be induced between two moving media, like that being discussed in [86].

5.1 Induced Cherenkov Friction on a Charged Particle

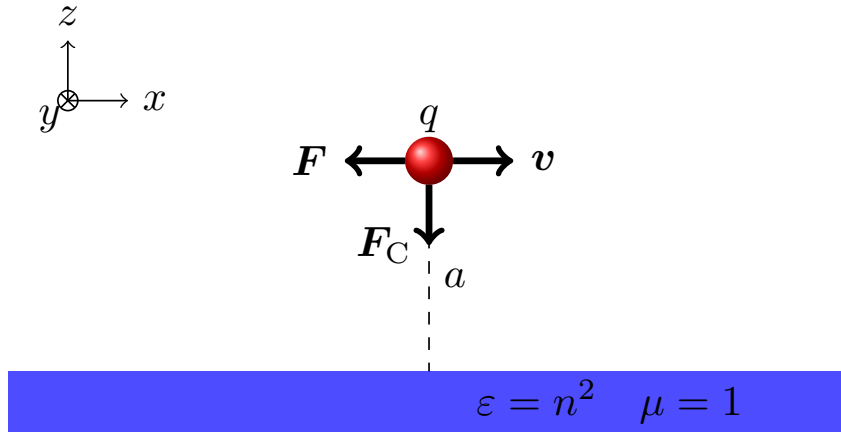


Figure 5.1: Illustration of a charged particle flying above a medium with a real index of refraction n .

Before diving into the quantum realm, let us first investigate the friction induced on a charged particle when it moves parallel to a dielectric with index of refraction n . The discussion here is in fact within the realm of classical electrodynamics, because the friction does not originate from fluctuations. Therefore, no quantization is involved. But, the setting here does differ from the classic setting for Cherenkov radiation, where the charged particle itself moves inside the medium. Here, the charged particle, q , moves with constant velocity, v , parallel to a dielectric plate in vacuum. For simplicity, we ignore the magnetic properties of the medium. The physical situation is illustrated in Fig. 5.1. The static Coulomb interaction between the surface and the charged particle, F_C , is normal to the planar surface. But, we shall see that there also exists a tangential component of the classical Lorentz force, F , which acts as a frictional force on the charged particle.

5.1.1 A nondispersive medium

The Lorentz force on a charged particle is

$$\mathbf{F} = q(\mathbf{E} + \mathbf{v} \times \mathbf{B}). \quad (5.1)$$

The trajectory of the charged particle shown in Figure 5.1 is

$$\mathbf{R}(t) = (x = vt, y = 0, z = a). \quad (5.2)$$

The Lorentz force in the direction of the particle's motion (x) acts as a frictional force on the particle,

$$F(t) = qE_x(t, \mathbf{R}(t)). \quad (5.3)$$

The current density due to the moving charged particle is

$$j_x(t, \mathbf{r}) = qv\delta(x - vt)\delta(y)\delta(z - a) \Rightarrow j_x(\omega; \mathbf{r}) = qe^{i\frac{\omega}{v}x}\delta(y)\delta(z - a). \quad (5.4)$$

The field induced by the current in Eq. (5.4) is

$$\begin{aligned} E_x(\omega; \mathbf{r}) &= -\frac{1}{i\omega} \int d\tilde{\mathbf{r}} G_{xx}(\omega; \mathbf{r}, \tilde{\mathbf{r}}) j_x(\omega; \tilde{\mathbf{r}}) \\ &= -\frac{q}{i\omega} \int \frac{dk_y}{2\pi} e^{(i\frac{\omega}{v}x + ik_y y)} G_{xx}\left(\omega, k_x = \frac{\omega}{v}, k_y; z, a\right). \end{aligned} \quad (5.5)$$

Notice only special modes $\omega = k_x v$ are selected to contribute to the frictional force,

$$F = q^2 \int \frac{d\omega}{2\pi} \left(-\frac{1}{i\omega}\right) \int \frac{dk_y}{2\pi} G_{xx}\left(\omega, k_x = \frac{\omega}{v}, k_y; a, a\right). \quad (5.6)$$

The frictional force in Eq. (5.6) is independent of time and independent of the sign of the charge. In addition, only the odd in ω part in G_{xx} will contribute to the frictional force.

According to Eq. (2.93), G_{xx} in a planar geometry reads

$$G_{xx}(\omega, \mathbf{k}_\perp; z, \tilde{z}) = \frac{k_x^2}{k^2} \partial_z \partial_{\tilde{z}} g^H + \frac{k_y^2}{k^2} \omega^2 g^E. \quad (5.7)$$

The scalar Green's functions are

$$g^{E,H}(\omega, k; z, \tilde{z}) = \frac{1}{2\kappa} e^{-\kappa|z-\tilde{z}|} + \frac{r^{E,H}}{2\kappa} e^{-\kappa(z+\tilde{z})} \quad (5.8)$$

where the reflection coefficients involve two different propagation wave numbers associated with the vacuum and the medium, respectively,

$$r^E = \frac{\kappa - \kappa_n}{\kappa + \kappa_n}, \quad r^H = \frac{\kappa - \kappa_n/n^2}{\kappa + \kappa_n/n^2}. \quad (5.9)$$

The vacuum propagation wave number, κ , is purely real for the contributing modes because

$$\kappa^2 = k^2 - \omega^2 = \left(\frac{\omega}{v}\right)^2 + k_y^2 - \omega^2 = \frac{\omega^2}{\gamma^2 v^2} + k_y^2 > 0. \quad (5.10)$$

It is also even in ω . As a result, the bulk part of the Green's function, which only involves κ , does not contribute to the friction.

The propagation wave number in the dielectric for the contributing modes, however, could become purely imaginary if

$$\kappa_n^2 = k^2 - \omega^2 n^2 = \kappa^2 - \omega^2(n^2 - 1) = \omega^2 \left(\frac{1}{v^2} - n^2\right) + k_y^2 < 0. \quad (5.11)$$

which can be satisfied in the integration region

$$k_y^2 < k_n^2 = \left(n^2 - \frac{1}{v^2}\right) \omega^2. \quad (5.12)$$

Such integration region is null unless

$$nv > 1, \quad (5.13)$$

which is precisely the standard Cherenkov condition. We assume n is constant in this section, so that the Cherenkov threshold velocity $v_C = 1/n$ is nondispersive in frequency.

Above the Cherenkov threshold, $v > v_C$, and in the integration region, $k_y^2 < k_n^2$,

$$\kappa_n \implies -i \operatorname{sgn}(\omega) \sqrt{\omega^2(n^2 - 1) - \kappa^2} = -i \operatorname{sgn}(\omega) \sqrt{k_n^2 - k_y^2} \quad (5.14)$$

becomes odd in ω and purely imaginary. The frictional force, therefore, only arises from the imaginary part of the Green's function,

$$F = -\frac{q^2}{4\pi^2} \int \frac{d\omega}{\omega} \int_{k_y^2 < k_n^2} dk_y \operatorname{Im} G_{xx} \left(\omega, k_x = \frac{\omega}{v}, k_y; a, a \right). \quad (5.15)$$

In view of Eq. (5.10), it is convenient to introduce polar coordinates as integration variables by letting

$$\frac{\omega}{\gamma v} = \kappa \cos \theta, \quad k_y = \kappa \sin \theta. \quad (5.16)$$

As a result,

$$F = -\frac{q^2}{4\pi^2} \int d\theta \frac{1}{\cos \theta} \int d\kappa \operatorname{Im} G_{xx} (\omega = \gamma v \kappa \cos \theta, k_x = \gamma \kappa \cos \theta, k_y = \kappa \sin \theta; a, a), \quad (5.17)$$

for which $k_n^2 > k_y^2$ translates to

$$\cos^2 \theta > \frac{1}{(\gamma^2 - 1)(n^2 - 1)} \quad (5.18)$$

independent of κ . This allows us to easily integrate κ out when plugging in the Green's function. Since κ is real definite and the friction arises from the imaginary part of κ_n , only the scattering part of the Green's function contributes to the friction through the imaginary reflection coefficients,

$$\begin{aligned} F &= -\frac{q^2}{8\pi^2(2a)^2} \int d\theta \frac{\cos \theta}{\gamma^2 \cos^2 \theta + \sin^2 \theta} [(\gamma^2 - 1) \sin^2 \theta \operatorname{Im} r^E + \gamma^2 \operatorname{Im} r^H] \\ &= -\frac{q^2}{32\pi^2 a^2} [f^E(\gamma, n) + f^H(\gamma, n)], \end{aligned} \quad (5.19)$$

where

$$\text{Im } r^E = \text{Im} \frac{2}{1 + \kappa_n/\kappa} = 2\text{sgn}(\cos \theta) \frac{\sqrt{(\gamma^2 - 1)(n^2 - 1) \cos^2 \theta - 1}}{(\gamma^2 - 1)(n^2 - 1) \cos^2 \theta}, \quad (5.20)$$

$$\text{Im } r^H = \text{Im} \frac{2}{\kappa + \kappa_n/n^2} = 2\text{sgn}(\cos \theta) \frac{\frac{1}{n^2} \sqrt{(\gamma^2 - 1)(n^2 - 1) \cos^2 \theta - 1}}{1 - \frac{1}{n^4} \sqrt{(\gamma^2 - 1)(n^2 - 1) \cos^2 \theta - 1}}. \quad (5.21)$$

Notice both the integrand in Eq. (5.19) and the integration region Eq. (5.18) are even in $\cos \theta$, which enables us to rewrite the integral with the new variable $x = \sin \theta$,

$$\begin{aligned} f^E(\gamma, n) &= \frac{4}{\sqrt{(\gamma^2 - 1)(n^2 - 1)}} \int_{-x_0}^{x_0} dx \frac{x^2}{x_1^2 - x^2} \frac{\sqrt{x_0^2 - x^2}}{1 - x^2} \\ f^H(\gamma, n) &= \frac{4n^2/v^2}{\sqrt{(\gamma^2 - 1)(n^2 - 1)}} \int_{-x_0}^{x_0} dx \frac{1}{x_1^2 - x^2} \frac{\sqrt{x_0^2 - x^2}}{x_2^2 - x^2}, \end{aligned} \quad (5.22)$$

with the shorthand notations

$$x_0^2 = 1 - \frac{1}{\sqrt{(\gamma^2 - 1)(n^2 - 1)}} < 1, \quad x_1^2 = \frac{1}{v^2} > 1, \quad x_2^2 = 1 + \frac{n^4 - 1}{\sqrt{(\gamma^2 - 1)(n^2 - 1)}} > 1. \quad (5.23)$$

The integrals in Eq. (5.22) are manifestly convergent and in fact can be integrated analytically,

$$\begin{aligned} f^E(\gamma, n) &= -\frac{4\pi}{\sqrt{(\gamma^2 - 1)(n^2 - 1)}} \left(1 + \sqrt{\frac{\gamma^2 - 1}{n^2 - 1}} - \frac{n\gamma}{\sqrt{n^2 - 1}} \right), \\ f^H(\gamma, n) &= \frac{4\pi}{\sqrt{(\gamma^2 - 1)(n^2 - 1)}} \left(\frac{\gamma^2 n^2}{\sqrt{(\gamma^2 + n^2)(n^2 - 1)}} - \frac{n\gamma}{\sqrt{n^2 - 1}} \right). \end{aligned} \quad (5.24)$$

The sum of the two contributions reads

$$f^{\text{tot}} = f^E + f^H = \frac{4\pi}{\sqrt{(\gamma^2 - 1)(n^2 - 1)}} \left(\frac{\gamma^2 n^2}{\sqrt{(\gamma^2 + n^2)(n^2 - 1)}} - \sqrt{\frac{\gamma^2 - 1}{n^2 - 1}} - 1 \right), \quad (5.25)$$

which can be shown to be positive for $nv > 1$ and to vanish at the threshold velocity v_C . Therefore, the induced Cherenkov friction is negative definite, that is, a true drag, and it only exists when the charged particle moves faster than the Cherenkov threshold velocity.

In the relativistic limit, we find

$$\gamma \gg n > 1 : f^{tot} \longrightarrow 4\pi. \quad (5.26)$$

It is quite surprising that the friction becomes independent of velocity and insensitive to the index of refraction of the dielectric in this limit. In the static situation,¹ the Coulomb force in the normal direction reads

$$F_C = -\frac{q^2}{4a^2} \frac{n^2 - 1}{n^2 + 1}. \quad (5.27)$$

The ratio of the (relativistic) tangential ICF to the normal force is therefore

$$\frac{F}{F_C} = \frac{1}{2\pi} \frac{n^2 + 1}{n^2 - 1}. \quad (5.28)$$

On the other hand, in the perfectly conducting limit,

$$n \gg \gamma > 1 : f^{tot} \sim 4\pi \frac{\sqrt{\gamma^2 - 1}}{n} \longrightarrow 0, \quad (5.29)$$

the friction on the charged particle vanishes. That is, a genuine frictionless surface needs to be not only perfectly smooth but also perfectly conducting!

5.1.2 A dispersive medium

In the last section, the assumption that the index of refraction is just a constant, independent of frequency, is undoubtedly an oversimplification. Let us in this section take into account the dispersion of the dielectric surface.

An immediate complication of worrying about the dispersion is that the Cherenkov condition, Eq. (5.13), now also becomes frequency dependent,

$$n(\omega)v > 1. \quad (5.30)$$

This condition selects the frequency modes that will contribute to the ICF in

¹Here, we are citing the familiar results of electrostatics [48, 49], ignoring the modification of the Coulomb force due to the relativistic motion. A more careful treatment would be examining the z component of the Lorentz force using the method outlined for computing the ICF in this section.

Eq. (5.15) and can be complicated depending on the specific form of $n(\omega)$.² Here, we will still make an assumption that $n(\omega)$ is purely real, which avoids the entanglement between the effect of induced Cherenkov radiation and that of the dissipation in the dielectric surface. As a consequence, $n(\omega)$ is an even function in ω .³

The integrand in Eq. (5.15) is then guaranteed to be even in both ω and k_y so that it can be rewritten as

$$F = -\frac{q^2}{\pi^2} \int_0^\infty \frac{d\omega}{\omega} \int_0^\infty dk_y \operatorname{Im} G_{xx}^s \left(\omega, k_x = \frac{\omega}{v}, k_y; a, a \right). \quad (5.31)$$

The integration range in Eq. (5.31) is only formal, because not all those modes with positive ω and k_y will contribute to the ICF. This can be seen by analyzing the two relevant propagation wave numbers. The vacuum propagation wave number is guaranteed to be real and even in ω ,

$$\kappa^2 = \sqrt{k_y^2 + k_1^2}, \quad k_1 = \frac{\omega}{\gamma v}. \quad (5.32)$$

Therefore, the only source for an imaginary part to arise in the Green's function is the propagation wave number in the medium, κ_n , and it so happens only if

$$\kappa_n^2 = k_y^2 - \omega^2 \left[n(\omega)^2 - \frac{1}{v^2} \right] < 0. \quad (5.33)$$

This requires not only the Cherenkov condition in Eq. (5.30) to hold, but also

$$k_n^2 = \omega^2 \left[n(\omega)^2 - \frac{1}{v^2} \right] > k_y^2. \quad (5.34)$$

Under these conditions, κ_n becomes purely imaginary and odd in ω ,

$$\kappa_n \implies -i \operatorname{sgn}(\omega) \sqrt{k_n^2 - k_y^2}. \quad (5.35)$$

The actual calculation differs from the nondispersive case in that we want to retain ω as an integration variable, since the index of refraction depends on ω

²If the permittivity of the medium can be modeled by a set of resonant oscillators, the Cherenkov modes usually lies below the resonance frequencies of each oscillator. Of course, the widths of the continuous Cherenkov band is very sensitive to the velocity of the particle [49].

³Since $\varepsilon = n^2$, the permittivity, ε , is real when n is real. As a generalized susceptibility, the real part of the permittivity must be even in ω . It then follows that $n(\omega)$ is even.

explicitly. The reflection coefficients should therefore be written as

$$\begin{aligned}\text{Im } r^E &= 2\text{sgn}(\omega) \frac{\sqrt{(k_1^2 + k_y^2)(k_n^2 - k_y^2)}}{k_1^2 + k_n^2}, \\ \text{Im } r^H &= 2\text{sgn}(\omega) \frac{\frac{1}{n^2} \sqrt{(k_1^2 + k_y^2)(k_n^2 - k_y^2)}}{(1 - \frac{1}{n^4})k_y^2 + (k_1^2 + \frac{1}{n^4}k_n^2)}.\end{aligned}\quad (5.36)$$

The ICF on the particle can be split into the contributions from the E mode and the H mode,

$$F = -\frac{q^2}{\pi^2} \int_{0, n(\omega)v > 1}^{\infty} d\omega \omega (f^E + f^H), \quad (5.37)$$

where f^E and f^H are

$$\begin{aligned}f^E &= \int_0^{k_n} dk_y \frac{k_y^2}{\frac{\omega^2}{v^2} + k_y^2} \frac{\sqrt{k_n^2 - k_y^2}}{k_1^2 + k_n^2} e^{-2\sqrt{k_1^2 + k_y^2}a}, \\ f^H &= \int_0^{k_n} dk_y \frac{1}{n^2 v^2} \frac{k_1^2 + k_y^2}{\frac{\omega^2}{v^2} + k_y^2} \frac{\sqrt{k_n^2 - k_y^2}}{(1 - \frac{1}{n^4})k_y^2 + (k_1^2 + \frac{1}{n^4}k_n^2)} e^{-2\sqrt{k_1^2 + k_y^2}a}.\end{aligned}\quad (5.38)$$

Both f^E and f^H are dimensionless functions. It is therefore useful to introduce the following dimensionless variables,

$$\frac{k_y}{k_n} = y, \quad \frac{\omega/v}{k_n} = \frac{1}{\sqrt{n^2 v^2 - 1}} = b, \quad \frac{k_1}{k_n} = \frac{b}{\gamma}, \quad x = 2\omega a, \quad (5.39)$$

so that Eq. (5.38) becomes

$$\begin{aligned}f^E(x, n, v) &= \int_0^1 dy \frac{y^2}{y^2 + b^2} \frac{\sqrt{1 - y^2}}{1 + \frac{b^2}{\gamma^2}} e^{-\frac{x}{v} \sqrt{\frac{y^2}{b^2} + \frac{1}{\gamma^2}}}, \\ f^H(x, n, v) &= \int_0^1 dy \frac{1}{n^2 v^2} \frac{y^2 + \frac{b^2}{\gamma^2}}{y^2 + b^2} \frac{\sqrt{1 - y^2}}{(1 - \frac{1}{n^4})y^2 + (\frac{b^2}{\gamma^2} + \frac{1}{n^4})} e^{-\frac{x}{v} \sqrt{\frac{y^2}{b^2} + \frac{1}{\gamma^2}}}.\end{aligned}\quad (5.40)$$

In the case of a constant n , the ω integral in Eq. (5.37) can be easily integrated and the results, of course, coincide with those found in Sec. 5.1.1. But, in general, one needs to first identify the frequency modes that satisfy the Cherenkov condition,

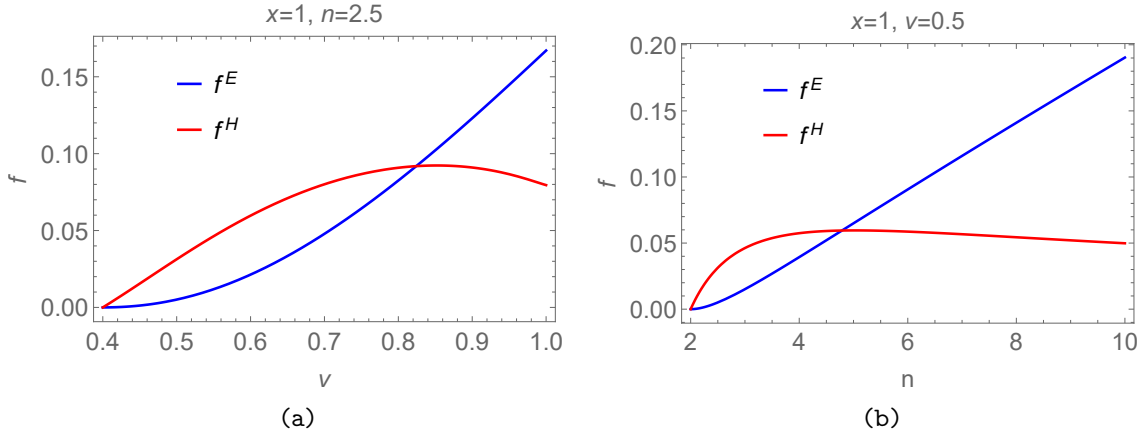


Figure 5.2: Plots of dimensionless functions shown in Eq. (5.40). (a) For $x = 1$, $n = 2.5$, f^E and f^H are plotted as functions of velocity for $v \in [0.4, 1.0]$. (b) For $x = 1$, $v = 0.5$, f^E and f^H are plotted as functions of the index of refraction for $n \in [2, 10]$.

$n(\omega)v > 1$. Due to the presence of the exponential factor appearing in Eq. (5.40), the Cherenkov modes with the lowest frequencies will contribute the most to the ICF on the charged particle, while the contributions from higher frequency modes will be suppressed. In addition, ICF is also exponentially suppressed with increasing distance.

For a particular frequency and a fixed distance such that $x = 2\omega a = 1$, we illustrate how the dimensionless functions in Eq. (5.40) vary with velocity and the index of refraction in Figure 5.2. It is seen from the plot that f^E monotonically increases with both v and n while f^H exhibits peaks in both. As a result, even though f^H dominates over f^E for velocities/index of refraction just above threshold, f^E eventually surpasses f^H for higher velocities and index of refraction.

5.2 Quantum Cherenkov Friction on a Neutral Polarizable Particle

In this section, we study instead the Cherenkov friction induced on a neutral but polarizable particle when it moves parallel to a planar dielectric plate at a distance. The physical situation is illustrated in Figure 5.3. We already know that there exists the famous Casimir-Polder force, which is normal to the surface. We have also discussed and calculated the frictional effect due to the surrounding blackbody

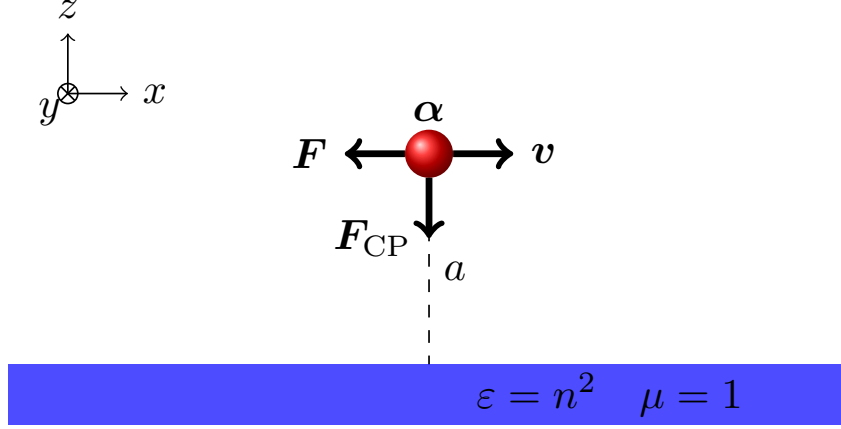


Figure 5.3: Illustration of a neutral but polarizable particle flying above a medium with a real index of refraction n .

radiation in Chapter 3. Here, we will focus on the frictional effect caused by the induced Cherenkov radiation.

The general formula for quantum friction on an intrinsically dissipative particle, Eq. (3.60), obtained through quantization of the classical Lorentz force law by FDT still applies here:

$$F = \int \frac{d\nu'}{2\pi} \frac{d^2\mathbf{k}'}{(2\pi)^3} (k'_x + \nu'v) \text{tr} \mathfrak{S}\boldsymbol{\alpha}'(\nu') \cdot \mathfrak{S}\mathbf{G}'(\nu', \mathbf{k}'_{\perp}; a, a) \times \left\{ \coth\left[\frac{\beta\gamma(\nu' + k'_x v)}{2}\right] - \coth\left(\frac{\beta'\nu'}{2}\right) \right\}. \quad (5.41)$$

The above is slightly generalized than Eq. (3.60) in that it takes into account a non-symmetric polarizability tensor or Green's tensor.

Unlike QVF in Chapter 3 and QFPC in Chapter 4, for which we performed the entire calculation in the rest frame of the particle, \mathcal{P} , here, the presence of a dielectric plate with finite permittivity makes the rest frame of radiation, \mathcal{R} , a preferred frame for the discussion, where we do not need worry about the transformation of material properties. Let us, therefore, use the frequency and momentum intrinsic to frame \mathcal{R} as integration variables by making the following variable changes:

$$\nu' = \gamma(\nu - k_x v), \quad k'_x = \gamma(k_x - \nu v). \quad (5.42)$$

This leads to

$$F = \int \frac{d\nu}{2\pi} \frac{d^2\mathbf{k}}{(2\pi)^3} \frac{k_x}{\gamma} \text{tr} \mathfrak{S}\boldsymbol{\alpha}' [\gamma(\nu - k_x v)] \cdot \mathfrak{S}\mathbf{G}' [\gamma(\nu - k_x v), \gamma(k_x - \nu v), k_y; a, a] \times \left\{ \coth\left(\frac{\beta\nu}{2}\right) - \coth\left[\frac{\beta'}{2}\gamma(\nu - k_x v)\right] \right\}. \quad (5.43)$$

For the configuration illustrated in Figure 5.3 where the polarizable particle moves in vacuum, the bulk contribution to the friction is precisely the QVF already discussed in Chapter 3.⁴ This allows us to set aside the bulk contribution and focus on the scattering contribution. Let us also assume that the polarizability tensor of the nanoparticle is isotropic so that

$$F = \int \frac{d\nu}{2\pi} \frac{d^2\mathbf{k}}{(2\pi)^3} \frac{k_x}{\gamma} \text{Im} \alpha' [\gamma(\nu - k_x v)] \cdot \text{Im} \text{tr} \mathbf{G}'^s [\gamma(\nu - k_x v), \gamma(k_x - \nu v), k_y; a, a] \times \left\{ \coth\left(\frac{\beta\nu}{2}\right) - \coth\left[\frac{\beta'}{2}\gamma(\nu - k_x v)\right] \right\}. \quad (5.44)$$

Now, we want to transform the trace of the Green's tensor from frame \mathcal{P} to frame \mathcal{R} . This can be done with the transformations for the Green's tensor provided in Appendix A. Here, we follow Ref. [30] and further rewrite the trace as a combination of the scalar Green's functions, g^E and g^H in frame \mathcal{R} :

$$\text{tr} \mathbf{G}'^s [\gamma(\nu - k_x v), \gamma(k_x - \nu v), k_y; a, a] = \sum_{\sigma=E,H} \phi_\sigma(\nu, \mathbf{k}_\perp) g_\sigma^s(\nu, \mathbf{k}_\perp). \quad (5.45)$$

Here, $\phi_{E,H}$ are real valued scalar functions

$$\begin{aligned} \phi_E &= [\gamma(\nu - k_x v)]^2 + 2\gamma^2 v^2 k_y^2 \left(1 - \frac{\nu^2}{k^2}\right), \\ \phi_H &= [\gamma(\nu - k_x v)]^2 + 2(k_x^2 + \gamma^2 k_y^2) \left(1 - \frac{\nu^2}{k^2}\right), \end{aligned} \quad (5.46)$$

and $g^{s,\sigma}$ are the scalar Green's functions in Eq. (2.95),

$$g^{s,\sigma}(\nu, \mathbf{k}) = \frac{1}{2\kappa} r^\sigma e^{-2\kappa a}, \quad (5.47)$$

⁴If the medium below fills the region where the polarizable particle moves, the situation is more parallel to the classic Cherenkov effect on charged particles, where the friction will be purely due to the bulk contribution. If, instead, the particle moves in a different medium, both the bulk and the scattering will contribute to the friction, which will result in two different Cherenkov conditions corresponding to the two different media.

which can develop imaginary parts through the propagation wave numbers in vacuum and in the medium, κ and κ_n .

There can be three different sources of dissipation in the particle-radiation system,

- ① *vacuum dissipation:* $\kappa^2 = k^2 - \nu^2 < 0$.
- ② *surface dissipation:* *the index of refraction is imaginary.* (5.48)
- ③ *induced Cherenkov dissipation:* $\kappa_n^2 = k^2 - \nu^2 n^2 < 0$.

In general, the three mechanisms listed above will interfere together, which renders the calculation complicated. Here, we wish to isolate the friction caused by the induced Cherenkov dissipation. Surface dissipation can be avoided by considering a dielectric surface with a real index of refraction, n . And we shall now see that the vacuum dissipation is turned off at zero temperature, $T = T' = 0$.

Using the evenness of the integrand in Eq. (5.44), the friction can be rewritten as

$$F = \frac{1}{4\pi^3\gamma} \int_{-\infty}^{\infty} d\nu \int_0^{\infty} dk_x \int_{-\infty}^{\infty} dk_y k_x \operatorname{Im} \alpha' [\gamma(\nu - k_x v)] \sum_{\sigma=E,H} \phi_{\sigma}(\nu, \mathbf{k}_{\perp}) \operatorname{Im} g^{s,\sigma}(\nu, \mathbf{k}_{\perp}) \times [\operatorname{sgn}(\nu) - \operatorname{sgn}(\nu - k_x v)]. \quad (5.49)$$

The difference of the sgn functions can be translated onto the integral limits for ν ,

$$F = \frac{1}{2\pi^3\gamma} \int_0^{\infty} dk_x \int_0^{k_x v} d\nu \int_{-\infty}^{\infty} dk_y k_x \operatorname{Im} \alpha' [\gamma(\nu - k_x v)] \sum_{\sigma=E,H} \phi_{\sigma}(\nu, \mathbf{k}_{\perp}) \operatorname{Im} g^{s,\sigma}(\nu, \mathbf{k}_{\perp}). \quad (5.50)$$

Apparently, the propagation wave number in vacuum, κ , is now real definite because

$$\kappa^2 = k_y^2 + k_1^2, \quad k_1^2 = k_x^2 - \nu^2 > 0. \quad (5.51)$$

There is therefore no vacuum dissipation. The only source of dissipation is in the propagation wave number in the medium, κ_n , which only develops an imaginary

part if

$$\kappa_n^2 = k_y^2 - k_n^2 < 0 \text{ and } k_n^2 = \nu^2 n^2 - k_x^2 > 0 \implies \nu > \frac{k_x}{n} \text{ and } k_y^2 < k_n^2. \quad (5.52)$$

Under these conditions, κ_n becomes purely imaginary,

$$\kappa_n \longrightarrow -i \operatorname{sgn}(\omega) \sqrt{k_n^2 - k_y^2}. \quad (5.53)$$

Taking these considerations into account, the ICF on the polarizable particle should be written as

$$F = \frac{1}{2\pi^3 \gamma} \int_0^\infty dk_x \int_{\frac{k_x}{n}}^{k_x v} d\nu \int_{-k_n}^{k_n} dk_y k_x \operatorname{Im} \alpha' [\gamma(\nu - k_x v)] \sum_{\sigma=E,H} \phi_\sigma(\nu, \mathbf{k}_\perp) \operatorname{Im} g^{s,\sigma}(\nu, \mathbf{k}_\perp), \quad (5.54)$$

from which we see that a nonvanishing friction automatically implies the Cherenkov condition,

$$n\nu > 1. \quad (5.55)$$

The expression for ICF obtained here precisely agrees that found in Ref. [30].

Now, for the purpose of evaluating the friction, let us write explicitly

$$\begin{aligned} \operatorname{Im} g^{s,E} &= \operatorname{Im} \frac{1}{\kappa + \kappa_n} e^{-2\kappa a} = \frac{\sqrt{k_n^2 - k_y^2}}{\nu^2(n^2 - 1)} e^{-2\sqrt{k_y^2 + k_1^2} a}, \\ \operatorname{Im} g^{s,H} &= \operatorname{Im} \frac{1}{\kappa + \kappa_n/n^2} e^{-2\kappa a} = \frac{\frac{1}{n^2} \sqrt{k_n^2 - k_y^2}}{(k_x^2 + k_y^2)(1 - \frac{1}{n^4}) - \nu^2(1 - \frac{1}{n^2})} e^{-2\sqrt{k_y^2 + k_1^2} a}. \end{aligned} \quad (5.56)$$

A model for the polarizability is also needed. We will again consider a nanoparticle made of gold, the imaginary part of which maybe described by Eq. (2.117) as

$$\operatorname{Im} \alpha(\omega) = V \frac{\omega_p^2 \omega \eta}{(\omega_1^2 - \omega^2)^2 + \omega^2 \eta^2}, \quad (5.57)$$

where V is the volume of the nanoparticle, $\omega_p = 9 \text{ eV}$ is plasma frequency of gold, $\omega_1 = \omega_p/\sqrt{3} = 5.20 \text{ eV}$ is the resonance frequency induced by the Lorenz-Lorentz relation, and $\eta = 0.035 \text{ eV}$ is the damping parameter of gold.

Now, we have all ingredients needed to evaluate the ICF in Eq. (5.54). Special attention needs to be paid to the fact that the frequency of the polarizability needs

to be Lorentz shifted before plugging into the ICF in Eq. (5.54). It is also convenient to scale out the dimensional factors in Eq. (5.54) using

$$\nu = \omega_1 u, \quad k_x = \omega_1 x, \quad k_y = \omega_1 y, \quad \eta = \omega_1 \delta, \quad w = 2\omega_1 a. \quad (5.58)$$

After the scaling, ICF on the nanoparticle can be written as,

$$F = \frac{V\omega_p^2\omega_1^3}{\pi^3} [f^E(n, \nu, \delta, w) + f^H(n, \nu, \delta, w)], \quad (5.59)$$

where the two dimensionless functions read

$$\begin{aligned} f^E(n, \nu, \delta, w) &= \int_0^\infty dx \int_{x/n}^{xv} du \int_0^{\sqrt{u^2 n^2 - x^2}} dy \frac{x(u-xv)\delta}{[1 - \gamma^2(u-xv)^2]^2 + \gamma^2(u-xv)^2 \delta^2} \\ &\quad \times \left[\gamma^2(u-xv)^2 + 2\gamma^2 v^2 y^2 \left(1 - \frac{u^2}{x^2 + y^2} \right) \right] \\ &\quad \times \frac{\sqrt{u^2 n^2 - x^2 - y^2}}{(n^2 - 1)u^2} e^{-w\sqrt{x^2 + y^2 - u^2}}, \\ f^H(n, \nu, \delta, w) &= \int_0^\infty dx \int_{x/n}^{xv} du \int_0^{\sqrt{u^2 n^2 - x^2}} dy \frac{x(u-xv)\delta}{[1 - \gamma^2(u-xv)^2]^2 + \gamma^2(u-xv)^2 \delta^2} \\ &\quad \times \left[\gamma^2(u-xv)^2 + 2(x^2 + \gamma^2 y^2) \left(1 - \frac{u^2}{x^2 + y^2} \right) \right] \\ &\quad \times \frac{\frac{1}{n^2} \sqrt{u^2 n^2 - x^2 - y^2}}{(x^2 + y^2) \left(1 - \frac{1}{n^4} \right) - u^2 \left(1 - \frac{1}{n^2} \right)} e^{-w\sqrt{x^2 + y^2 - u^2}}. \end{aligned} \quad (5.60)$$

The above expressions allow the index of refraction to be dispersive, that is, depending on u . Here, however, we will assume it to be a constant, which allows us to numerically integrate over the dimensionless frequency u and give an estimate of the ICF. This differs from the discussion in [30], where more emphasis is put on the spectrum of the ICF.

For a fixed $n = 2.5$,⁵ the Cherenkov threshold velocity is $v_C = 0.4$, below which the ICF will vanish. The magnitude of the friction obviously scales with the size of the nanoparticle. For example, the volume of a nanosphere is $V = \frac{4}{3}\pi r^3$, where r is the radius of the nanosphere. The other length in the problem is the

⁵This is close to the index of refraction of diamond at a wavelength of $\lambda = 589$ nm.

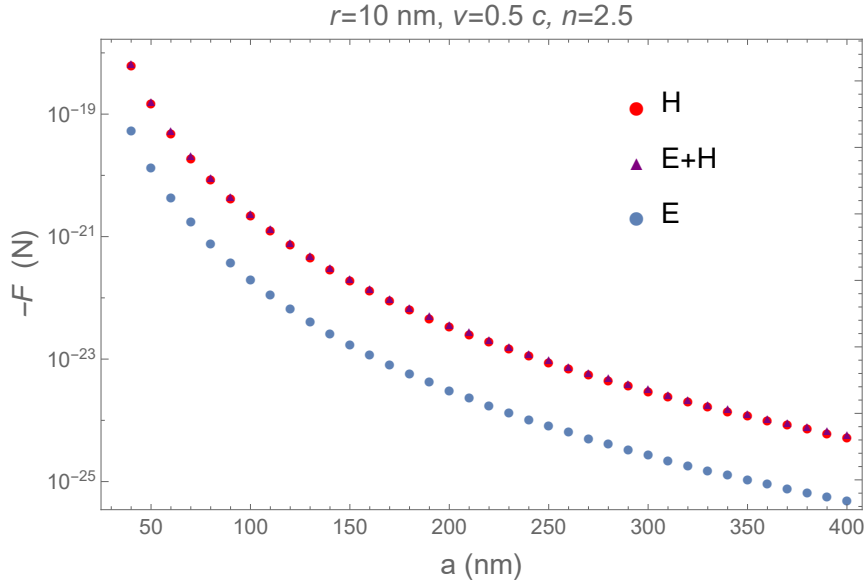


Figure 5.4: A gold nanosphere of radius $r = 10 \text{ nm}$ is moving with a constant velocity, $v = 0.5c$, above a planar dielectric plate with index of refraction, $n = 2.5$. The magnitude of the induced Cherenkov friction on the nanosphere is plotted as a function of the separation between the nanosphere and the plate for $a \in [40 \text{ nm}, 400 \text{ nm}]$. The E mode contribution, the H mode contribution and the total friction are indicated by blue dots, red dots and purple dots, respectively.

distance between the particle and the dielectric plate, a . To minimize any other surface effects, a should be at least several times greater than r . As can be seen in Eq. (5.60), the magnitude of the force should decay with increasing distance due to the exponential factor. A question then arises as to whether the size effect or the distance effect is more prominent. That is, can a bigger friction be achieved by considering a larger nanosphere, even though it is farther away from the surface? Let us now fix the velocity to be $v = 0.5$ and compare numerically the friction for a smaller nanosphere of radius, $r = 10 \text{ nm}$ at a distance $a = 100 \text{ nm}$ to that for a larger nanosphere with $r = 100 \text{ nm}$ at a distance of $a = 1000 \text{ nm} = 1 \mu\text{m}$:

$$\begin{aligned}
 r = 10 \text{ nm}, \quad a = 100 \text{ nm} &\implies F = -2.45 \times 10^{-21} \text{ N}, \\
 r = 100 \text{ nm}, \quad a = 1000 \text{ nm} &\implies F = -2.42 \times 10^{-24} \text{ N}.
 \end{aligned}
 \tag{5.61}$$

This suggests that the decay of ICF with distance is more prominent than the size effect of the nanoparticle.

In Figure 5.4, we illustrate the distance dependence of ICF on a moving gold nanosphere for fixed velocity. Apparently, for $v = 0.5c$, the friction is dominated

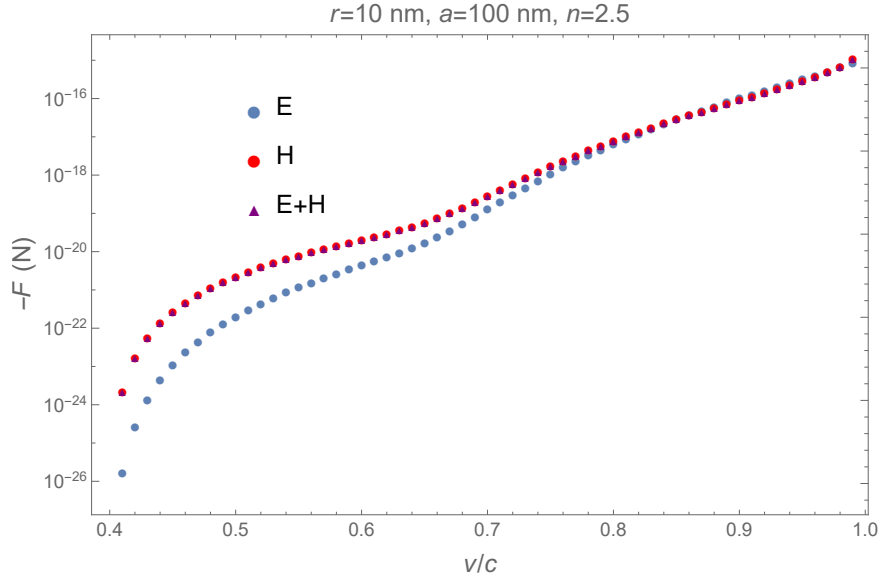


Figure 5.5: A gold nanosphere of radius $r = 10$ nm is moving above a planar dielectric plate with index of refraction, $n = 2.5$ at a fixed distance, $a = 100$ nm. The magnitude of the induced Cherenkov friction on the nanosphere is plotted as a function of the velocity of the nanosphere for $v \in [0.4, 0.99]$. The E mode contribution, the H mode contribution and the total friction are indicated by blue dots, red dots and purple triangles, respectively.

by the contributions from the H mode. When the distance between the particle and the surface is just four times the radius of the particle ($a = 4r = 40$ nm), the magnitude of ICF reaches $-F = 6.89 \times 10^{-19}$ N.

In Figure 5.5, the velocity dependence of ICF is illustrated instead for a nanosphere moving at a fixed distance, $a = 10r = 100$ nm above the dielectric surface. The friction is completely dominated by the H mode contribution for smaller velocities just above the Cherenkov threshold. For higher velocity, however, it is clearly seen that the E mode contribution becomes more and more important and even surpasses that of the H mode at some highly relativistic velocities. The largest magnitude of the friction on the plot is for $v = 0.99$, where it reaches $-F = 1.10 \times 10^{-15}$ N, well within the current experimental reach for minute forces. Of course, the above is just a very rough estimate, particularly in view that we have not allowed dispersion in the dielectric surface. Nonetheless, it does indicate that one might be able to observe the induced Cherenkov friction on a gold (metal) nanosphere if it could be made to move at relativistic speeds.

Chapter 6

Conclusions and Outlook

In this thesis, we have discussed fluctuation-induced-frictional effects on atoms and nanoparticles. These particles possess neither charge nor intrinsic dipole moments. But, they are polarizable and can be polarized by electromagnetic fields. Even without any external fields, the neutral but polarizable particles can be polarized by the quantum and thermal fluctuations of electromagnetic fields. When the particles acquire a nonzero velocity, frictional forces and radiative heat transfer can be induced on the particles. In this thesis, we calculate these quantum frictional effects by quantizing the first principles in classical electrodynamics, namely the Lorentz force law and the Joule heating law, with the fluctuation-dissipation theorem (FDT). Such a unified approach is applied to the calculation of the quantum frictional effects in several simple backgrounds. First, we discuss the quantum vacuum friction (QVF) and quantum vacuum radiative heat transfer (QVRHT) for particles moving in vacuum (free space, not in contact with or close to any other object). The nonequilibrium steady state (NESS) is defined as the state where QVRHT vanishes in the rest frame of the particle, \mathcal{P} . These discussions are based on our recently published papers [21, 22], both of which feature a fully-relativistic treatment. Next, we explore the quantum friction on the particle moving parallel to a perfectly conducting plate (QFPC). This frictional force has been unaddressed by the theoretical community until recently by us [23]. Both QVF and QFPC vanish at zero temperature and QFPC is best understood as QVF modified by the perfectly conducting boundary condition. Finally, we study the friction on a particle moving in vacuum, parallel to a nondissipative dielectric plate with a finite index of refraction.

tion. In this case, even at zero temperature, if the particle's velocity exceeds the speed of light in the dielectric plate, it will experience an induced Cherenkov friction (ICF). The zero-temperature ICF on a neutral particle arises purely from the quantum fluctuations. Both QVF and QFPC reflect that the electromagnetic vacuum itself can be dissipative, while ICF reflects the dissipative nature of the modified (by nondissipative material) electromagnetic vacuum. Discussion of finite-temperature ICF would require a consideration of both mechanisms, which is not detailed in this thesis.

Another obvious extension to the discussions already presented here is to allow the dielectric plate to be dissipative. Quantum frictional effects on particles passing above a dissipative surface had been studied by other groups for years, for example, in Refs. [87, 88, 89, 62]. However, the analyses in these works are restricted to zero-temperature and nonrelativistic regime. A finite-temperature and fully-relativistic treatment of such a situation is in fact very hard because several different dissipation mechanisms would be at work and interfere with each other. We hope the straightforward approach we supply here may prove advantageous in attacking this task systematically.

Furthermore, fluctuation-induced effects are not confined to frictional force and radiative heat transfer. Analogous to the quantum frictional force on a moving particle, a rotating particle experiences a quantum frictional torque which will slow down its rotation, either in vacuum [90, 91] or in the presence of a surface [92]. More intriguingly, a spontaneous torque can be induced on a nonreciprocal particle ($\alpha_{ij} \neq \alpha_{ji}$) sitting in vacuum if the particle is not in equilibrium with the surrounding environment. The nonreciprocity can be activated by a magnetic field, which breaks the time-reversal symmetry¹ of the system apart from the applied magnetic field [94]. A concrete example of a magnetic-field-induced nonsymmetric permittivity tensor for n-doped InSb was used in Ref. [95]. On the contrary, spontaneous forces (first order in the susceptibility) on nonreciprocal particles seem to require not only a time-reversal symmetry-breaking mechanism, but also a surface. Consideration of the spontaneous effects together with the frictional effects leads to potentially observable terminal linear velocity and terminal angular velocity of

¹A comprehensive tutorial on the origin of nonreciprocity and its relationship with time-reversal symmetry breaking can be found in Ref. [93].

the nonreciprocal particle. In Ref. [61], we investigate these nonreciprocal effects. Moreover, a quantum propulsion force (second order in the local susceptibility) on a reciprocal extended body at rest is actually possible, provided that the body is not in thermal equilibrium with the environment and exhibits inhomogeneity across its volume [96, 97].

Numerical estimates of QVF for a gold atom and QFPC for a cesium atom are provided in this thesis. In both of these situations, the quantum frictional forces are too tiny to be observed at room temperature, but they are proportional to T^8 and, therefore, it is hoped that they might be measured at higher temperatures. However, the temperature must not exceed the ionization temperature of the atom, T_i , above which the atom will no longer stay neutral. In addition, the analysis presented in this thesis assumes a static polarizability for atoms, which could only be justified up to the temperature corresponding to the first excitation energy of the atom, T_1 . For temperatures in between T_1 and T_i , a more careful analysis is needed to include the first order frictional effect because the polarizability of the atom develops an imaginary part at the atomic transition frequencies, the contribution of which to the quantum friction cannot be ignored. If we further consider the finite width of each resonance, additional off-resonance first-order frictional effects need to be taken into account as well.

Apart from temperature, the quantum frictional forces also depend on velocity. They are generally too small to be observed unless the velocity of the particle reaches a fraction of the speed of light. An immediate question arises as of how to accelerate the neutral atoms. The solution is to combine the ion accelerators with a neutralizer where fast ions can be converted to neutral atoms with little change in momentum. In this way, MeV energy has been successfully achieved for argon beam and copper beam in Refs. [98, 99], respectively. ²

However optimistic we try to be, it seems the task of directly measuring the quantum frictional forces is challenging. Therefore, it is desirable to find other signatures for the quantum frictional effects. In the introduction, we mention that some authors have proposed that the geometric phase might be a fruitful venue for the investigation of quantum frictional effects [32, 33, 34]. Here, we provide

²For copper, 1 MeV is equivalent to a velocity of $0.0058c$, while for argon, it is equivalent to $0.0073c$.

another one based on the calculations we had done. In Ref. [22], we study the QVRHT on a moving nanoparticle and find that the radiative heat transfer always tends to bring the nanoparticle to its NESS temperature, which would be different from the environment temperature. We therefore propose that the deviation of the NESS temperature from the environment temperature could serve as a feasible signature for the quantum vacuum frictional effects. For a gold nanosphere moving at half of the speed of light, at temperatures lower than 1000 K,³ the deviation of its NESS temperature from the temperature of the environment can reach 18%. In fact, for nonrelativistic velocities, the deviation is approximately described by $\Delta = \frac{2}{3}v^2$, which seems to be detectable even at much lower velocities.

³In practice, we should not consider temperatures much higher than this, since gold melts at 1337 K.

Appendix A

Lorentz Transformations of Dipole, Field and Green's Tensor

When the particle moves with a velocity relative the radiation background, there exist naturally two frames to describe the physics, the rest frame of radiation, \mathcal{R} , and the rest frame of the particle, \mathcal{P} . We find the quantization is often easier done in frame \mathcal{P} . Therefore, in most calculations throughout the thesis, we will try to first transform the dipole and the fields in the first-principle expressions into frame \mathcal{P} and then apply the fluctuation-dissipation theorem to it. But when it comes to evaluate the quantized expression, the electromagnetic Green's tensor must be transformed back to frame \mathcal{R} , where we know its form. As a result, Lorentz transformations between the two frames are frequently performed for the dipole, the electromagnetic fields and the Green's tensor. In this appendix, we describe how these quantities transform under a Lorentz boost in the x direction with speed v . Primes are used throughout for quantities and coordinates in frame \mathcal{P} . In order to apply these directly to the problems in the main text, an underlying planar symmetry in the x - y plane is assumed. That is, the z coordinates are prevented from being transformed into the Fourier space.

The transformations of different components of dipole moment in the frequency space are

$$d_x(\omega) = d'_x(\gamma\omega), \quad d_y(\omega) = \gamma d'_y(\gamma\omega), \quad d_z(\omega) = \gamma d'_z(\gamma\omega). \quad (\text{A.1})$$

In the time domain, the transformations are

$$d_x(t) = \frac{1}{\gamma} d'_x\left(\frac{t}{\gamma}\right), \quad d_y(t) = d'_y\left(\frac{t}{\gamma}\right), \quad d_z(t) = d'_z\left(\frac{t}{\gamma}\right). \quad (\text{A.2})$$

In spacetime coordinates, the transformations of different components of the electric field read

$$\begin{aligned} E'_x(\mathbf{r}', t') &= E_x(\mathbf{r}, t), \\ E'_y(\mathbf{r}', t') &= \gamma[E_y(\mathbf{r}, t) - vB_z(\mathbf{r}, t)], \\ E'_z(\mathbf{r}', t') &= \gamma[E_z(\mathbf{r}, t) + vB_y(\mathbf{r}, t)], \end{aligned} \quad (\text{A.3})$$

where the transformation of the spacetime coordinates are

$$t = \gamma(t' + vx'), \quad x = \gamma(x' + vt'), \quad y = y', \quad z = z'. \quad (\text{A.4})$$

In frequency-momentum space, these transformations become

$$\begin{aligned}
E'_x(\omega', \mathbf{k}'_{\perp}; z') &= E_x(\omega, \mathbf{k}_{\perp}; z), \\
E'_y(\omega', \mathbf{k}'_{\perp}; z') &= \gamma [E_y(\omega, \mathbf{k}_{\perp}; z) - vB_z(\omega, \mathbf{k}_{\perp}; z)], \\
E'_z(\omega', \mathbf{k}'_{\perp}; z') &= \gamma [E_z(\omega, \mathbf{k}_{\perp}; z) + vB_y(\omega, \mathbf{k}_{\perp}; z)],
\end{aligned} \tag{A.5}$$

where the transformation of the coordinates are

$$\omega = \gamma(\omega' + k'_x v), \quad k_x = \gamma(k'_x + \omega' v), \quad k_y = k'_y, \quad z = z'. \tag{A.6}$$

The transformation of the components of the Green's tensor can be obtained by considering the Lorentz transformation of the fields and applying the FDT in both frames consistently. Here, the transformations of the material properties like ϵ or μ are never invoked because we always express \mathbf{G}' in terms of \mathbf{G} (instead of the other way around) as below:

$$\begin{aligned}
G'_{xx}(\omega', \mathbf{k}'_{\perp}; z', \tilde{z}') &= G_{xx}(\omega, \mathbf{k}_{\perp}; z, \tilde{z}), \\
G'_{yy}(\omega', \mathbf{k}'_{\perp}; z', \tilde{z}') &= \frac{1}{\omega^2} \left(\omega'^2 G_{yy} + \gamma^2 k_y'^2 v^2 G_{xx} + \omega' \gamma k_y' v G_{xy} + \omega' \gamma k_y' v G_{yx} \right) (\omega, \mathbf{k}_{\perp}; z, \tilde{z}), \\
G'_{zz}(\omega', \mathbf{k}'_{\perp}; z', \tilde{z}') &= \frac{1}{\omega^2} \left(\omega'^2 G_{zz} + \gamma^2 v^2 \partial_z \partial_{\tilde{z}} G_{xx} + i\omega' \gamma v \partial_{\tilde{z}} G_{zx} - i\omega' \gamma v \partial_z G_{xz} \right) (\omega, \mathbf{k}_{\perp}; z, \tilde{z}), \\
G'_{xy}(\omega', \mathbf{k}'_{\perp}; z', \tilde{z}') &= \frac{1}{\omega} \left(\omega' G_{xy} + \gamma k_y' v G_{xx} \right) (\omega, \mathbf{k}_{\perp}; z, \tilde{z}), \\
G'_{yx}(\omega', \mathbf{k}'_{\perp}; z', \tilde{z}') &= \frac{1}{\omega} \left(\omega' G_{yx} + \gamma k_y' v G_{xx} \right) (\omega, \mathbf{k}_{\perp}; z, \tilde{z}), \\
G'_{zx}(\omega', \mathbf{k}'_{\perp}; z', \tilde{z}') &= \frac{1}{\omega} \left(\omega' G_{zx} - i\gamma v \partial_z G_{xx} \right) (\omega, \mathbf{k}_{\perp}; z, \tilde{z}), \\
G'_{xz}(\omega', \mathbf{k}'_{\perp}; z', \tilde{z}') &= \frac{1}{\omega} \left(\omega' G_{xz} + i\gamma v \partial_{\tilde{z}} G_{xx} \right) (\omega, \mathbf{k}_{\perp}; z, \tilde{z}), \\
G'_{yz}(\omega', \mathbf{k}'_{\perp}; z', \tilde{z}') &= \frac{1}{\omega^2} \left(\omega'^2 G_{yz} - i\gamma^2 k_y' v^2 \partial_{\tilde{z}} G_{xx} + i\omega' \gamma v \partial_{\tilde{z}} G_{yx} - \omega' \gamma k_y' v G_{xz} \right) (\omega, \mathbf{k}_{\perp}; z, \tilde{z}), \\
G'_{zy}(\omega', \mathbf{k}'_{\perp}; z', \tilde{z}') &= \frac{1}{\omega^2} \left(\omega'^2 G_{zy} + i\gamma^2 k_y' v^2 \partial_z G_{xx} - i\omega' \gamma v \partial_z G_{xy} - \omega' \gamma k_y' v G_{zx} \right) (\omega, \mathbf{k}_{\perp}; z, \tilde{z}),
\end{aligned} \tag{A.7}$$

where the transformation of the coordinates are

$$\omega = \gamma(\omega' + k'_x v), \quad k_x = \gamma(k'_x + \omega' v), \quad k_y = k'_y, \quad z = z', \quad \tilde{z} = \tilde{z}'. \tag{A.8}$$

Appendix B

The Absence of Zero Temperature Quantum Friction in the Presence of a Diaphanous Medium

In this appendix, we supply a proof for why no zero temperature quantum friction (QF) should arise for a nondissipative particle in the vacuum or in the presence of a perfectly conducting (PC) plate. Further, we extend the claim to include the case where a diaphanous, nondissipative medium with the property $\varepsilon\mu = 1$ exist in the environment.

The QF for a nondissipative particle is second order in the intrinsic polarizability of the particle, $\alpha(\omega)$. See Eq. (4.1). At zero temperature, it can be rewritten as the following:

$$F = 2 \int_0^\infty \frac{d\omega}{2\pi} \int \frac{d^2\mathbf{k}_\perp}{(2\pi)^2} \frac{d^2\bar{\mathbf{k}}_\perp}{(2\pi)^2} \bar{k}_x \text{tr} \alpha(\omega) \cdot \Im \mathbf{G}'(\omega, \mathbf{k}_\perp; a, a) \cdot \alpha(\omega) \cdot \Im \mathbf{G}'(\omega, \bar{\mathbf{k}}_\perp; a, a) \times [\text{sgn}(\omega + \bar{k}_x v) - \text{sgn}(\omega + k_x v)]. \quad (\text{B.1})$$

To obtain Eq. (B.1), we have exchanged k_x and \bar{k}_x for the second term in Eq. (4.1) and used the evenness of the integrand under the total reflection of its frequency and wave vector arguments $(\omega, \mathbf{k}_\perp, \bar{\mathbf{k}}_\perp) \rightarrow (-\omega, -\mathbf{k}_\perp, -\bar{\mathbf{k}}_\perp)$. In order to make the argument clearer, let us change the \mathbf{k}_\perp and $\bar{\mathbf{k}}_\perp$ into dimensionless variables using ω as a positive scale,

$$k_x = \omega x, \quad k_y = \omega y, \quad \bar{k}_x = \omega \bar{x}, \quad \bar{k}_y = \omega \bar{y}. \quad (\text{B.2})$$

The friction now reads

$$F = \frac{1}{16\pi^5} \int_0^\infty d\omega \omega^5 \int dx dy d\bar{x} d\bar{y} \bar{x} \text{tr} \alpha(\omega) \cdot \Im \mathbf{G}'(\omega, \omega x, \omega y) \cdot \alpha(\omega) \cdot \Im \mathbf{G}'(\omega, \omega \bar{x}, \omega \bar{y}) \times [\text{sgn}(1 + \bar{x}v) - \text{sgn}(1 + xv)], \quad (\text{B.3})$$

where we have suppressed the spatial z coordinates of the Green's tensors. The difference in the sgn functions can be translated back into limits for the x and \bar{x} integrals, leading to

$$F = \frac{1}{8\pi^5} \int_0^\infty d\omega \omega^5 \int dy d\bar{y} \left[\int_{-\infty}^{-\frac{1}{v}} dx \int_{-\frac{1}{v}}^\infty d\bar{x} - \int_{-\frac{1}{v}}^\infty dx \int_{-\infty}^{-\frac{1}{v}} d\bar{x} \right] \bar{x} \times \text{tr} \alpha(\omega) \cdot \Im \mathbf{G}'(\omega, \omega x, \omega y) \cdot \alpha(\omega) \cdot \Im \mathbf{G}'(\omega, \omega \bar{x}, \omega \bar{y}). \quad (\text{B.4})$$

By exchanging x and \bar{x} again for the second term inside the bracket of Eq. (B.4), we find the frictional force becomes

$$F = \frac{1}{8\pi^5} \int_0^\infty d\omega \omega^5 \int dy d\bar{y} \int_{-\infty}^{-\frac{1}{v}} dx \int_{-\frac{1}{v}}^\infty d\bar{x} (\bar{x} - x) \times \text{tr} \boldsymbol{\alpha}(\omega) \cdot \Im \mathbf{G}'(\omega, \omega x, \omega y) \cdot \boldsymbol{\alpha}(\omega) \cdot \Im \mathbf{G}'(\omega, \omega \bar{x}, \omega \bar{y}). \quad (\text{B.5})$$

Now, the limit on x prevents the vacuum propagation wave number of the first reduced Green's tensor, κ , from developing an imaginary part, because of

$$\kappa^2 = k^2 - \omega^2 = \omega^2(x^2 + y^2 - 1) > 0, \quad x < -\frac{1}{v}. \quad (\text{B.6})$$

For the simplest vacuum situation where only the diagonal components of the Green's tensor contribute to the integral (see Appendix A of Ref. [21] for a detailed discussion), the anti-Hermitian part reduces to the ordinary imaginary part. But the only possible source of an imaginary part for the first Green's tensor in Eq. (B.5), κ , is now real definite. As a result, the zero temperature QVF vanishes.

For backgrounds other than vacuum, zero temperature quantum friction exists in general because the propagation wave number associated with the medium can become imaginary since

$$\kappa_n^2 = k^2 - \omega^2 n^2 = \omega^2(x^2 + y^2 - \varepsilon\mu) \quad (\text{B.7})$$

does not have a definite sign unless the index of refraction is smaller or less than 1,

$$n^2 = \varepsilon\mu \leq 1. \quad (\text{B.8})$$

In particular, for a diaphanous medium with the special property,

$$\varepsilon\mu = 1, \quad (\text{B.9})$$

the propagation wave number associated with the diaphanous medium coincides with the vacuum one, $\kappa_n = \kappa$. This nice coincidence renders the reflection coefficients in Eq. (2.97) to be real definite as long as ε and μ are real,

$$r^E = \frac{\mu - 1}{\mu + 1} = \frac{1 - \varepsilon}{1 + \varepsilon}, \quad r^H = \frac{\varepsilon - 1}{\varepsilon + 1}. \quad (\text{B.10})$$

Therefore, the only source of the imaginary part in the scalar Green's functions Eq. (2.95) is still just κ , which turns out to be real definite recalling Eq. (B.6). It can be further checked that the anti-Hermitian part of \mathbf{G}' vanishes unless κ develops an imaginary part even though the off-diagonal components of the Green's tensor and the transformation between \mathbf{G}' and \mathbf{G} needs to be taken into account. Therefore, we conclude that $\Im \mathbf{G}' = 0$ even if a diaphanous medium is present in the background, and as a result, zero temperature QF for such case must be absent.

Now, apparently, both the perfect conductor defined by Eq. (2.101) and Eq. (2.102) and the vacuum can be deemed as members of the family of diaphanous materials, for which the total reflection coefficient $r^E + r^H = 0$.

Appendix C

Analytical Method for Extracting Limits of QFPC

In this appendix, we provide a systematic analytical method for extracting the nonrelativistic limit, the small z (large separation/high temperature) limit and the large z (small separation/low temperature) limit of QFPC discussed in Chapter 4. We will illustrate the method with the most interesting contribution, F^{XZ} . The method, though, applies to other contributions as well. A static polarizability is still assumed throughout this appendix.

Let us first review the expression for F^{XZ} . We find in Eq. (4.12),

$$F^{\text{XZ}} = \frac{\alpha_{xx}(0)\alpha_{zz}(0)}{32\pi^3(2a)^8} f^{\text{XZ}}(v, z) = \frac{\alpha_{xx}(0)\alpha_{zz}(0)}{32\pi^3(2a)^8} \int_0^\infty dx x^7 \mathcal{F}^{\text{XZ}}(x, v, z) \quad (\text{C.1})$$

and \mathcal{F}^{XZ} is defined in Eq. (4.9d), which can be rewritten using the half-integer Bessel functions ¹,

$$J_{\frac{5}{2}}(x) = \sqrt{\frac{2x}{\pi}} j_2(x) = -\sqrt{\frac{2}{\pi x^{\frac{5}{2}}}} [3x \cos(x) + (x^2 - 3) \sin(x)] \quad (\text{C.2})$$

as

$$\mathcal{F}^{\text{XZ}}(x, v, z) = -\sqrt{\pi} 2^{\frac{3}{2}} x^{-\frac{3}{2}} J_{\frac{5}{2}}(x) \int_{-1}^1 du u \sqrt{1-u^2} J_1(x\sqrt{1-u^2}) \frac{1}{e^{x\gamma z(1+uv)} - 1}. \quad (\text{C.3})$$

Now, the key step of the analysis is to expand the thermal occupation factor in Eq. (C.3) as a Maclaurin series in the v variable, but retaining the implicit dependence of γ on v ,

$$\frac{1}{e^{x\gamma z(1+uv)} - 1} = \sum_{n=0}^{\infty} \frac{v^n}{n!} \left[\frac{\partial^n}{\partial v^n} \frac{1}{e^{x\gamma z(1+uv)} - 1} \right] \Big|_{v=0} = \sum_{n=0}^{\infty} \frac{v^n u^n}{n!} (x\gamma z)^n \frac{\partial^n}{\partial (x\gamma z)^n} \frac{1}{e^{x\gamma z} - 1}, \quad (\text{C.4})$$

Doing that, we obtain

$$\begin{aligned} \mathcal{F}^{\text{XZ}}(x, v, z) &= -\sqrt{\pi} 2^{\frac{3}{2}} x^{-\frac{3}{2}} J_{\frac{5}{2}}(x) \sum_{n=0}^{\infty} \frac{v^n}{n!} z^n \frac{\partial^n}{\partial z^n} \frac{1}{e^{x\gamma z} - 1} \\ &\quad \times \int_{-1}^1 du u^{n+1} \sqrt{1-u^2} J_1(x\sqrt{1-u^2}). \end{aligned} \quad (\text{C.5})$$

¹The other contributions can all be rewritten using Bessel functions with different half-integer orders.

Noticing that, in Eq. (C.5), any even n terms vanishes on account of the symmetry of the u integral, we immediately conclude, in the nonrelativistic limit, the leading term should be linear in v , given by the $n = 1$ term,

$$\mathcal{F}_{\text{NR}}^{\text{XZ}}(x, v, z) = -v\sqrt{\pi} 2^{\frac{3}{2}} x^{-\frac{3}{2}} J_{\frac{5}{2}}(x) z \frac{\partial}{\partial z} \frac{1}{e^{xz} - 1} \int_{-1}^1 du u^2 \sqrt{1-u^2} J_1(x\sqrt{1-u^2}). \quad (\text{C.6})$$

We find integration formula 6.683-6 found in [100], for given $\text{Re } \rho > -1$ and $\text{Re } \mu > -1$,

$$\int_0^{\pi/2} d\theta J_\mu(a \sin \theta) (\sin \theta)^{\mu+1} (\cos \theta)^{2\rho+1} = 2^\rho \Gamma(\rho+1) a^{-\rho-1} J_{\rho+\mu+1}(a). \quad (\text{C.7})$$

We can now carry out the u integral in Eq. (C.7) by making a change of variable, $u = \cos \theta$, and finding

$$\mathcal{F}_{\text{NR}}^{\text{XZ}}(x, v, z) = -4\pi v x^{-3} J_{\frac{5}{2}}^2(x) z \frac{\partial}{\partial z} \frac{1}{e^{xz} - 1}. \quad (\text{C.8})$$

The function f_{XZ} is to be obtained by integrating on x as shown in Eq. (C.1)

$$f_{\text{NR}}^{\text{XZ}} = -8vz \frac{\partial}{\partial z} \int_0^\infty dx \frac{[3x \cos x + (x^2 - 3) \sin x]^2}{x} \frac{1}{e^{xz} - 1}. \quad (\text{C.9})$$

Realizing that $z \frac{\partial}{\partial z}$ only acts on the exponential factor and can be exchanged for $x \frac{\partial}{\partial x}$ allows us to integrate by part on x and arrive at

$$f_{\text{NR}}^{\text{XZ}} = 8v \int_0^\infty dx [x(2x^2 + 3) + x^2(x^2 - 6) \sin(2x) + x(4x^2 - 3) \cos(2x)] \frac{1}{e^{xz} - 1}, \quad (\text{C.10})$$

where the first term in the bracket is obviously easy to integrate, while the next two terms can be generated by differentiation using the formula 3.951-12 in [100],

$$\int_0^\infty dx \frac{\sin(bx)}{e^x - 1} = \frac{\pi}{2} \coth(b\pi) - \frac{1}{2b}. \quad (\text{C.11})$$

This leads to

$$\begin{aligned} f_{\text{NR}}^{\text{XZ}} &= 8v \left\{ \int_0^\infty dx \frac{(2x^3 + 3x)}{e^{xz} - 1} + \left[\frac{d^4}{db^4} - 4 \frac{d^3}{db^3} + 6 \frac{d^2}{db^2} - 3 \frac{d}{db} \right] \left[\frac{\pi}{2z} \coth\left(\frac{b\pi}{z}\right) - \frac{1}{2b} \right] \right\} \Big|_{b=2} \\ &= v \left(\frac{16\pi^4}{15z^4} + \frac{4\pi^2}{z^2} - 18 \right. \\ &\quad + \left\{ \frac{32\pi^5}{z^5} \left[3 \coth^2\left(\frac{2\pi}{z}\right) - 2 \right] \coth\left(\frac{2\pi}{z}\right) + \frac{32\pi^4}{z^4} \left[3 \coth^2\left(\frac{2\pi}{z}\right) - 1 \right] \right. \\ &\quad \left. \left. + \frac{48\pi^3}{z^3} \coth\left(\frac{2\pi}{z}\right) + \frac{6\pi^2}{z^2} \right\} \text{csch}^2\left(\frac{2\pi}{z}\right) \right). \end{aligned} \quad (\text{C.12})$$

We therefore obtain in Eq. (C.12) the nonrelativistic limit valid for arbitrary z values.

Now, we turn to find the small z (vacuum/high temperature) limit and the large z (short distance/low temperature) limit of f^{XZ} for arbitrary velocities, which requires us to consider all the odd $n = 2m + 1$ terms in Eq. (C.5),

$$\mathcal{F}^{\text{XZ}}(x, v, z) = -\pi J_{\frac{5}{2}}(x) \sum_{m=0}^{\infty} \frac{v^{2m+1}}{m!} 2^{2-m} x^{-(m+3)} J_{m+\frac{5}{2}}(x) z^{2m+1} \frac{\partial^{2m+1}}{\partial z^{2m+1}} \frac{1}{e^{x\gamma z} - 1}, \quad (\text{C.13})$$

As a result, we have

$$f^{\text{XZ}}(v, z) = -\pi \sum_{m=0}^{\infty} \frac{v^{2m+1}}{m!} 2^{2-m} z^{2m+1} \frac{\partial^{2m+1}}{\partial z^{2m+1}} \int_0^{\infty} dx x^{4-m} J_{\frac{5}{2}}(x) J_{m+\frac{5}{2}}(x) \frac{1}{e^{x\gamma z} - 1}, \quad (\text{C.14})$$

which may be cast in forms suitable for small or large z by employing representations of the integrand (other than the thermal occupation factor) that are appropriate for large or small x , respectively.

For $z \ll 1$, we use the finite series representation

$$J_{n+\frac{1}{2}}(x) = \sqrt{\frac{2}{\pi x}} \left[\sin\left(x - \frac{\pi}{2}n\right) \sum_{k=0}^{\lfloor \frac{n}{2} \rfloor} \frac{(-1)^k (n+2k)!}{(2k)!(n-2k)!} (2x)^{-2k} \right. \\ \left. + \cos\left(x - \frac{\pi}{2}n\right) \sum_{k=0}^{\lfloor \frac{n-1}{2} \rfloor} \frac{(-1)^k (n+2k+1)!}{(2k+1)!(n-2k-1)!} (2x)^{-(2k+1)} \right], \quad (\text{C.15})$$

appropriate for large x to generate an expansion for $f^{\text{XZ}}(v, z)$. We will be content to establish the leading-order term for small z , which derives from the leading-order term in the above representation for large x :

$$J_{n+\frac{1}{2}}(x) \sim \sqrt{\frac{2}{\pi x}} \sin\left(x - \frac{\pi}{2}n\right), \quad x \rightarrow \infty. \quad (\text{C.16})$$

Using Eq. (C.16) in Eq. (C.14) and keeping only the $m = 0$ term, corresponding to the leading x -power in the integrand, we readily obtain, as $z \rightarrow 0$,

$$f^{\text{XZ}}(v, z) \sim -8vz \frac{\partial}{\partial z} \int_0^{\infty} dx x^3 \sin^2 x \frac{1}{e^{x\gamma z} - 1} \sim -4vz \frac{\partial}{\partial z} \Gamma(4)\zeta(4)(\gamma z)^{-4} = \frac{16\pi^4 v}{15\gamma^4 z^4}. \quad (\text{C.17})$$

It is interesting to note the appearance of the Planck-Einstein transformed temperature, $T_\gamma \equiv \frac{T}{\gamma}$, in this (high-temperature) limit. Note Eq. (C.17) captures not only the correct z dependence but also the velocity dependence of f^{XZ} in the small z limit. Taking further the nonrelativistic limit amounts to ignoring the γ^4 factor, which agrees with Eq. (C.12). The agreement of Eq. (C.17) with the numerical data for $v = 0.5$ is also illustrated in Fig. C.1.

For $z \gg 1$, we use instead

$$J_\mu(x) J_\nu(x) = \sum_{n=0}^{\infty} \frac{(-1)^n (\mu + \nu + n + 1)_n}{n! \Gamma(\mu + n + 1) \Gamma(\nu + n + 1)} \left(\frac{x}{2}\right)^{\mu + \nu + 2n}, \quad (\text{C.18})$$

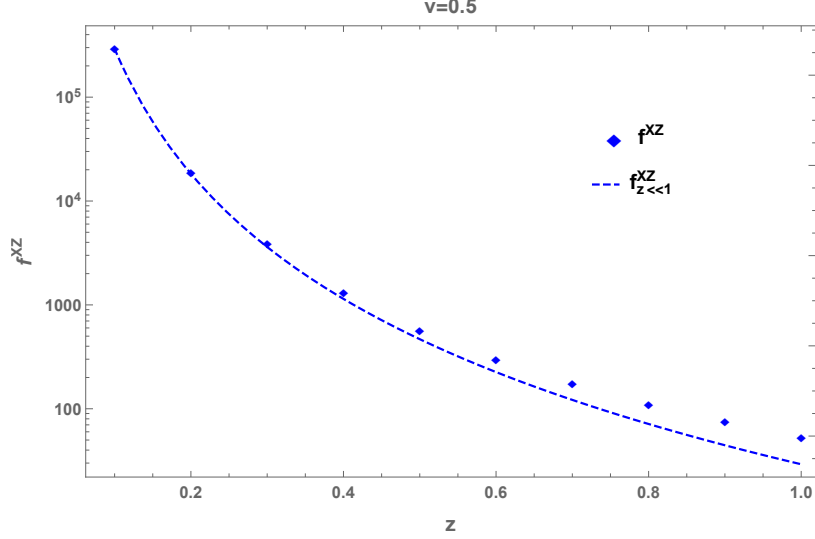


Figure C.1: At fixed velocity $v = 0.5$, the numerical results for f^{XZ} (dots) and its small z approximation (dashed line) obtained in Eq. (C.17) are shown for $z \in [0, 1]$.

appropriate for small x to generate an expansion for $f^{XZ}(v, z)$. In this case, the leading x -power in the integrand in Eq. (C.14) is independent of m , so all terms must be included, resulting in

$$\begin{aligned}
f^{XZ}(v, z) &\sim -\pi \sum_{m=0}^{\infty} \frac{v^{2m+1}}{m!} \frac{2^{-(3+2m)}}{\Gamma(\frac{7}{2}) \Gamma(m + \frac{7}{2})} z^{2m+1} \frac{\partial^{2m+1}}{\partial z^{2m+1}} \int_0^{\infty} dx x^9 \frac{1}{e^{x\gamma z} - 1} \\
&= -\pi \sum_{m=0}^{\infty} \frac{v^{2m+1}}{m!} \frac{2^{-(3+2m)}}{\Gamma(\frac{7}{2}) \Gamma(m + \frac{7}{2})} z^{2m+1} \frac{\partial^{2m+1}}{\partial z^{2m+1}} \Gamma(10) \zeta(10) (\gamma z)^{-10} \\
&= \pi \sum_{m=0}^{\infty} \frac{v^{2m+1}}{m!} \frac{2^{-(3+2m)}}{\Gamma(\frac{7}{2}) \Gamma(m + \frac{7}{2})} \frac{(2m+10)! \zeta(10)}{(\gamma z)^{10}} \\
&= \frac{2^8 \zeta(10) v}{15 \gamma^{10} z^{10}} \sum_{m=0}^{\infty} v^{2m} (m+1)(m+2)(m+3)(m+4)(m+5)(2m+7)(2m+9) \\
&= \frac{2^{11} 3 \zeta(10)}{z^{10}} \gamma^6 v (21 + 30v^2 + 5v^4), \quad z \rightarrow \infty, \tag{C.19}
\end{aligned}$$

where we have used the identity

$$\gamma^{2n} = \frac{1}{(n-1)!} \frac{d^{n-1}}{d(v^2)^{n-1}} \frac{1}{1-v^2} = \frac{1}{(n-1)!} \sum_{m=0}^{\infty} v^{2m} (m+1)(m+2) \cdots (m+n-1). \tag{C.20}$$

The result obtained in Eq. (C.19) is precisely that found in Eq. (4.14).

List of Publications

Prachi Parashar, Kimball A. Milton, Yang Li, Hannah Day, Xin Guo, Stephen A. Fulling, Inés Cavero-Peláez. Quantum electromagnetic stress tensor in an inhomogeneous medium. *Phys. Rev. D* **97**, 125009, (2018).

Yang Li, Kimball A. Milton, Xin Guo, Gerard Kennedy, Stephen A. Fulling. Casimir forces in inhomogeneous media: renormalization and the principle of virtual work. *Phys. Rev. D* **99**, 125004, (2019).

Kimball A. Milton, Yang Li, Xin Guo, Gerard Kennedy. Electrodynamic friction of a charged particle passing a conducting plate. *Phys. Rev. Research* **2**, 023114, (2020).

Kimball A. Milton, Hannah Day, Yang Li, Xin Guo, Gerard Kennedy. Self-force on moving electric and magnetic dipoles: Dipole radiation, Vavilov-Čerenkov radiation, friction with a conducting surface, and the Einstein-Hopf effect. *Phys. Rev. Research* **2**, 043347 (2020).

Xin Guo, Kimball A. Milton, Gerard Kennedy, William P. McNulty, Nima Pourtalomi, Yang Li. Energetics of quantum vacuum friction: Field fluctuations. *Phys. Rev. D* **104**, 116006 (2021).

Xin Guo, Kimball A. Milton, Gerard Kennedy, William P. McNulty, Nima Pourtalomi, Yang Li. Energetics of quantum vacuum friction. II. Dipole fluctuations and field fluctuations. *Phys. Rev. D* **106**, 016008 (2022).

Yang Li, Kimball A. Milton, Prachi Parashar, Gerard Kennedy, Nima Pourtalomi, Xin Guo. Casimir self-entropy of nanoparticles with classical polarizabilities: Electromagnetic field fluctuations. *Phys. Rev. D* **106**, 036002 (2022).

Xin Guo, Kimball A. Milton, Gerard Kennedy, Nima Pourtalomi. Quantum friction in the presence of a perfectly conducting plate. *Phys. Rev. A* **107**, 062812 (2023).

Kimball A. Milton, Xin Guo, Gerard Kennedy, Nima Pourtalomi, Dylan M. DelCol. Vacuum torque, propulsive forces, and anomalous tangential forces: Effects of non-reciprocal media out of thermal equilibrium. *arXiv: 2306.02197* (2023).

Bibliography

- [1] M. Planck. Über das Gesetz der Energieverteilung im Normal-spectrum. *Ann. d. Phys.*, 4:553, 1901.
- [2] M. Planck. Über die Begründung des Gesetzes der schwarzen. *Ann. d. Phys.*, 37:642, 1912.
- [3] A. Einstein and L. Hopf. Statistische Untersuchung der Bewegung eines Resonators in einem Strahlungsfeld. *Ann. Phys. (Leipzig)*, 338:1105, 1910.
- [4] A. Einstein and O. Stern. Einige Argumente für die Annahme einer molekularen Agitation beim absoluten Nullpunkt. *Ann. Phys. (Leipzig)*, 40:551, 1913.
- [5] P. W. Milonni. *The quantum vacuum*. Academic Press, San Diego, 1993.
- [6] H. B. G. Casimir. On the attraction between two perfectly conducting plates. *Proc. K. Ned. Akad. Wet.*, 51:793, 1948.
- [7] H. B. G. Casimir and D. Polder. The Influence of Retardation on the London-van der Waals Forces. *Phys. Rev.*, 73:4, 1948.
- [8] S. K. Lamoreaux. Demonstration of the Casimir Force in the 0.6 to 6 μm Range. *Phys. Rev. Lett.*, 78:5, 1997.
- [9] C. I. Sukenik, M. G. Boshier, V. Sandoghdar D. Cho, and E. A. Hinds. Measurement of the Casimir-Polder Force. *Phys. Rev. Lett.*, 70:5, 1992.
- [10] K. A. Milton. *The Casimir effect*. World Scientific, New Jersey, 2001.
- [11] J. B. Pendry. Shearing the vacuum – quantum friction. *J. Phys. Condens. Matter*, 9:10301, 1997.
- [12] E. V. Teodorovich. Contribution of macroscopic van der Waals interactions to frictional force. *Proc. R. Soc. Lond. A*, 362:71, 1978.
- [13] L. S. Levitov. Van der Waals friction. *Europhys. Lett.*, 8:499, 1989.
- [14] J. S. Høye and I. Brevik. Friction force between moving harmonic oscillators. *Physica A*, 181:413, 1992.
- [15] J. S. Høye and I. Brevik. Friction force with non-instantaneous interaction between moving harmonic oscillators. *Physica A*, 196:241, 1993.

-
- [16] V. Mkrtchian, V. A. Parsegian, R. Podgornik, and W. M. Saslow. Universal thermal radiation drag on neutral objects. *Phys. Rev. Lett.*, 91:220801, 2003.
- [17] G. Łach, M. DeKieviet, and U. D. Jentschura. Einstein–Hopf drag, Doppler shift of thermal radiation and blackbody drag: Three perspectives on quantum friction. *Cent. Eur. J. Phys.*, 10:763, 2012.
- [18] K. Sinha and P. W. Milonni. Dipoles in blackbody radiation: momentum fluctuations, decoherence, and drag force. *J. Phys. B: At. Mol. Opt. Phys.*, 55:204002, 2022.
- [19] K. A. Milton, Y. Li, X. Guo, and G. Kennedy. Electrodynamic friction of a charged particle passing a conducting plate. *Phys. Rev. Research*, 2:023114, 2020.
- [20] K. A. Milton, H. Day, Y. Li, X. Guo, and G. Kennedy. Self-force on moving electric and magnetic dipoles: Dipole radiation, Vavilov–Čerenkov radiation, friction with a conducting surface, and the Einstein-Hopf effect. *Phys. Rev. Research*, 2:043347, 2020.
- [21] X. Guo, K. A. Milton, G. Kennedy, W. P. McNulty, N. Pourtolami, and Y. Li. Energetics of quantum vacuum friction: Field fluctuations. *Phys. Rev. D*, 104:116006, 2021.
- [22] X. Guo, K. A. Milton, G. Kennedy, W. P. McNulty, N. Pourtolami, and Y. Li. Energetics of quantum vacuum friction. II. Dipole fluctuations and field fluctuations. *Phys. Rev. D*, 106:016008, 2022.
- [23] X. Guo, K. A. Milton, G. Kennedy, and N. Pourtolami. Quantum friction in the presence of a perfectly conducting plate. *Phys. Rev. A*, 107:062812, 2023.
- [24] M. Kardar and R. Golestanian. The “friction” of vacuum, and other fluctuation-induced forces. *Rev. Mod. Phys.*, 71:1233, 1999.
- [25] A. I. Volokitin and B. N. J. Persson. *Electromagnetic Fluctuations at the Nanoscale*. Springer, Berlin, 2017.
- [26] F. Intravaia, R. O. Behunin, C. Henkel, K. Busch, and D. A. R. Dalvit. Failure of local thermal equilibrium in quantum friction. *Phys. Rev. Lett.*, 117:100402, 2016.
- [27] M. Oelschläger. *Fluctuation-induced phenomena in nanophotonic systems*. PhD thesis, Institut für Physik, Humboldt-Universität zu Berlin, 2020.
- [28] D. Reiche, F. Intravaia, and K. Busch. Wading through the void: Exploring quantum friction and nonequilibrium fluctuations. *APL Photonics*, 7:030902, 2022.
- [29] M. Oelschläger, D. Reiche, C. H. Egerland, K. Busch, F. Intravaia. Electromagnetic viscosity in complex structured environments: From blackbody to quantum friction. *Phys. Rev. A*, 106:052205, 2022.

-
- [30] G. Pieplow and C. Henkel. Cherenkov friction on a neutral particle moving parallel to a dielectric. *J. Phys.: Condens. Matter*, 27:214001, 2015.
- [31] K. A. Milton, J. S. Høye, and I. Brevik. The reality of Casimir friction. *Symmetry*, 8:29, 2016.
- [32] M. Belén Farías, Fernando C. Lombardo, Alejandro Soba, Paula I. Villar, and Ricardo S. Decca. Towards detecting traces of non-contact quantum friction in the corrections of the accumulated geometric phase. *npj Quantum inf.*, 6:25, 2020.
- [33] L. Viotti, F. C. Lombardo, and P. I. Villar. Enhanced decoherence for a neutral particle sliding on a metallic surface in vacuum. *Phys. Rev. A*, 103:032809, 2021.
- [34] F. C. Lombardo, R. S. Decca, L. Viotti, and P. I. Villar. Detectable signature of quantum friction on a sliding particle in vacuum. *Adv. Quantum Technol.*, 4:2000155, 2021.
- [35] K. McDonald. On the history of the radiation reaction. <http://kirkmcd.princeton.edu/examples/>, 2017.
- [36] M. Lesiuk, M. Przybytek, and B. Jeziorski. Theoretical determination of polarizability and magnetic susceptibility of neon. *Phys. Rev. A*, 102:052816, 2020.
- [37] M. Sonnleitner and S. M. Barnett. The Röntgen interaction and forces on dipoles in time-modulated optical fields. *Eur. Phys. J. D*, 71:336, 2017.
- [38] J. B. Johnson. Thermal Agitation of Electric Charge in Conductors. *Phys. Rev.*, 32:97, 1928.
- [39] H. Nyquist. Thermal Agitation of Electric Charge in Conductors . *Phys. Rev.*, 32:110, 1928.
- [40] H. B. Callen and T. A. Welton. Irreversibility and Generalized Noise. *Phys. Rev.*, 83:34, 1951.
- [41] R. Kubo. Statistical-Mechanical Theory of Irreversible Processes. I. *J. Phys. Soc. Jpn*, 12:570, 1957.
- [42] R. Kubo. The fluctuation-dissipation theorem. *Rep. Prog. Phys.*, 29:255, 1966.
- [43] P. C. Martin and J. Schwinger. Theory of Many-Particle Systems. I. *Phys. Rev.*, 115:1342, 1959.
- [44] N. Borghini. Topics in nonequilibrium physics. <https://www.physik.uni-bielefeld.de/~borghini/Teaching/Nonequilibrium16/>. Accessed: 2023-03-16.
- [45] L. P. Kadanoff and P. C. Martin. Hydrodynamic Equations and Correlation Functions. *Ann. Phys.*, 24:419, 1963.

-
- [46] M. Khaleghy and F. Qassemi. Relativistic temperature transformation revisited, one hundred years after relativity theory, 2005.
- [47] A. Sihvola, I. V. Lindell, H. Wallén, P. Ylä-Oijala. Material realizations of perfect electric conductor objects. *ACES*, 25:1007, 2010.
- [48] J. Schwinger, L. L. DeRaad, Jr., K. A. Milton, and W.-y. Tsai. *Classical Electrodynamics*. Perseus/Taylor and Francis, Reading, MA, 1998.
- [49] J. D. Jackson. *Classical Electrodynamics*. Wiley, New York, 1999.
- [50] V. A. Parsegian. *Van der Waals forces*. Cambridge, New York, 2006.
- [51] J. S. Høye, I. Brevik, J. B. Aarseth, and K. A. Milton. Does the transverse electric zero mode contribute to the Casimir effect for a metal? *Phys. Rev. E*, 67:056116, 2003.
- [52] F. Bloch. Zum elektrischen Widerstandsgesetz bei tiefen Temperaturen. *Z. Phys.*, 59:208, 1930.
- [53] E. Grüneisen. Die Abhängigkeit des elektrischen Widerstandes reiner Metalle von der Temperatur. *Ann. Phys. (Leipzig)*, 408:530, 1933.
- [54] A. Lambrecht and S. Reynaud. Casimir force between metallic mirrors. *Eur. Phys. J. D*, 8:309, 2000.
- [55] E. D. Palik. *Handbook of Optical Constants of Solids*. Academic Press, New York, 1995.
- [56] Basic Atomic Spectroscopic Data. https://physics.nist.gov/PhysRefData/Handbook/atomic_number.htm. Accessed: 2023-04-10.
- [57] G. Łach, M. DeKieviet, and U. D. Jentschura. Enhancement of blackbody friction due to the finite lifetime of atomic levels. *Phys. Rev. Lett.*, 108:043005, 2012.
- [58] G. V. Dedkov and A. A. Kyasov. Tangential force and heating rate of a neutral relativistic particle mediated by equilibrium background radiation. *Nucl. Instrum. Methods Phys. Res. B*, 268:599, 2010.
- [59] G. V. Dedkov and A. A. Kyasov. Thermal Radiation of a Blackbody Moving in Equilibrium Gas of Photons. *Zhurnal Tekhnicheskoi Fiziki*, 91:1075, 2021.
- [60] K. Sinha and P. W. Milonni. Dipoles in blackbody radiation: momentum fluctuations, decoherence and drag force. *J. Phys. B*, 55:204002, 2022.
- [61] K. A. Milton, X. Guo, G. Kennedy, N. Pourtolami, and D. Delcol. Vacuum torque, propulsive forces and anomalous tangential forces: Effects of nonreciprocal media out of equilibrium, 2023. arXiv:2306.02197.
- [62] D. Reiche, F. Intravaia, J.-T. H., K. Busch, and B.-L. Hu. Nonequilibrium thermodynamics of quantum friction. *Phys. Rev. A*, 102:050203(R), 2020.

-
- [63] C. Farías, V. A. Pinto, and P. S. Moya. What is the temperature of a moving body? *Sci. Rep.*, 7:17657, 2017.
- [64] J. Jung and T. G. Pedersen. Exact polarizability and plasmon resonances of partly buried nanowires. *Opt. Express*, 19:22775, 2011.
- [65] G. Pieplow and C. Henkel. Fully covariant radiation force on a polarizable particle. *New J. Phys.*, 15:023027, 2013.
- [66] G. V. Dedkov and A. A. Kyasov. Fluctuation-electromagnetic interaction under dynamic and thermal nonequilibrium conditions. *Phys. Usp.*, 60:559, 2017.
- [67] P. R. Berman, R. W. Boyd, and P. W. Milonni. Polarizability and the optical theorem for a two-level atom with radiative broadening. *Phys. Rev. A*, 74:053816, 2006.
- [68] U. D. Jentschura and K. Pachucki. Functional form of the imaginary part of the atomic polarizability. *Eur. Phys. J. D*, 69:118, 2015.
- [69] P. Schwerdtfeger and J. K. Nagle. 2018 table of static dipole polarizabilities of the neutral elements in the periodic table. *Mol. Phys.*, 117:1200, 2019.
- [70] T. M. Miller and B. Bederson. Atomic and molecular polarizabilities—a review of recent advances. volume 13 of *Advances in Atomic and Molecular Physics*, pages 1–55. Academic Press, 1978.
- [71] U. D. Jentschura, G. Łach, M. DeKieviet, and K. Pachucki. One-loop dominance in the imaginary part of the polarizability: application to blackbody and noncontact van der Waals friction. *Phys. Rev. Lett.*, 114:043001, 2015.
- [72] C. M. Brown and M. L. Ginter. Absorption spectrum of Au I between 1300 and 1900 Å. *J. Opt. Soc. Am.*, 68(2):243, Feb 1978.
- [73] J. C. Ehrhardt and S. P. Davis. Precision wavelengths and energy levels in gold*. *J. Opt. Soc. Am.*, 61(10):1342, Oct 1971.
- [74] D. M. Harber, J. M. Obrecht, J. M. McGuirk, and E. A. Cornell. Measurement of the Casimir-Polder force through center-of-mass oscillations of a Bose-Einstein condensate. *Phys. Rev. A*, 72:033610, 2005.
- [75] J. M. Obrecht, R. J. Wild, M. Antezza, L. P. Pitaevskii, S. Stringari, and E. A. Cornell. Measurement of the Temperature Dependence of the Casimir-Polder Force. *Phys. Rev. Lett.*, 98:063201, 2007.
- [76] M. Krüger and M. Rauscher. Colloid-colloid and colloid-wall interactions in driven suspensions. *J. Chem. Phys.*, 127:034905, 2007.
- [77] K.-H. Weber and Craig J. Sansonetti. Accurate energies of ns, np, nd, nf, and ng levels of neutral cesium. *Phys. Rev. A*, 35:4650, 1987.
- [78] B. Cordero, V. Gómez, A. E. Platero-Prats, M. Revés, J. Echeverría, E. Cremades, F. Barragán, and S. Alvarez. Covalent radii revisited. *Dalton Trans.*, pages 2832–2838, 2008.

-
- [79] I. I. Beterov, I. I. Ryabtsev, D. B. Tretyakov and V. M. Entin. Quasiclassical calculations of blackbody-radiation-induced depopulation rates and effective lifetimes of Rydberg nS , nP , and nD alkali-metal atoms with $n \leq 80$. *Phys. Rev. A*, 79:052504, 2009.
- [80] P. A. Cherenkov. Visible luminescence of pure liquids under the influence of γ -radiation. *Dokl. Akad. Nauk SSSR*, 2:451, 1934.
- [81] P. A. Cherenkov. Visible Radiation Produced by Electrons Moving in a Medium with Velocities Exceeding that of Light. *Phys. Rev.*, 52:378, 1937.
- [82] I. M. Frank and I. E. Tamm. Coherent visible radiation of fast electrons passing through matter. *Compt. Rend. Acad. Sci. URSS*, 14:107, 1937.
- [83] I. M. Frank. Doppler effect in a refractive medium. *Izv. Acad. Nauk. SSSR*, 6:3, 1937.
- [84] I. M. Frank. Vavilov-Cherenkov radiation for electric and magnetic multipoles. *Usp. Fiz. Nauk. SSSR*, 144:251, 1984.
- [85] V.L. Ginzburg. V radiation by uniformly moving sources: Vavilov–cherenkov effect, doppler effect in a medium, transition radiation and associated phenomena. volume 32 of *Progress in Optics*, pages 267–312. Elsevier, 1993.
- [86] M. F. Maghrebi, R. Golestanian, and M. Kardar. Quantum Cherenkov radiation and noncontactfriction. *Phys. Rev. A*, 88:042509, 2013.
- [87] S. Scheel and S. Y. Buhmann. Casimir-polder forces on moving atoms. *Phys. Rev. A*, 80:042902, 2009.
- [88] G. Barton. On van der Waals friction. II: Between atom and half-space. *New J. Phys.*, 12:113045, 2010.
- [89] F. Intravaia, R. O. Behunin, and D. A. R. Dalvit. Quantum friction and fluctuation theorems. *Phys. Rev. A*, 89:050101(R), 2014.
- [90] A. Manjavacas and F. J. García de Abajo. Vacuum friction in rotating particles. *Phys. Rev. Lett.*, 105:113601, 2010.
- [91] A. Manjavacas and F. J. García de Abajo. Thermal and vacuum friction acting on rotating particles. *Phys. Rev. A*, 82:063827, 2010.
- [92] A. Manjavacas and F. J. García de Abajo. Rotational quantum friction. *Phys. Rev. Lett.*, 109:123604, 2012.
- [93] V. S. Asadchy, M. S. Mirmoosa, A. Díaz-Rubio, S.-H. Fan, and S. A. Tretyakov. Tutorial on electromagnetic nonreciprocity and its origins. *Proceedings of the IEEE*, 108(10):1684–1727, 2020.
- [94] D. Pan, H. Xu, and F. J. García de Abajo. Magnetically activated rotational vacuum friction. *Phys. Rev. A*, 99:062509, 2019.

-
- [95] L.-X. Zhu and S.-H. Fan. Persistent Directional Current at Equilibrium in Nonreciprocal Many-Body Near Field Electromagnetic Heat Transfer. *Phys. Rev. A*, 117:134303, 2016.
- [96] B. Müller and M. Krüger. Anisotropic particles near surfaces: Propulsion force and friction. *Phys. Rev. A*, 93:032511, 2016.
- [97] M. T. H. Reid, O. D. Miller, A. G. Polimeridis, A. W. Rodriguez, E. M. Tomlinson, and S. G. Johnson. Photon torpedoes and Rytov pinwheels: Integral-equation modeling of non-equilibrium fluctuation-induced forces and torques on nanoparticles, 2017. arXiv:1708.01985.
- [98] R. Rajeev, T. M. Trivikram, K. P. M. Rishad, V. Narayanan, E. Krishnakumar, and M. Krishnamurthy. A compact laser-driven plasma accelerator for megaelectronvolt-energy neutral atoms. *Nature Phys.*, 9:185, 2013.
- [99] M. Dalui, T. M. Trivikram, J. Colgan, J. Pasley, and M. Krishnamurthy. Compact acceleration of energetic neutral atoms using high intensity laser-solid interaction. *Scientific Reports*, 7:3871, 2017.
- [100] I. S. Gradshteyn and I. M. Ryzhik. *Table of Integrals, Series and Products*. Academic Press, Waltham, MA, 7th edition, 2014.